



CLIMAAX
climate ready regions

Deliverable Phase 2 – Climate risk assessment

climate aDapTalon for vulnerABLE regions using the “CLIMAAX” framEwork (DATABLe)

Greece, Region of Central Macedonia

Document Information

Deliverable Title	Phase 2 – Climate risk assessment
Brief Description	This report outlines the data collection and application processes for regional and local data in the Region of Central Macedonia (RCM), utilizing the CLIMAAX framework, with a focus on two (2) selected hazards: floods and wildfires. The required data, methodologies, and tools for implementing the framework in the RCM were primarily sourced from the CLIMAAX project digital handbook, with minor modifications applied as necessary.
Project name	climate aDapTalon for vulnerABLE regions using the “CLIMAAX” framEwork (DATABLE)
Country	Greece
Region/Municipality	RCM
Leading Institution	RCM
Author(s)	<ul style="list-style-type: none"> ● Ioannis Kompatsiaris (CDXi¹) ● Stefanos Vrochidis (CDXi) ● Ilias Gialampoukidis (CDXi) ● Anastasia Moutzidou (CDXi) ● Konstantinos Karystinakis (CDXi) ● Konstantinos Vlachos (CDXi) ● Athanasios Arvanitidis (CDXi)
Deliverable submission date	02/03/2026
Final version delivery date	02/03/2026
Nature of the Deliverable	R – Report
Dissemination Level	PU - Public

Version	Date	Change editors	Changes
1.0	10/11/2025	Nikolaos Papadopoulos (RCM)	Initial structure of the document. Preliminary guidelines and descriptions were included.
1.1	20/10/2025	Nikolaos Papadopoulos (RCM)	Corrections and updates. Preliminary format of the document.
2.0	10/11/2025	CDXi	Update Floods and Wildfire workflows.
2.1	18/01/2026	CDXi	Update on regional data collection
3.0	18/01/2026	Nikolaos Papadopoulos	Reviewing and final updates.

¹ CDXi Solutions P.C.: <https://cdxi.gr/>.

		(RCM)	
3.1	16/02/2026	CDXi	Updates on data collection from local authorities
3.1.1	16/02/2026	CDXi	Additional flooding workflow was added.
3.2	02/03/2026	Nikolaos Papadopoulos (RCM)	Reviewing and final updates of the new version.

Table of Contents

Document Information..... 2

Table of Contents..... 4

List of Figures..... 6

List of Tables..... 7

Abbreviations and acronyms 9

Executive summary..... 11

1 Introduction..... 12

 1.1 Background 12

 1.2 Main objectives of the project 12

 1.3 Project team..... 12

 1.4 Outline of the document’s structure..... 13

2 Climate risk assessment – Phase 2 14

 2.1 Scoping..... 14

 2.1.1 Objectives 14

 2.1.2 Context..... 14

 2.1.3 Participation and risk ownership 15

 2.1.4 Application of principles 16

 2.1.5 Stakeholder engagement 16

 2.2 Risk Exploration 17

 2.2.1 Screen risks (selection of main hazards)..... 17

 2.2.2 Choose Scenario 20

 2.3 Regionalized Risk Analysis 21

 2.3.1 Hazard #1 - Floods..... 21

 2.3.1.1 River floods (discharges) – European data..... 22

 2.3.1.2 River floods (flood maps) – Regional data..... 30

 2.3.1.3 Flooding buildings and population exposure 47

 2.3.2 Hazard #2 – Wildfires..... 53

 2.3.2.1 Wildfire – FWI Response Model – European data 54

 2.3.2.2 Wildfire – FWI (ML) 63

 2.4 Key Risk Assessment Findings..... 70

 2.4.1 Mode of engagement for participation 71

 2.4.2 Gather output from Risk Analysis step..... 71

 2.4.3 Assess Severity 71

 2.4.4 Assess Urgency..... 72

 2.4.5 Understand Resilience Capacity 72

 2.4.6 Decide on Risk Priority..... 72

2.5	Monitoring and Evaluation	73
2.6	Work plan Phase 3	73
3	Conclusions Phase 2- Climate risk assessment.....	74
4	Progress evaluation	75
5	Supporting documentation	76
6	References	77
	Appendix	79

List of Figures

Figure 1: A schematic depiction of RCM along with selected water bodies across the region.....	12
Figure 2: Selected area for the example application of the workflow.....	23
Figure 3: Daily timeseries of river discharges (m ³ /s) based on six (6) different GCM-RCM climate model combinations for the period 1991-2006.	24
Figure 4: Flow-duration curve based on six (6) different GCM-RCM climate model combinations for the period 1991-2006.....	24
Figure 5: Monthly mean river discharges (m ³ /s) for the selected catchment ID for historical GCM-RCM, scenarios, and time periods.	25
Figure 6: Extreme River discharges (m ³ /s) for the selected catchment ID for different GCM-RCM and scenarios combinations for 10-year and 50-year return periods.	26
Figure 7: Relative change in extreme river discharges for the selected catchment ID for different GCM-RCM and selected scenarios combinations and for 10-year and 50-year return periods.....	27
Figure 8: Timeseries of river discharges taken from GRDC 6262310 data.	28
Figure 9: Modelled discharge timeseries based on six (6) GCM-RCM climate model combinations as well as the values from the observational dataset from GRDC 6262310.....	29
Figure 10: Flow-duration curve based on modelled river discharges for six (6) GCM-RCM combinations for the GRDC 6262310.....	29
Figure 11: Mean River discharges for GRDC 6262310.....	30
Figure 12: The areas depicted are, from top to bottom and left to right: Anthemountas River (top left), Chalkidiki (top right), the delta of the Axios and Loudias Rivers (middle left), Paralia Katerini (middle right), and the West Side of Thessaloniki (bottom).	34
Figure 13: River Flood Inundation Depth Across Return Periods (RP50, RP100, RP1000) in Central Macedonia.....	35
Figure 14: Aqueduct floods (baseline ca.1980): River Inundation Depth for a 1-in-100 Year Event Across Selected Central Macedonia Case-Study Areas.	36
Figure 15: LUISA Land Cover (2018, 100 m): Categorical Land-Use Maps for Selected Case-Study Areas. Top left represents Chalkidiki, top right Paralia Katerini, bottom left, Delta of Axios, and bottom right a selected area in the Wider area of Thessaloniki (zoomed in).	37
Figure 16: Flood hazard mapping based on the regional high-resolution river flood map dataset for the present-day scenario for the wider area of the West Side of Thessaloniki, and for the wider Axios Delta area.	38
Figure 17: River flood potential for various return periods in both study cases. The upper section illustrates the Wider Area of Thessaloniki, while the lower section shows the Delta area.	39
Figure 18: Flood map for the baseline scenario (ca. 1980) for 1 in 100 years return period for the two (2) selected example areas: on the left, the wider area of the West Side of Thessaloniki, and on the right, the Axios Delta wider area.	40
Figure 19: Flood maps for the RCP4.5 emission scenario, for return periods 1 in 100 years for 2030, 2050, and 2080 projections.....	41
Figure 20: Flood maps for the RCP8.5 emission scenario, for return periods 1 in 100 years for 2030, 2050, and 2080 projections.....	42
Figure 21: LUISA Land Cover map for the selected area. On the left the wider area of the West Side of Thessaloniki, and on the right the Axios Delta.	43
Figure 22: Depth-damage curves as given by the JRC (left). Vulnerability curves for the first ten (10) LUISA land cover types are given following the "LUISA_damage_info_curves_greece.xlsx".	43
Figure 23: River flood damages for extreme river flow scenarios in current day climate. The same scheme is followed with the previous figures regarding the areas that are depicted.	45
Figure 24: Maps of flood and associated damages for extreme river water level scenarios in current climate 1 in 100-year extreme event.	46

Figure 25: River flood maps for the case study areas for selected return periods for the given bounding box shapefile. 47

Figure 26: Difference in the river flood maps for the case study areas for selected return periods. 48

Figure 27: Population map for the case study areas for the selected bounding box areas. 48

Figure 28: Unclassified buildings for the case study areas. 49

Figure 29: Mean flood depth maps for the 50-, 100-, and 1000-year return periods. 50

Figure 30: Mean flood depth damage to buildings based on the flood maps for 50-, 100-, and 100-years return periods. 51

Figure 31: Critical infrastructure with 50-, 100-, and 1000-year return periods are depicted. 52

Figure 32: Exposed population for 50-, 100-, and 1000-years return periods. 52

Figure 33: Displaced population for 50-, 100-, and 1000-years return periods. 53

Figure 34: Day of Year Statistics of FWI in EL52 for the period from 1981 to 2010. 55

Figure 35: FWI probability of exceedance based on a Gumbel fitted distribution model together with the estimated probability of exceedance (left). Number of days in the fire season for EL52 (right). 56

Figure 36: Response surfaces of FWI exceedance probability and fire season length under temperature and precipitation changes in EL52. 57

Figure 37: Projected changes in mean dt and dp for RCM under RCP8.5. 59

Figure 38: Spatially aggregated projections of temperature and precipitation change under RCP4.5. 59

Figure 39: EL52 | RCP8.5: Climate-projection distributions overlaid on the $FWI \geq 60$ exceedance response Surface (2030s–2090s). 60

Figure 40: Response probability plot for exceeding FWI threshold in a year for EL52 under RCP 8.5. 60

Figure 41: Ensemble statistics of spatially resolved $FWI \geq 60$ exceedance probability in a year, for 2000-2020s and 2030-2050s decades. 61

Figure 42: Population distribution and projected total population change under SSP4 for EL52. ... 62

Figure 43: Affected Population as a Function of Wildfire Hazard Level ($FWI \geq 60$) under RCP4.5... 62

Figure 44: Affected Population under a High Wildfire Hazard Threshold ($FWI \geq 60, P \geq 30\%$). 63

Figure 45: DEM and Aspect figures for the selected area of Thessaloniki. 65

Figure 46: Figure of the Land Cover map (top), and the original and modified CLC (down). 66

Figure 47: Rasterized historical fires map. The sparsity of the map is related to the number of fire events occurred in the selected area of Thessaloniki in the given period between 2020 and 2024. 67

Figure 48: Wildfire susceptibility and hazard mapping for the RCM under historical climate (1991–2010) and future scenario RCP4.5 (2021–2040; CLMcom_CCLM). (left) Wildfire susceptibility (probability) under future climate: RCP4.5, 2021–2040 (CLMcom_CCLM). (middle) Wildfire hazard classes under historical climate: 1991–2010 (HIST_199110). (right) Wildfire hazard classes under future climate: RCP4.5, 2021–2040 (CLMcom_CCLM). 68

Figure 49: Vulnerability indicators for Thessaloniki (100 m resolution): continuous normalized surfaces and three-class categorical maps (population, economic, ecological). 69

Figure 50: Exposure datasets for Thessaloniki used in the risk analysis, shown as (top) vector layers and (bottom) rasterized previews within the study-area boundary, including point-based assets (hospitals, hotels, schools, shelters) and road network classes (primary, secondary, and tertiary roads). 69

Figure 51: Wildfire risk maps for Thessaloniki under historical (1991–2010) and future (2021–2040, RCP4.5; CLMcom_CCLM) climate conditions, showing categorized risk levels (low, moderate-low, moderate-high, high) for three vulnerability dimensions: population (to (top row), economic (middle row), and ecological (bottom row). 70

List of Tables

Table 1: National and regional datasets and sources related to floods workflow(s). 17

Table 2: National and regional datasets and sources related to wildfire workflow(s).....	18
Table 3: National and regional datasets and sources related to both hazards.	18
Table 4:Data overview for all flood related workflows.	21
Table 5: Summary table of the mutable variables and parameters.	22
Table 6: Catchment details of the selected area.	23
Table 7: Data for selected station as given by the GRDC.....	28
Table 8: Catchment ID characteristics.	28
Table 9: Names and codes for identifying the major rivers in EL9, EL10, and EL11.....	32
Table 10: Maximum damage for reconstruction in €/m ² for the first land use codes.	44
Table 11: Codes with the highest economic damages for Axios Delta and the wider area of the West Side of Thessaloniki.	44
Table 12: Overview of the FWI response model: Assumptions, capabilities, and limitations.	54
Table 13: Workflows' data availability and progress status.	54
Table 14: Table of ranked years for precipitation and temperature perturbations for estimating the maximum return period of FWI (only the first ten (10) values are displayed for demonstration). ...	55
Table 15: Model output values for combined variations in perturbations of dp and dt respectively.	56
Table 16: Risk priority table for the selected hazards for the RCM.....	73
Table 17: Overview key performance indicators.	75
Table 18:Overview milestones.	75

Abbreviations and acronyms

Abbreviation / acronym	Description
AHM	Annual Heat-Moisture Index
CDS	Copernicus Climate Data Store
CLIMAAX	CLIMAtE risk and vulnerability Assessment framework and toolbox
CMIP6	Coupled Model Intercomparison Project Phase 6
CRA	Climate Risk Assessment
CSV	Comma-separated-values file format
DDbelow0	Degree-days below 0°C
DDabove18	Degree-days above 18°C
DEM	Digital Elevation Model
ECMWF	European Centre for Medium-Range Weather Forecasts
ERA5	ECMWF Reanalysis v5
EU-DEM	European Digital Elevation Model
EURO-CORDEX	Coordinated Downscaling Experiment - European Domain
FWI	Fire Weather Index
GeoJSON	Geographic JavaScript Object Notation
GeoTIFF	Geographic Tagged Image File Format
GCM	General Circulation Model
GFDL-ESM2M	Geophysical Fluid Dynamics Laboratory Earth System Model version 2 - Medium resolution
GRDC	Global Runoff Data Center
GRIB	General Regularly-distributed Information in Binary form
gpkg	Geopackage open format
HadGEM2-ES	Hadley Centre Global Environment Model version 2 - Earth System
IPCC	Intergovernmental Panel on Climate Change
IPSL-CM5A-LR	Institut Pierre-Simon Laplace Climate Model version 5A - Low Resolution
JRC	Joint Research Centre
KPI	Key Performance Indicator
LUISA	Land Use-based Integrated Sustainability Assessment
MAP	Annual total precipitation
MAT	Annual mean temperature
MIROC-ESM-CHEM	Model for Interdisciplinary Research on Climate - Earth System Model with Chemistry
ML	Machine Learning
MWMT	Mean warmest month temperature
NorESM1-M	Norwegian Earth System Model version 1 - Medium resolution
NUTS	Nomenclature of territorial units for statistics
PE	probability of exceedance
PPT_at	Mean autumn precipitation
PPT_sm	Mean summer precipitation
PPT_sp	Mean spring precipitation

PPT_wt	Mean spring precipitation
RCM	Region of Central Macedonia
RCP	Representative Concentration Pathways
RP/rp	Return period
shp	Shapefile format
SHM	Summer Heat-Moisture Index
SSPs	Shared Socioeconomic Pathways
Tave_sm	Mean summer temperature
TD	Continentality
Tmax_sm	Maximum summer temperature
WoldPop	World Population
WUI	Wildland Urban Interface

Executive summary

Phase 2 of the CLIMAAX project in the RCM aimed to advance understanding of climate risks for flooding and wildfires through the structured application of four (4) workflows: river flood maps, river flood discharge estimation, FWI (ML), and a Fire Weather Index-based wildfire response model. The primary objective was to establish a robust, reproducible analytical baseline using EU datasets, rather than to deliver a fully regionalized risk assessment at this stage. This approach prepares for deeper regional refinement once locally held data become accessible. For flooding, Phase 2 implemented workflows that translate climate-driven signals into river discharge indicators, and utilized the use of regionally created flooding maps for different rerun periods, enabling comparison of flood hazard patterns under both current and projected climate conditions. For wildfires, the FWI response model was used to assess how variations in temperature and precipitation affect the probability of exceeding critical fire danger thresholds and the duration of the fire season. Additionally, an alternative, data-driven approach using local datasets for RCM was applied for hazard and risk assessment. All workflows were applied consistently at the regional scale to ensure methodological coherence, transparency of assumptions, and alignment with the CLIMAAX Handbook. Concurrently, Phase 2 emphasized data scoping and readiness. Extensive efforts were made to identify, document, and formally request relevant regional and national datasets from competent authorities, including flood hazard and risk maps, forest and burned-area mapping, and population statistics. Although many of these datasets were sourced from local authorities and used for the workflows, some remain theoretically available, but their use within the project remains in a pending status due to administrative and procedural constraints.

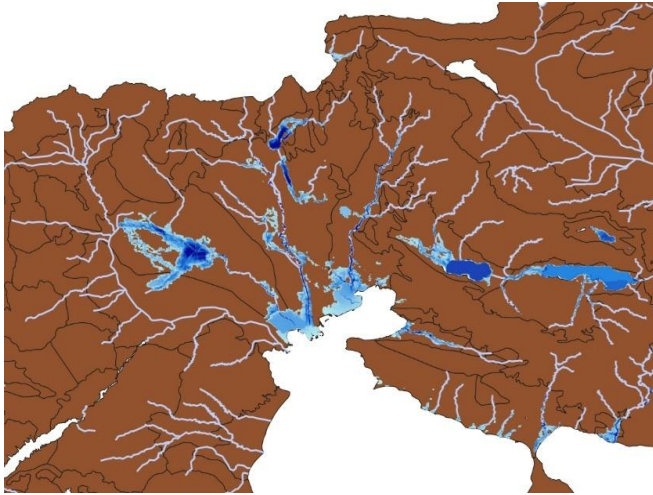
Key lessons from Phase 2 highlight the value of European datasets as a coherent baseline for cross-hazard comparison, while also acknowledging their limitations in spatial detail and local contextual accuracy. The analysis identified areas where regional data would most enhance results, particularly in refining exposure, damage estimation, and decision relevance. Resource allocation was efficient, prioritizing high-impact analytical steps and reuse of CLIMAAX workflows, although this approach necessarily limited the depth of validation. Overall, Phase 2 provides a structured reference point for flood and wildfire risk analysis in RCM, strengthens technical readiness within the regional authority, and positions the project to transition, in subsequent phases, toward fully regionalized, decision-supportive climate risk assessment.

1 Introduction

1.1 Background

RCM serves as a second-level local self-government authority, comprising seven regional units

Figure 1: A schematic depiction of RCM along with selected water bodies across the region.



(Imathia, Thessaloniki, Pella, Kilkis, Pieria, Serres, and Halkidiki) and Civil Protection departments. It serves nearly two million residents. RCM is responsible for governmental functions and implements policies on environmental protection, resilience, climate change adaptation, and disaster and risk management. Additionally, it operates with local authorities, stakeholders, and scientific institutions to develop policies and action plans tailored to regional needs. Figure 1 shows the RCM's coverage area and the borders of each regional unit in the northern part of the country, depicting some representative water bodies. The regional

flood maps provided by governmental bodies, when compared with the original source of flooding maps in the CLIMAAX project, already identify related data gaps and highlight the need for a unified data contribution context that precisely aligns with CLIMAAX's aims.

1.2 Main objectives of the project

Phase 2 aims to enhance the relevance of climate risk assessment in RCM by transitioning from initial scoping to a structured, decision-oriented application of the CLIMAAX framework, utilizing regional sources and data. This phase aims to improve the consistency and usability of risk information for floods and wildfires, the main hazards for RCM for the CLIMAAX project, by using regional data, thereby informing preparedness and adaptation processes, reinforcing readiness to integrate climate risk concerns into regional decision-making for adaptation actions. Employing this framework in Phase 2 would ensure methodological consistency across different hazards and support the ongoing refinement of risk analysis. Incorporating local data further increases the assessment by accurately mirroring regional conditions and priorities, enhancing spatial attributes, and enabling context-specific interpretation of the two (2) hazards (floods and wildfires). Obtaining regional data, especially from a central national source, is not agnostic to layers of bilateral talks and collaboration between departments, even within the same governmental body. This friction, overall, adds an additional layer of workload, especially in cases where regional data are distributed under specific licenses.

1.3 Project team

The contractor's legal representative oversees project management, acting as the formal point of contact with the contracting authority, representing the consortium in contractual and legal matters, monitoring execution, and supervising internal coordination and financial administration. The CDXi team implements the project in collaboration with RCM and is structured around a

Project Manager and a Deputy Project Manager, who coordinate the Expert Team. The Project Manager oversees the overall technical execution of the project, including activity design and implementation, supervision of the work plan, approval of deliverables, and timelines. The Deputy Project Manager assists the Project Manager by coordinating activities, allocating tasks, managing scheduling, and reporting progress. Project team members perform assigned technical tasks, communicate with relevant staff of the contracting authority, participate in meetings, and ensure timely delivery of outputs.

1.4 Outline of the document's structure

This report describes the activities undertaken during Phase 2 of the climate risk assessment in the RCM, with a primary objective of gathering, selecting, modifying, and applying regional and local data within the CLIMAAX workflows. Additionally, the newly added workflows for floods and wildfires using European datasets were executed. The CDXi team, in collaboration with the RCM team, reviewed the methodology, collected and analyzed available materials when possible, and established the basis for technical implementation, applying the methodologies where feasible. The report's structure reflects this sequence.

- Section 2.1 outlines the initial scoping activities, including the definition of assessment objectives, a description of the regional context, and the identification of relevant stakeholders.
- Section 2.2 details the selection and implementation of technical workflows, such as hazard prioritization, and the processing of available regional datasets.
- Section 2.3 presents an overview of climate risks identified through the analysis, as well as initial results, including risk maps, damage estimates, and output interpretation.
- Section 2.4 provides a summary of the preliminary key risk assessment for the RCM.

This deliverable presents the results from the CLIMAAX technical workflows, including the river and coastal floods workflow for river floods (flood maps and flood building damage and population exposure), river flood discharge map, the Fire Weather Index (FWI) response model methodology, and the current database of regional and local data. All outputs are designed to inform further adaptation planning and to provide an initial basis for stakeholder engagement and policy development in the Phase 3 of the project. Each workflow offers a unique theme for engagement in further discussions in Phase 3, without excluding the application of the workflows for even more specific case studies, as provided by the experts.

2 Climate risk assessment – Phase 2

This chapter presents an overview of Phase 2 of the Climate Risk Assessment (CRA) conducted by the RCM as part of the CLIMAAX project. In the initial phase, the main activities focused on clarifying objectives, understanding the regional context, and selecting the most relevant climate-related hazards while applying the CLIMAAX framework using European datasets, in keeping with the hazard selection of Phase 1. Building on this basis, Phase 2 shifted the main focus to the collection of regional (and/or local) datasets. The objective was to systematically map all available governmental bodies, open data portals, and geoportals, identify potential data gaps, and ensure the region had a robust basis for risk assessment. Due to bureaucratic procedures, the application of the regional datasets is still ongoing. However, sets of data were provided from the local authorities and ministries, allowing the realization of a number of workflows.

2.1 Scoping

2.1.1 Objectives

For RCM, the CRA focuses on two (2) hazards of high relevance to the region: flooding and wildfires. Fluvial flooding is assessed using flood maps, flood building damage and exposure, and river discharge indicators. Wildfires are assessed using a response-model approach that links temperature and precipitation changes to FWI exceedance, and an FWI index based on an ML (Machine Learning) approach. The purpose of the assessment is to translate climate change signals into comparable, hazard-specific risk information. Regional authorities can use these findings to support planning, preparedness, and adaptation dialogues. Expected outcomes include improved understanding of future hazard trajectories and their uncertainties across climate scenarios. The assessment also identifies the relative importance of these hazards over time, which will be the main aim of Phase 3. CRA outputs provide a technical reference to support regional planning, flood risk management discussions, wildfire preparedness strategies, and the integration of climate risk considerations into regional development and adaptation policies, in collaboration with local civil protection units and fire departments. The scope of CRA Phase 2 is constrained by the availability and accessibility of regional data. Regionally relevant datasets for flooding maps, river discharge, wildfire-related factors, exposure, and vulnerability were identified and requested. However, access to some datasets within the Phase 2 timeframe is still pending due to administrative and procedural constraints. Consequently, the assessment was implemented using both regional and European-scale climate datasets for the CLIMAAX workflows, including the newly added workflows. These challenges were addressed by explicitly defining the CRA as a strategic assessment, clearly documenting (when possible) assumptions and uncertainties, and maintaining coordination with institutional stakeholders to prepare the ground for regionalization of outputs.

2.1.2 Context

The Phase 2 outputs for flooding and wildfires can be placed directly under the RCM monitoring logic by treating them as (i) climate-indicator tracking inputs and (ii) risk-relevant evidence for evaluating actions. For floods, the river discharge indicators/projections provide a climate-related time series that can be monitored alongside other related indices to describe how the flood-generating potential of river systems evolves across scenarios, in collaboration with the

decentralized administration and its flood-related departments². These outputs can feed the RCM's strategic decisions as a hazard-relevant indicator set, and they can also be used in thematic mapping to support the network of data collection function of the geoportals (for floods and wildfires, respectively) by standardizing regional flood-relevant layers for repeated updates. For wildfires, the FWI response model outputs (probability of exceeding an FWI threshold, its evolution by decade/scenario, and spatial ensemble statistics) align even more explicitly with regional awareness and emphasis on tracking extremes, because they translate projected temperature/precipitation change into a consistent wildfire-danger indicator that can be monitored over time, mapped, and reported. These belong to climate-indicator monitoring and also support result indicators by providing a reference baseline against which prevention and preparedness measures (e.g., forest management and fire-prevention actions) can be reviewed over successive reporting cycles. Taken together, discharge-based flood indicators and FWI-based wildfire indicators provide a practical, transferable set of monitoring layers for a data network and indicator system capable of producing progress reports and thematic maps, while remaining compatible with future enhancements as regional datasets become available for validation and operational use. The importance of river and coastal flooding was already described in the Phase 1 deliverable, where flood maps were used for the calculation of the fluvial flooding hazard in the RCM based on river flood depth maps for different return periods, covering both high- and coarse-resolution datasets both for modeled (source: [JRC](#)) and future (source: [Aqueduct Floods](#)) river flood hazard maps. While in the first deliverable a general idea about the potential hazards was given for each sub-region, for the example case of Thessaloniki, and for the whole region, in Phase 2, due to the volume and restrictions of data, dedicated areas were identified following a plan for creating representative case studies that will serve as generators for further cases. Thus, the aim will shift further from grasping a rather wide area and will focus on toy model cases.

2.1.3 Participation and risk ownership

In Phase 2 of the CLIMAAX project, stakeholder involvement focused on targeted institutional coordination and data gathering rather than broad participatory engagement. Engagement was carried out through structured discussions within the RCM and bilateral exchanges with qualified public authorities responsible for flood and wildfire management. These interactions aimed to align the scope of the climate risk assessment with existing regional responsibilities, operational practices, and data availability, rather than to validate results or co-produce outputs. The main stakeholders involved and willing to participate in CLIMAAX-related meetings included the local units of Civil Protection, the regional Fire Service authorities, and the flood management department of the Decentralized Administration of Macedonia and Thrace. Engagement took place through one in-person coordination meetings and follow-up exchanges by email and technical communication. These actors expressed interest in CLIMAAX's objectives, supported data collection efforts where possible, and indicated their willingness to remain involved in subsequent phases, particularly when results could inform operational planning and preparedness. However, it is important to acknowledge that there is currently no agreed regional risk threshold, which introduces significant decision uncertainty. Stakeholder feedback during Phase 2 mainly concerned the potential usefulness of CLIMAAX outputs for future planning, the need for clearer, hazard-specific indicators, and the importance of aligning results with existing flood risk

² See for example here: [Main ProbstasiaYdaton – ΑΠΟΚΕΝΤΡΩΜΕΝΗ ΔΙΟΙΚΗΣΗ ΜΑΚΕΔΟΝΙΑΣ ΘΡΑΚΗΣ](#).

management and Civil Protection frameworks. Difficulties encountered were related to data availability and administrative procedures, including delays in accessing regional datasets and limitations in data sharing across public authorities, even where data were nominally open but not available in usable formats. Additionally, frequent updates to local portals, resulted in a non-unified data access procedure. Risk ownership in the region is currently organized under the regional Civil Protection and sectoral governance framework. Responsibility for identifying, assessing, and mitigating flood and wildfire risks lies with the RCM. At this stage, no specific stakeholder groups representing vulnerable populations or exposed communities were directly engaged in Phase 2, and no formally defined regional thresholds for acceptable or tolerable risk are documented. These aspects are recognized as gaps and are expected to be addressed progressively through the informed discussions in Phase 3.

2.1.4 Application of principles

Phase 2 involves CLIMAAX principles through clear methodological and procedural decisions. It preaches social justice, equity, and inclusivity by explicitly considering vulnerability, especially in flood- and fire-related impacts and in focus groups. Quality and transparency were maintained through even workflow logic, straightforward information about the datasets and for each hazard, and traceable inputs and outputs to support review and updates.

2.1.5 Stakeholder engagement

Stakeholder engagement during Phase 2 focused on direct coordination with institutional bodies responsible for climate risk management and emergency response in the RCM. Engagement was carried out via organized discussions, of any format, with the RCM project team and representatives of key public authorities, including the Decentralized Administration of Macedonia and Thrace, the Ministry of Environment, Civil Protection authorities, and senior leadership of the Fire Service at the regional level, including the Head of the Fire Station responsible for the wider region (see also an example in the Appendix). These stakeholders were selected due to their high-level responsibilities in planning, operational coordination, risk management, and emergency response for floods and wildfires, respectively. Engagement activities included an in-person meeting at RCM headquarters, followed by regular email communication. In these, project objectives, Phase 2 scope, and key methodological choices were outlined, emphasizing the CLIMAAX framework and faster methods of collecting regional data. Information was presented clearly, focusing on its use in CLIMAAX workflows. The project received strong interest from participating stakeholders. Senior representatives expressed clear expectations regarding the assessment results and demonstrated active support for the project, particularly by assisting with all necessary bureaucratic issues related to accessing relevant regional datasets and by advising on institutional processes. Stakeholders also indicated strong interest in continued participation during Phase 3, with the intention of exploring how CLIMAAX outputs could be incorporated into tactical plans, preparedness planning, and risk management procedures. Feedback from stakeholders confirmed the project's relevance to regional climate risk governance and also highlighted limitations in data access, potential data gaps, and administrative procedures. Although efforts were made to support data provision and, where possible, accelerate internal processes, formal data-sharing requirements slowed integration. The main difficulties encountered related to the availability, circulation, and usability of data across public authorities, including

cases where formally open datasets were not provided in directly usable formats (for example, there was no straightforward access to *geotiff* format documents for flood scenarios). In spite of these constraints, Phase 2 engagement strengthened institutional coordination and established a solid basis for continued collaboration and data integration in the next phases of the project.

2.2 Risk Exploration

2.2.1 Screen risks (selection of main hazards)

RCM is increasingly exposed to climate-related hazards that pose significant risks to infrastructure, economic activities, and public safety. Based on the initial screening carried out in Phase 1 and refined in Phase 2, in line with the CLIMAAX methodology, the primary hazards relevant to the regional context remain river and coastal flooding and wildfires. No new hazard categories were introduced at this stage; however, the screening has been strengthened through the application of two (2) hazard-specific workflows and the systematic use of national and regional datasets provided by public authorities. River flooding continues to pose a major hazard, particularly in the region's main river basins. Low-lying floodplains are highly sensitive to intense precipitation events and peak river discharges. Recurrent flooding affects agricultural land, residential areas, road networks, and critical infrastructure, leading to economic losses and long-term disruption. Communities in flood-prone rural areas, especially those with limited structural protection, are particularly vulnerable. In Phase 2, this hazard screening was refined using a flood-discharge-oriented workflow. Additionally, wildfires remain a recurrent and escalating hazard in RCM, particularly during the dry summer season. Elevated temperatures, increased heatwave frequency, increased humidity, and the accumulation of flammable biomass from land abandonment significantly increase fire danger. In Phase 2, wildfire screening was advanced through the implementation of an FWI-based response workflow, allowing fire danger to be evaluated as a function of projected temperature and precipitation changes. This approach enables a consistent assessment of both current and future wildfire conditions and supports the identification of periods and areas with heightened fire risk. Across all hazards, the screening step explicitly integrates data from regional, and national authorities, including flood hazard maps, river discharge information, forest and burned-area mapping, land use data, and population statistics. The screening currently relies on hazard-oriented and preparatory outputs, while the full quantitative coupling of regional datasets within the selected CLIMAAX workflows will be undertaken in subsequent analysis steps, once all national and regional data inputs are fully available.

Table 1: National and regional datasets and sources related to floods workflow(s).

Dataset	Data type	Authority
River flood maps	Geotiff	YPEKA
River flood maps – future scenarios	Geotiff	YPEKA
River water systems	Geotiff	YPEKA
Vegetation and Land use	Geotiff	YPEKA
Protected areas	Geotiff	YPEKA

Historical flood events	Geotiff	YPEKA
Areas of potential flood events	Geotiff	YPEKA
Flood hazard areas – Low and high probability scenario	Geotiff	YPEKA
Flood risk zones – Low, medium, and high probability scenario	Geotiff	YPEKA
Flood risk zones	Geotiff	YPEKA
Coastal water systems	Geotiff	Decentralized Government
(Daily) River runoff time series	Netcdf	YPEKA
Sub-watersheds/-catchments ³	shp	Decentralized Government
Flood depth maps	Netcdf	Civil protection
Water level time series (and statistical indicators)	Netcdf	HNMS

Table 2: National and regional datasets and sources related to wildfire workflow(s).

Dataset	Data type	Authority
Burnt Forest Areas	Geotiff	gOFI
Cartographic data (Fire)	Geotiff	gOFI
Posted forest maps	Geotiff	Greek Cadastre⁴
Total burned areas of all types	Geotiff	FMRS
Fuel type mapping	Geotiff	FMRS

Table 3: National and regional datasets and sources related to both hazards.

Dataset	Data type	Authority
Digital cartographic base maps at 1:5,000 scale (Population and Housing Census 2021)	Geotiff	ELSTAT
Population and population density of Kallikratis municipalities (Population Census 2021, ELSTAT)	Geotiff	ELSTAT/YPEKA
Digital Elevation Model (DEM) from the LSO project (5 m resolution)	Geotiff/Netcdf	Greek Cadastre

Primary hazard data - Floods

National flood hazard geoportal (YPEN Geoportal⁵): The Ministry of Environmental and Energy offers a platform that has a key role as a state-mandated repository for the majority of the official

³ See also: [Γεωπύλη – Σχέδια Διαχείρισης ΔΑΠ](#)

⁴ See also: [Ψηφιακός Χάρτης Κτηματολογίου](#)

flood mapping in Greece. It hosts legally defined flood hazard and flood risk maps for high-, medium-, and low-probability scenarios (e.g., 50-, 100-, and 1000-year Return Periods (RPs)). Critically, it includes future projections under different climate pathways. CLIMAAX role: This is the definitive source for the physical flood threat. It provides the spatial data on where, how deep, and how likely flooding occurs today and under future climates. This forms the "hazard" layer for all subsequent exposure and risk analysis within the CLIMAAX framework.

Flood risk management plans: This category includes formal documents such as the "Flood Risk Management Plan for Central Macedonia" and the "Strategic Environmental Impact Assessment for Central Macedonia"⁶. They serve a binary role as reports and as data-rich containers. They include geospatial annexes with thematic maps (land use, soil, geology), methodological descriptions for hazard modeling, and crucially, economic parameters. However, not all data are in usable formats, or the initial sources are not accessible. CLIMAAX role: These documents provide the essential context and calibration for hazard data. They provide a historical baseline for model validation and the methodological transparency required for EU compliance to translate flood water depth into economic loss, thereby moving the assessment from "hazard" to quantified "risk."

INSPIRE Geospatial data catalogues⁷: This refers to Greece's national implementation of the EU INSPIRE Directive, which mandates standardized, interoperable geospatial data services. It provides foundational layers, such as administrative boundaries, hydrographic networks (rivers and lakes), and protected sites, via standard web services (primarily WMS, and occasionally WFS). CLIMAAX role: This is the interoperability backbone. It might offer reference data from Greece that can be ingested and combined with data from other EU sources within the CLIMAAX toolbox.

Primary hazard data - Wildfires

Official forest service and fire mapping data: This hub includes the Burned Area Mapping Service, which delineates wildfire perimeters annually. It also maintains the validated, legal Forest Maps that define forested land tenure and type, as well as aggregated statistics on total burned area. CLIMAAX role: This data provides the historical validity for wildfires. Burned-area perimeters can be used as an extra layer to the FWI workflow. The official forest maps could also be a key dataset for defining the Wildland-Urban Interface (WUI).

Academic and research consortium data: Led by specialized laboratories at the Aristotle University of Thessaloniki, such as the Laboratory of Forest Management and Remote Sensing⁸, this hub generates advanced, high-resolution data. Its core output is detailed Fuel Type and Load Maps that classify vegetation by flammability and energy content. CLIMAAX role: Fuel maps could be used as an additional layer to the FWI workflows(s) to generate fire hazard maps, or can be used in CLIMAAX workflows as layers to the given EU datasets for FWI.

Exposure and vulnerability data

Socio-economic and demographic data: The primary source is the Hellenic Statistical Authority (ELSTAT⁹), specifically the 2021 population-housing census data, which provides population counts and density at the municipal level. This is complemented by geospatial backgrounds from

⁵ See also INSPIRE related link.

⁶ See also: pkm.gov.gr/perifereiaiko-sxedio-prosarmogis-sti/sympε-πεοσπκα-πικμ/

⁷ geoportal.ypen.gr/geonetwork/srv/gre/catalog.search#/home

⁸ See also FMRS and gOFFI links in Table 2.

⁹ See also links in Table 2.

the Ministry of Environment's portal, which enable the precise georeferencing of this demographic data. CLIMAAX role: This defines the "people" component of exposure. By spatially joining this population data with hazard layers, this approach has the potential to support CLIMAAX in calculating the metric of the extent of exposure of individuals and households to a climate threat, transforming a natural hazard map into a risk map.

Terrain data: The authoritative source for terrain data is the national 5-meter resolution Digital Elevation Model (DEM) produced by the Hellenic Cadaster. For granular asset data, local portals, such as the Municipality of Thessaloniki's, provide vector datasets of buildings, roads, and critical infrastructure. CLIMAAX role: The LSO DEM could be used as a layer for all flood-related workflows.

Contextual vulnerability data: This data is often embedded within the broader planning documents, such as the thematic maps in Flood Risk Management Plans. A key dataset is the map of Protected Areas, including Natura 2000 sites and national parks, which identifies zones of high ecological value and sensitivity. CLIMAAX role: This data might add additional input to the "susceptibility" dimension of the risk equation. It allows CLIMAAX to weigh the consequences of a hazard. For example, a flood in an industrial zone versus in a protected wetland has different types of risk. Identifying vulnerable ecosystems or socially vulnerable communities (via demographic cross-analysis) enables the risk assessment to prioritize areas with the most severe or irreversible impacts.

Data integration: the practical application within CLIMAAX creates a logical pipeline from data to decision. For floods, models using the regional DEM and official rainfall curves generate inundation maps, hazard layers, and future RCP scenarios. For fires, fuel maps from gOFFI drive provide additional exposure layers. These layers can be computationally overlaid with population data from ELSTAT rather than WorldPop¹⁰ and with asset inventories from local portals to calculate exposure. This profile provides the evidence base for prioritizing actions in regional adaptation strategies and investing in mitigation measures.

2.2.2 Choose Scenario

Climate conditions were determined based on the CLIMAAX Framework and regional planning practices. Concentration pathways were selected, mainly a stabilization and a high-emissions scenario. These scenarios represent a possible range of future conditions relevant to river flood discharges and wildfire danger. Hazard indicators were generated and subsequently linked to current and projected population distributions to produce exposure risk outputs. This approach was applied explicitly to wildfire risk by combining FWI exceedance probabilities with population data to estimate the affected population over time. For flood risk, the analysis emphasized changes in hazard intensity and spatial extent under future climate scenarios. The analysis included multiple time horizons consistent with regional, national, and European planning processes. In the RCM, scenario premises project an intensification of wildfire risk, driven by rising average and extreme temperatures (without excluding prolonged drought periods). These trends are especially relevant during the fire season, as FWI projections indicate more frequent and extended exceedances of high-risk thresholds. In the short term, hazard conditions support the need to strengthen fire prevention measures and monitoring systems in WUI areas. Medium-term

¹⁰ [WorldPop](#)

scenarios suggest an extended fire season and an increase in extreme fire-danger days, while long-term high-emissions scenarios indicate a potential expansion of fire-prone zones into areas previously unexposed. These projections enable the labeling of changes in fire seasonality, frequency, and spatial patterns, providing a rigid basis for informed spatial planning and for evaluating fire mitigation strategies across regional areas.

2.3 Regionalized Risk Analysis

River flood risk was calculated through the implementation of a discharge-based hazard workflow (river discharge signals), while wildfire risk was assessed using the FWI response-surface model driven by projected temperature and precipitation changes (probability of exceeding an FWI threshold). Both workflows were implemented using EU datasets to ensure consistency across scenarios. In parallel, regional and local datasets were identified, collected and requested from competent authorities. Exposure was addressed for wildfires through population-based metrics using future socio-economic projections, and via an FWI ML workflow. New outputs include response-model-based wildfire hazard indicators and affected-population curves, as well as scenario-comparable flood discharge indicators. Indirect impacts were not explicitly quantified. Dataset limitations primarily relate to spatial detail and the absence of locally calibrated exposure and vulnerability data, as documented in the accompanying tables and to be addressed in later phases.

2.3.1 Hazard #1 - Floods

Based on the update data of the latest version of the CLIMAAX workflow, for the river and coastal floods workflow, the additional “River floods (discharges)” pipeline was selected to be included aiming for using both datasets from European and regional entities. In the table below, a summation list of the workflows for the river and coastal floods can be seen.

Table 4: Data overview for all flood related workflows.

Workflow	EU data	Deliverable/Progress	Regional data	Deliverable/Progress
River floods (flood maps)	Obtained	1/Achieved	Obtained	2/Achieved
River floods (discharges)	Obtained	1/Not available	Not available	2/Achieved
Coastal floods	Obtained	1/Achieved	Not available	2/Not available
Flood building damage and population exposed	Obtained	1/Achieved	Obtained	2/Achieved

2.3.1.1 River floods (discharges) – European data

This workflow uses the dataset of European-wide hydrological climate impact indicators (provided by SMHI¹¹ and the CDS), allowing for accessing the projected changes in river discharges due to climate change, using two types of data: (i) gridded (E-HYPEgrid model¹²) and catchment-level (E-HYPEcatch model). The following variables are used in this workflow: (i) catchment-level data, (ii) daily timeseries of river discharges for a historical period, (iii) monthly-means of river discharges, (iv) extreme river discharges for different return periods and their relative changes for different climate models, scenarios (RCP2.6, RCP4.5 and RCP8.5) and timeframes (2011-2040, 2041-2070, and 2071-2100). Relative change of extreme river discharges is available for 2, 5, 10, and 50-year return periods.

2.3.1.1.1 Hazard assessment

Obtaining data

Catchment-level river discharge data were obtained from the E-HYPEcatch models using a consistent retrieval workflow that encompasses all available model realizations. Historical daily discharge time series for 1991-2005 were collected to derive representative long-term statistics, while historical monthly mean discharges for 1971-2000 were acquired to assess longer-term river discharge statistics under historical climate conditions. Monthly mean river discharges were also obtained for the future periods (2011-2040, 2041-2070, and 2071-2100), under RCP4.5 and RCP8.5 scenarios, iterating across the selected GCM-RCMs (General Circulation Models-Representative Concentration Pathways) pairs, ensemble member combinations, and specified hydrological models. Additionally, extreme river discharge indicators for the 10-year and 50-year return periods were retrieved for both the historical climate and the same future periods, provided as absolute values and as relative changes from the reference period.

River flooding using river discharge statistics

The following table shows a summary of the data, variables, and other related information used to run this workflow:

Table 5: Summary table of the mutable variables and parameters.

Variables	Values/Description
<i>loc_name</i>	RCM
<i>loc</i>	22.8911, 40.6344
Catchment ID in the E-HYPEcatch dataset	9729471
Daily river discharges	<i>ds_day</i>
Mean river discharges	<i>ds_mon</i>
Absolute extreme river discharges	<i>ds_flood</i>
Relative extreme river discharges	<i>ds_flood_rel</i>
Daily discharge timeseries	<i>ds_day_sel</i>

¹¹ <https://www.smhi.se/>

¹² <https://confluence.ecmwf.int/pages/viewpage.action?pagelId=283570322>

Sub-basins

`data_folder_subbasins`

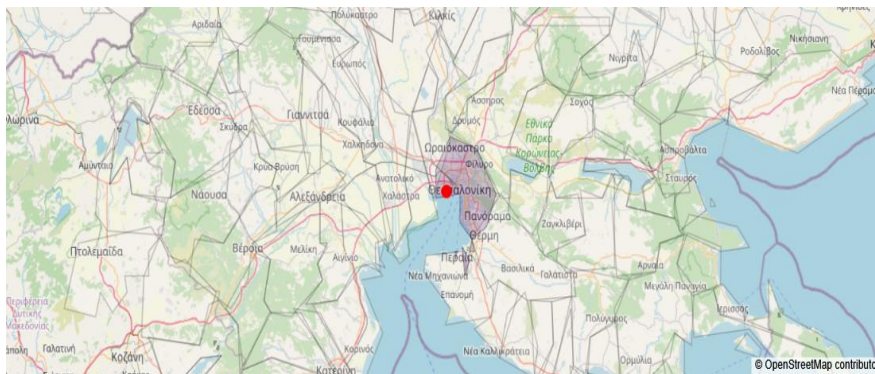
For the catchment of interest, the GeoDataFrame will provide the following table:

Table 6: Catchment details of the selected area.

	SUBID	HAROID	Geometry
SUBID			
9729471	9729471.0	9729471.0	MULTIPOLYGON (((22.92917 40.49583, 22.92084 40...

For this workflow, the example will demonstrate the applicability and transferability of the CLIMAAX methodology by focusing on a part of the Metropolitan area of Thessaloniki where the region's largest population resides. If needed, the workflow can be easily modified by adjusting the initially selected coordinates at the beginning, which results in a different catchment ID and geometry geodata frame.

Figure 2: Selected area for the example application of the workflow.



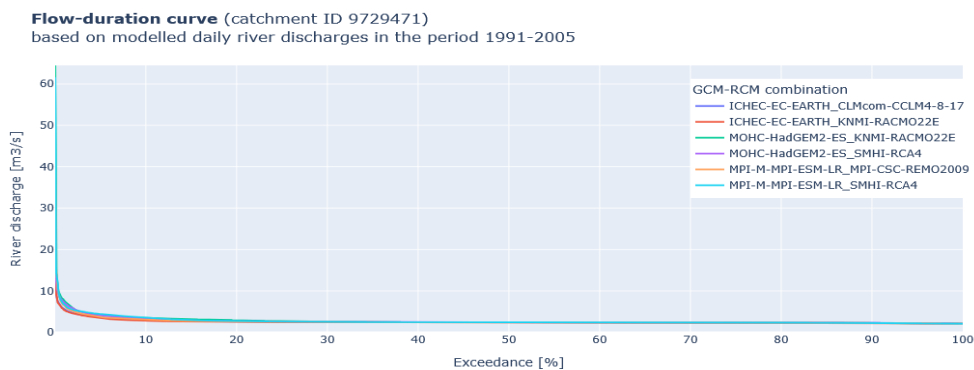
Daily historical river discharge timeseries are first subset to the selected catchment (`ds_day_sel`), computed, and saved for reuse. In the first figure, the dataset is plotted (default 2001-2005 vs. full 1991-2005 period) with separate panels for each GCM-RCM pairs and multiple lines per panel for different catchment models, illustrating variability and model-related uncertainty. Since these climate model runs are not constrained by real-world observations, the daily series are used to compare patterns across model combinations rather than individual past events. In the second figure, daily discharges are averaged across catchment models to produce a single timeseries per GCM-RCM pairs, which is plotted to support a clearer comparison between climate model simulations. In Figure 3, where the daily discharges are modelled against observations, it is shown that the observed GRDC discharge series is smoother and lower in magnitude, while the GCM-RCM simulations display sharper peaks and higher extremes. It is likely that the models do not reproduce individual historical events but instead represent plausible climate realizations. The wide spread between modelled series might indicate differences between GCM-RCM pairs. In Figure 3, which shows separate panels by GCM-RCM and multiple catchment models, it is shown that within each GCM-RCM panel, the different catchment model realizations follow very similar trajectories, whereas clear differences appear between panels. This confirms that uncertainty in daily discharge behavior is dominated by the choice of GCM-RCM pair, with hydrological model differences mainly affecting fine-scale.

Figure 3: Daily timeseries of river discharges (m³/s) based on six (6) different GCM-RCM climate model combinations for the period 1991-2006.



Further, daily river discharge values were processed to derive a flow-duration curve for modelled datasets. The calculation was based on ranking daily discharges in descending order and expressing each value as an exceedance probability over the analyzed period (which falls into the range between 1991 and up to 2005). The resulting flow-duration curves were used to assess how well the models represent both typical discharge conditions and high-flow events, taking into account the limited temporal coverage of the observational record.

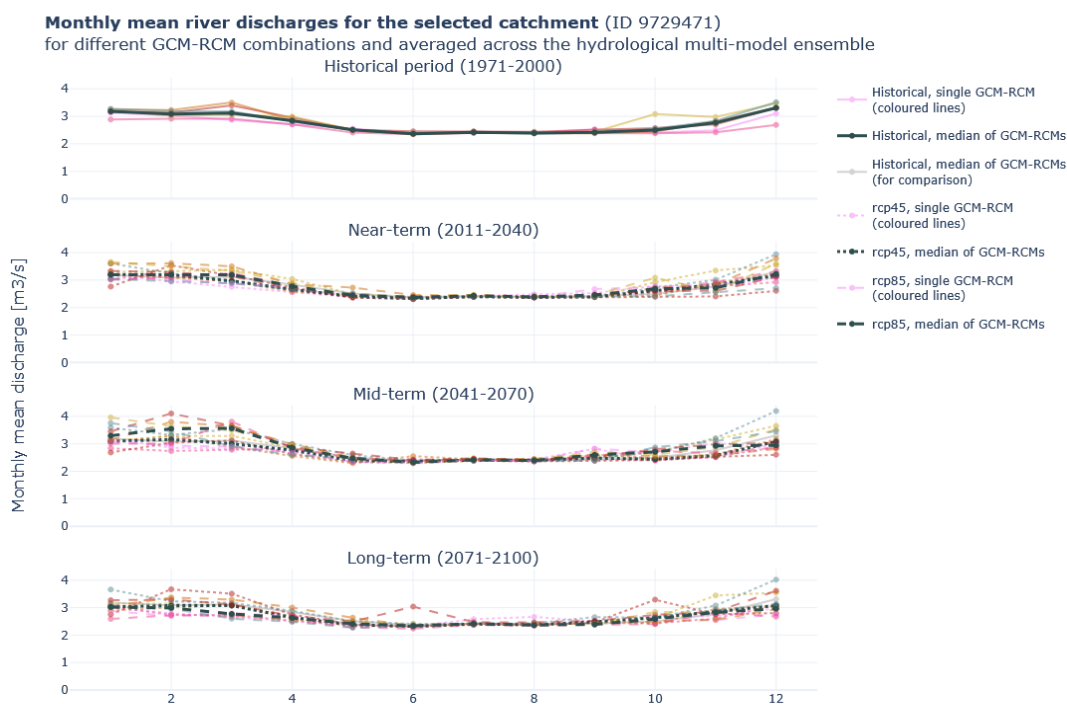
Figure 4: Flow-duration curve based on six (6) different GCM-RCM climate model combinations for the period 1991-2006.



The flow-duration curve indicates that modelled discharges are broadly of the same order of magnitude, showing that the models are able to represent high-flow conditions at a comparable

scale. However, GCM-RCM pairs produce higher extremes than observed, pointing to differences in the upper tail of the discharge distribution (below ~5-10%, steep curve). At moderate and high exceedance levels, the shape of the modelled curves is generally similar to the observed curve, suggesting a reasonable representation of background and seasonal flows. The divergence, combined with the limited observational time coverage, highlights uncertainty in the simulation of extremes rather than a complete mismatch in discharge behavior. Following the analysis of daily discharge variability and extremes, the next step focuses on seasonal behavior by examining monthly mean river discharges. Aggregating daily values to monthly means allows assessment of how the annual discharge cycle changes across climate scenarios and future time periods, highlighting potential shifts in seasonality rather than individual events.

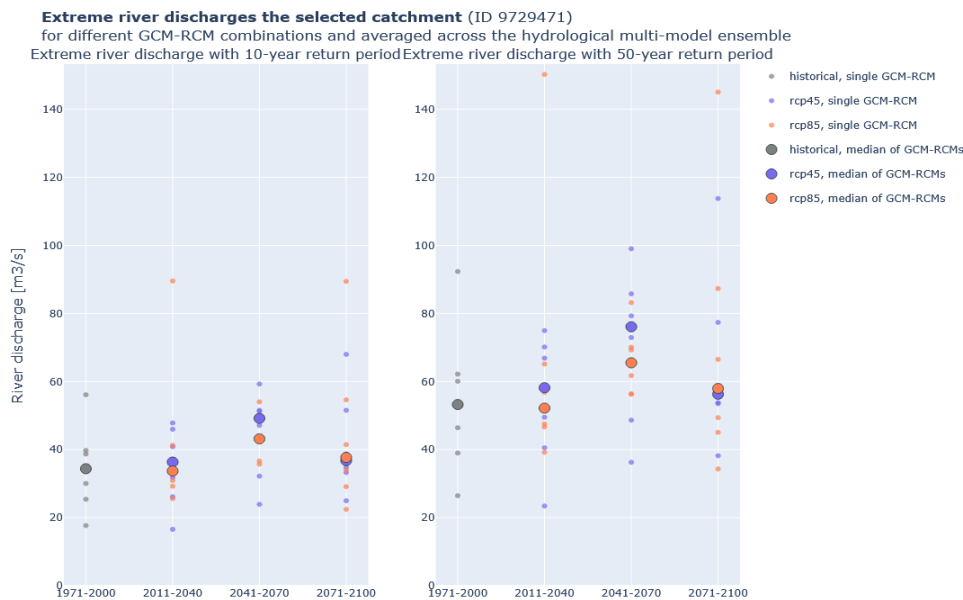
Figure 5: Monthly mean river discharges (m³/s) for the selected catchment ID for historical GCM-RCM, scenarios, and time periods.



Based on a qualitative visual comparison of the monthly mean discharge curves, the figure suggests a tendency towards slightly wetter conditions in future periods, particularly under mid- and long-term scenarios, although this pattern is not uniform across all months and varies between GCM-RCM pairs. The most noticeable differences relative to the historical period appear during late autumn and winter, where future median curves are generally positioned above the historical median, while summer months show comparatively small changes and remain closely clustered. Peak monthly discharges, which in the historical period occur mainly in late winter to early spring, appear less sharply defined in future scenarios and in some cases show a modest shift in timing, with increased winter contributions. These observations are based on relative differences in curve shape and position rather than on quantitative thresholds, and are intended to highlight broad seasonal tendencies rather than precise numerical changes.

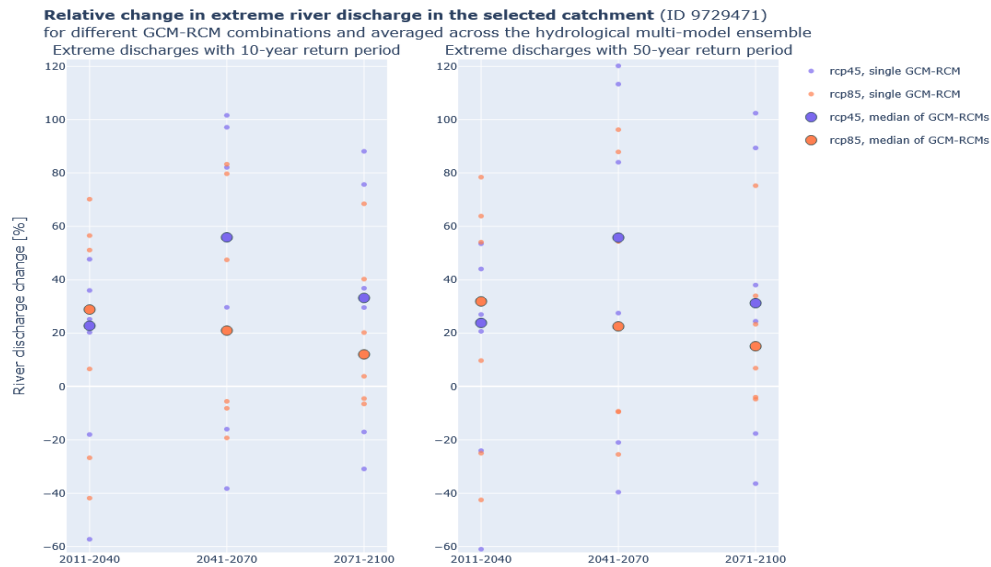
Following the assessment of seasonal changes in mean river discharge, the next step examines changes in extreme river discharges using estimated (10- and 50-year) return period flows. These indicators provide an exploratory view of how flood-related extremes may evolve under different climate scenarios and time horizons, with results shown as individual GCM-RCM pair values, and their ensemble medians.

Figure 6: Extreme River discharges (m³/s) for the selected catchment ID for different GCM-RCM and scenarios combinations for 10-year and 50-year return periods.



Based on a qualitative visual comparison of the plotted median points across time periods, median extreme discharges generally increase from the historical period towards the near- and mid-term, with no clear monotonic trend extending uniformly into the long term, indicating that changes in extremes are not strictly linear over time. Uncertainty across climate models is substantial in both the medium and long term, as shown by the wide vertical spread of individual GCM-RCM points around the median for each period, particularly for the 50-year return period. This spread appears comparable for RCP4.5 and RCP8.5; RCP8.5 tends to include higher upper-range values, suggesting a slightly broader range of possible extremes rather than a consistently larger median response. Differences between scenarios' medians are present indicating that model choice contributes more to uncertainty in projected extreme discharges than the difference between the two emission scenarios at the catchment scale considered. Finally, Figure 7 presents the relative changes in extreme river discharges for the 10- and 50-year return periods, expressed with respect to the historical reference period. Focusing on relative changes allows for a consistent comparison across climate model combinations while reducing the influence of systematic biases in absolute discharge magnitudes. The figure illustrates how the magnitude and direction of changes in flood-related extremes vary across emission scenarios and future time horizons.

Figure 7: Relative change in extreme river discharges for the selected catchment ID for different GCM-RCM and selected scenarios combinations and for 10-year and 50-year return periods.



When considering only the ensemble median values across climate models, the relative changes in extreme river discharges suggest a general tendency towards increasing extremes in the medium- and long-term periods for both the 10- and 50-year return levels. Differences between RCP4.5 and RCP8.5 median values are present but relatively small, with RCP8.5 occasionally indicating slightly larger increases, particularly for the 50-year return period. The uncertainty range across climate models is large, as shown by the wide spread of individual GCM-RCM projections around the median, comprising both positive and negative relative changes. The largest outliers do not consistently correspond to the same GCM-RCM combination across periods or return levels, indicating that inter-model variability is substantial and that no single climate model dominates the extreme-response behavior.

River flooding using river discharge statistics: validation with observations

Observed river discharge data used for model evaluation are obtained from the Global Runoff Data Centre (GRDC), which provides freely accessible daily discharge time series from gauging stations worldwide. The GRDC dataset is accessed through the official GRDC data portal, and the relevant station is selected and downloaded in standardized GRDC export format. After download, the daily discharge file is identified by its unique station number, which is subsequently used within the workflow to locate the data, extract station metadata, and enable direct comparison with modelled river discharge outputs for the corresponding catchment. It is worth to mention that for the GRDC stations located in Greece, the availability of observational discharge data is more limited compared to other European countries. In cases, continuous daily discharge records are missing or incomplete, and not all stations provide both daily and monthly statistics over sufficiently long and overlapping periods. This restricts the direct comparison of modelled and observed discharge characteristics, particularly for analyses that require long daily time series or consistent daily/monthly aggregation.

Table 7: Data for selected station as given by the GRDC.



Data description	Value
Catchment area	9729471.0
Coordinates	latitude 40.85° N, longitude 22.15° E
grdc_nr	6262310
Catchment ID in the E-HYPEcatch dataset	9000493

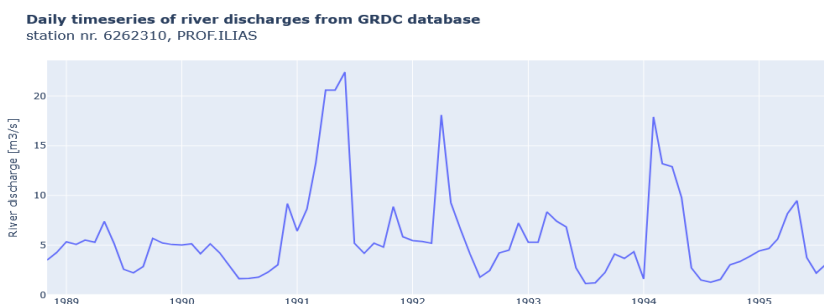
For the catchment of interest, the GeoDataFrame will provide the following table:

Table 8: Catchment ID characteristics.

	SUBID	HAROID	Geometry
SUBID			
9000493	9000493.0	9000773.0	POLYGON ((22.17084 40.92083, 22.17084 40.85417...

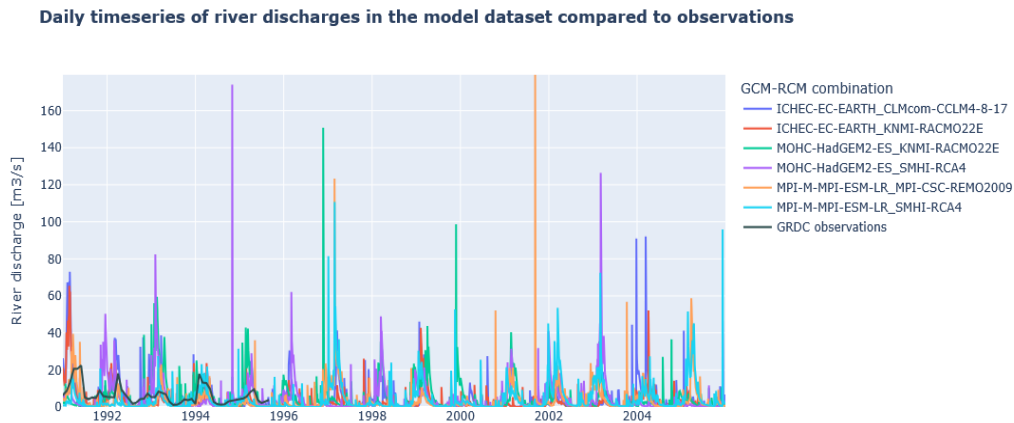
An example is the GRDC station “*PROF. ILIAS*” on the Moglenitsas river in Greece for which monthly discharge observations are available only from 1988 onwards, while daily records are not consistently available. Such data gaps need to be accounted for when interpreting model-observation comparisons in Greece and underline the heterogeneous availability of hydrological observations across Europe. Timeseries data are visualized in Figure 8 below.

Figure 8: Timeseries of river discharges taken from GRDC 6262310 data.



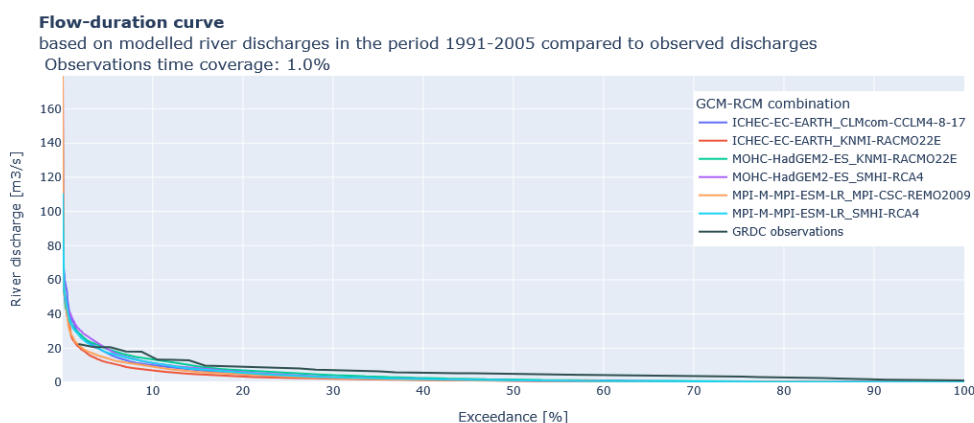
River discharges are compared in Figure 9 showing simulated discharge time series together with GRDC measurements for the selected catchment over the period 1991-2005. The modelled discharges correspond to averages across the hydrological catchment models and are displayed separately for each GCM-RCM pair, while the GRDC record serves as a reference. Clear differences in magnitude, variability, and temporal evolution are visible between the simulations and observations, indicating that the climate model outputs represent plausible realizations of discharge variability rather than reproducing the timing of individual historical events. Accordingly, the figure supports evaluation of discharge ranges and overall variability, rather than event-scale agreement between modelled and observed flows.

Figure 9: Modelled discharge timeseries based on six (6) GCM-RCM climate model combinations as well as the values from the observational dataset from GRDC 6262310.



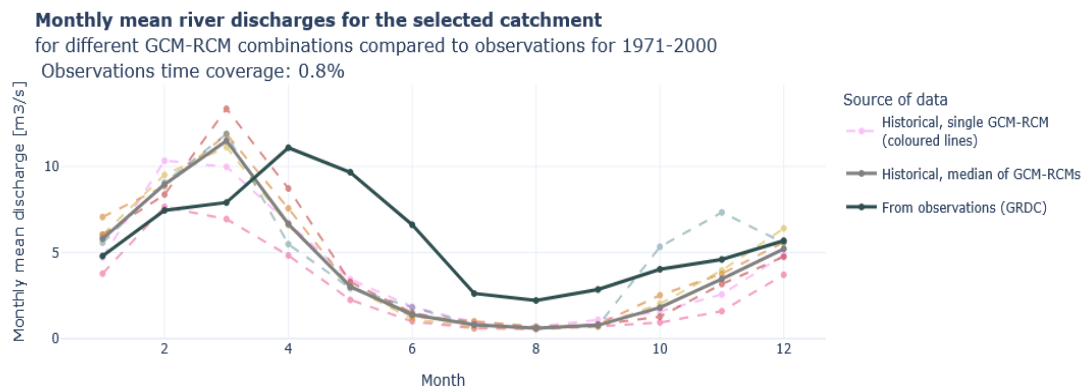
To further evaluate the consistency of the output for river discharges, distribution-based and seasonal diagnostics are examined. These complementary views allow assessment of how well the model ensemble represents the overall discharge distribution and the timing of the seasonal cycle, providing insight into differences in magnitude, and seasonal structure between simulations and observations. The flow-duration curve (daily discharges, 1991-2005; see Figure 10) presents the flow-duration curve derived from river discharge values, comparing the modelled discharge distributions (shown separately for each GCM-RCM pair) with GRDC observations for the same catchment. For consistency, the observational series is clipped to the exact model period (1991-2005), resulting in 5,479 daily values, and the observation time coverage over this period is calculated as 100%. The flow-duration curves are computed by ranking discharges from highest to lowest and expressing them against exceedance probability.

Figure 10: Flow-duration curve based on modelled river discharges for six (6) GCM-RCM combinations for the GRDC 6262310.



The monthly mean seasonal cycle (historical period 1971-2000) figure (see Figure 11) compares the seasonal pattern of river discharge using monthly mean values for the historical reference period (1971-2000). Modelled monthly means are first averaged across hydrological catchment models and then plotted for each GCM-RCM combination.

Figure 11: Mean River discharges for GRDC 6262310.



Taken together, the flow-duration curve and the monthly mean seasonal cycle indicate that the model ensemble broadly captures the overall range and seasonal structure of river discharges, while differences remain relative to observations. The flow-duration curves reveal systematic deviations between discharge distributions, particularly across higher flows, highlighting differences in the representation of variability and extremes. The comparison of monthly means further shows that, although the timing of the seasonal cycle is generally reproduced, discrepancies in magnitude persist across months.

2.3.1.2 River floods (flood maps) – Regional data

Hazard data is expected to be processed based on river flood depth maps provided by YPEN (the Ministry of Environment and Energy). The raster datasets are available in two ways: (i) via the official YPEN's portal for floods, where simplified versions of the maps can be sourced for visualization purposes, and (ii) via an official request from the government bodies and departments related to floods and disasters. The second format refers to the full-sized raster. The datasets will represent the depths under three (3) return periods (RP): 50, 100, and 1000 years. The file format (GeoTIFF (Geographic Tagged Image File Format) raster files) and their resolution are expected to be processed using the Jupyter notebook template as provided in the CLIMAAX flood workflow. The LUISA Land Use dataset at 100m resolution will be used in a raster format for the land use classification for each grid cell (assigning flood depth values to land use pixels), and identify land use classes (e.g., residential, industrial, etc.) that fail within the socio-economic activities located within the premises of the study's flood zones in the RCM. Further, JRC damage curves will allow for modelling vulnerability and estimating economic losses as a function of flood depth by land use category. Regional adaptations, as introduced in a previous deliverable (see Deliverable 1, p. 18), will be documented in a modified Excel file. Depth-damage functions are expressed as damage ratios for each land use type, allowing for an indirect measurement of flood exposure and its translation into economic consequences (where damage estimates are expressed in Euros). The bounding box that covers the region of interest (ROI) will be given in WGS84 (World Geodesic System) coordinates (EPSG:4326) and, if needed, reprojection to

EPSG:2100 will be performed. The [Bounding Box Tool](#) was selected for collecting the coordinates¹³.

2.3.1.2.1 Hazard assessment

Moving from a broader study area covering the whole region to a specific example, a list of potential areas of interest will be provided. Each area offers a specific set of characteristics that can serve as a case study for the application of regional data (flood maps for return periods of 50, 100, and 1000 years). These return periods differ from those in European databases, primarily due to the wider interval between return periods. The selected areas provide a foundation for further consideration and discussions with stakeholders, including representatives from local authorities, civil protection units, and fire departments, during Phase 3 of the CLIMAAX project. Due to ongoing bureaucratic procedures, EL11 data is still being acquired; therefore, only areas from EL9 and EL10 are considered. Unique codes for each river have been previously mentioned in this deliverable. The areas include: (i) Anthemous (Anthemountas) river (EL10), (ii) Paralia Katerini (EL9), (iii) Chalkidiki, (iv) the Delta of Axios and Loudias rivers, (v) an area near the wider Delta region, and (vi) an area on the West Side of Thessaloniki. Details for each area are provided below.

- i. The Anthemous river traverses areas from the prefecture of Chalkidiki to Thessaloniki. Although not extensive, it covers regions similar to those of the Axios, Loudias, and Strymonas rivers, and its terminus is near populated areas and the city's main airport. This river exemplifies data gaps: the Aqueduct maps lack flood coverage in this area, rendering them unsuitable for direct comparison with coarse-grained Aqueduct flood maps. Nevertheless, it serves as a valuable example of how even small rivers can influence local climate and pose challenges for prefectures and municipalities.
- ii. Paralia Katerini is a prominent tourist destination in EL9, located in the prefecture of Pieria near the capital, Katerini. Flood maps indicate a significant hazard for many areas in the prefecture, particularly in southern Pieria. Paralia and its surrounding areas attract the majority of tourists between May and September, playing a crucial role in the region's economic stability. Climate change poses a risk to the local economy, presenting significant challenges for local residents and municipal authorities in managing flood hazards.
- iii. Chalkidiki is characterized by a high vulnerability score, making it suitable for the study of hazard events, including compound and cascade events. Many rivers in Chalkidiki follow a similar pattern: they originate inland and terminate in coastal areas. Therefore, a single representative case study can illustrate general trends while recognizing the importance of individual area assessments for strategic resilience planning. Phase 3 of the CLIMAAX project will further demonstrate the need to develop a comprehensive strategy to address the prefecture's vulnerability.
- iv. The Delta of the Axios and Loudias rivers is a significant habitat supporting numerous bird and animal species. This area faces a high risk of flooding, as indicated by JRC data and coarse-resolution Aqueduct products. Nearby is an industrial zone of Thessaloniki and a village that hosts one of the city's three universities. In addition to the general area, a toy

¹³Due to the limitations of the Bounding Box tool (which draws a rectangle), any potential improvement to the region of interest can be achieved in GIS software, where a polygon can be drawn and the area extracted.

model of the industrial area was developed to assess whether the workflow can effectively capture the complexity of such mixed-use regions. This serves as an example (v).

- v. An area on the West Side of Thessaloniki was selected due to indications in regional flood maps that a former riverbed now presents a potential flood risk. This risk arises from the city's expansion into previously peripheral areas, where natural waterways have been altered or removed, increasing vulnerability to cascade hazards. Although not a primary example, including a general figure for this area across the three return periods would provide valuable comparative insight.

Rivers' "sieve"

All selected areas retain the potential to represent an "optimal" scenario, enabling the display of a broad range of data transferable across risk phases. Such an approach would also, in theory, strengthen the improvement of exposure and vulnerability estimates generated by providing inputs at a finer spatial scale for representative areas which serve as templates for similar cases or for areas facing the same climate-hazard problems. However, given the structural complexity of the river network, and taking into account that rivers often flow through multiple Administrative sub-regions, and multiple smaller tributaries converge into larger basins. This approach allows for a more manageable yet sufficiently representative estimation, facilitating the creation of templates for flood maps applicable to various areas within the RCM.

The unique identification number assigned to each river in Greece serves as a formal criterion for evaluating both accessibility and transferability. The table below presents several rivers relevant to Regional Climate Modeling (RCM). Additionally, the table includes rivers that are not among the most significant, yet their potential contribution to flooding events remains noteworthy¹⁴.

The following codes, unique to each river, enable reproducible data across regions. Henceforth, this data will be considered as referenced and will not be reiterated in the text to optimize space. To introduce representative examples of the CLIMAAX River and Coastal Floods workflow (River Floods; flood maps), a set of examples will be presented using regional/local data. In some cases, the examples coincide and can be compared with European data, for example, using the sparser Aqueduct flood maps, and in some cases, the opposite is true. Both cases, serves its cope: the former evaluates already existed results and provide a first flood for further discussions in terms of policy making and improving of strategies (which will serve as data for the forthcoming deliverable in the third phase) and the later will show precisely the need of regional data and a simple but intuitive way to identify and even introduce data gaps in some cases, where the local information provides a real case study, reflecting to the original EU sourced data.

Table 9: Names and codes for identifying the major rivers in EL9, EL10, and EL11.

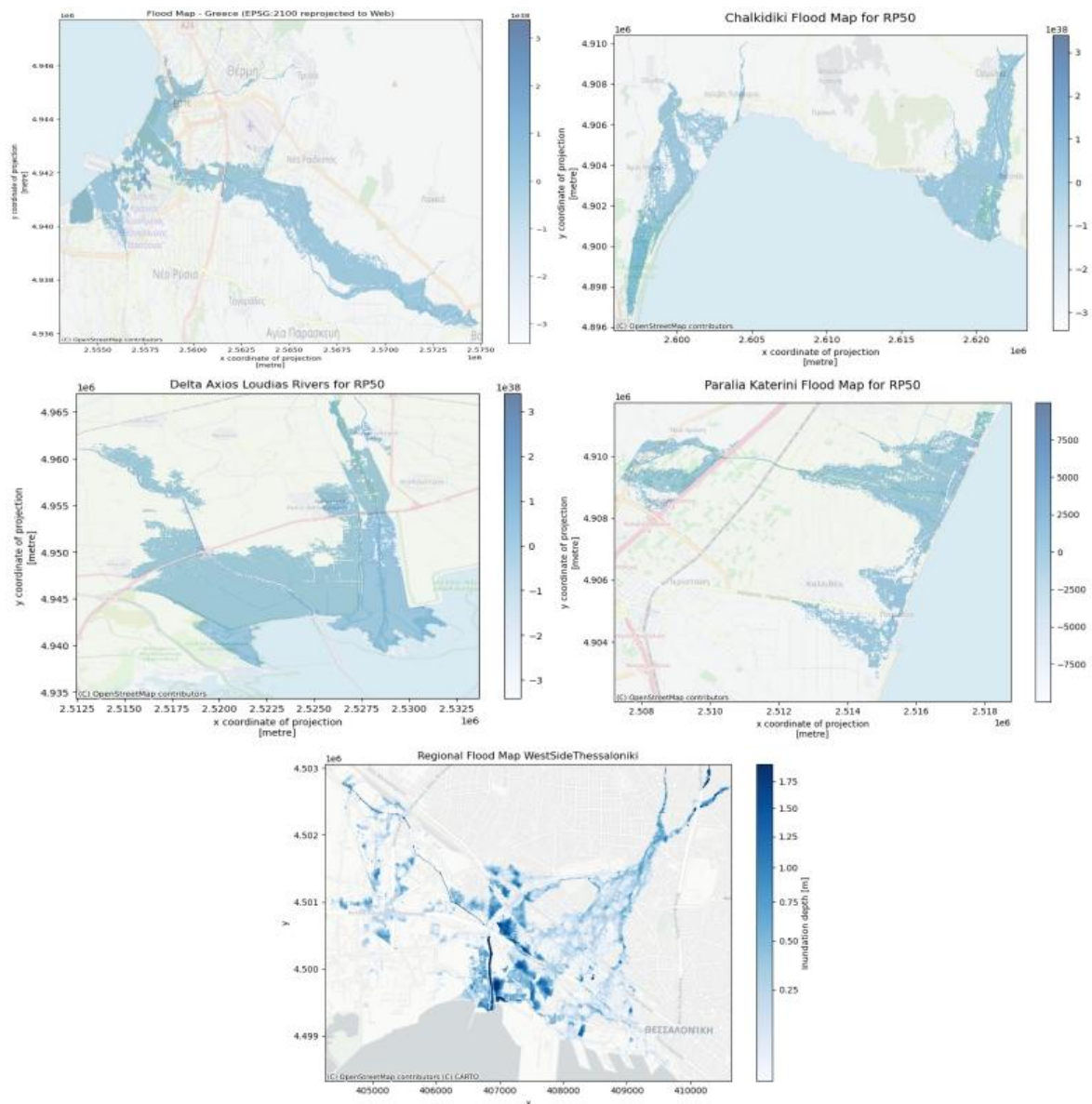
Name (Greek)	Name (English)	EU_CD	BASIN_CD/EL#
KONTIXA	KONTIXA	GR0009000400200170N	09
ΝΥΦΟΠΗΓΗ	NYFOPIGI	GR0009000400200220N	09

¹⁴ The encoding for the river names in the original source file is Windows-1253.

ΑΛΙΑΚΜΟΝΑΣ	ΑΛΙΑΚΜΟΝ	GR0009000400200550N	09
		GR0009000400200570N	09
		GR0009000400200330N	09
		GR0009000400200380N	09
		GR0009000400200110H	09
		GR0009000400200100H	09
ΤΡΙΠΟΤΑΜΟΣ	ΤΡΙΠΟΤΑΜΟΣ	GR0009000400200150N	09
		GR0009000400200160N	09
ΞΗΡΟΠΟΤΑΜΟΣ	ΧΙΡΟΠΟΤΑΜΟΣ	GR0009000400200510N	09
		GR0010000400220150N	10
		GR0010000400220130N	10
ΑΣΠΡΟΠΟΤΑΜΟΣ	ΑΣΠΡΟΠΟΤΑΜΟΣ	GR0009000400200270N	09
		GR0009000400200280N	09
		GR0009000400200430N	09
		GR0009000400200440N	09
ΜΑΥΡΟΠΟΤΑΜΟΣ	ΜΑΥΡΟΠΟΤΑΜΟΣ	GR0009000400200260N	09
		GR0009000400200240N	09
		GR0009000400200250N	09
ΨΑΡΟΡΡΕΜΑ	PSAROREMA	GR001000040F210180N	10
		GR001000040F210170N	10
ΓΑΛΛΙΚΟΣ	GALLIKOS	GR0010000400220190N	10
		GR0010000400220120N	10
		GR0010000400220180N	10
		GR0010000400220110N	10
		GR0010000400220100N	10
ΑΝΘΕΜΟΥΣ	ANTHEMOUS	GR0010000400230120N	10
		GR0010000400230110N	10
		GR0010000400230100H	10
ΒΑΤΟΝΙΑΣ	VATONIAS	GR0010000400290130N	10
		GR0010000400290100N	10
		GR0010000400290120N	10
		GR0010000400290120N	10
ΓΟΡΓΟΠΗΣ	GORGOPIS	GR001000040F210250N	10
		GR001000040F210240N	10
		GR001000040F210230N	10
		GR001000040F210220N	10
ΑΞΙΟΣ (ΒΑΡΔΑΡΗΣ)	AXIOS (VARDARIS)	GR001000040F210210N	10
		GR001000040F210110N	10
ΒΑΡΔΑΡΟΒΑΣΗ	VARDAROVASI	GR001000040F210130N	10
		GR001000040F210120H	10
ΛΟΥΔΙΑΣ	LOUDIAS	GR0010000400200100A	10
		GR0010000400200110A	10
ΖΑΜΟΥΝΗ	ZAMOUNI	GR0010000400300100N	10
		GR0010000400300100N	10
		GR0010000400300080N	10
ΣΤΡΥΜΩΝ	STRYMON	GR001100040B230420N	11
		GR001100040B230110N	11
		GR001100040B230100N	11

Figure 12 illustrates flooding maps corresponding to a 50-year return period scenario for the selected areas within the RCM.

Figure 12: The areas depicted are, from top to bottom and left to right: Anthemountas River (top left), Chalkidiki (top right), the delta of the Axios and Loudias Rivers (middle left), Paralia Katerini (middle right), and the West Side of Thessaloniki (bottom).



In Figure 13 a multi-panel comparison of river flood potential can be seen for several sub-areas around RCM. For each area, the three maps show inundation depth for different return periods (typically RP 50, RP 100, and RP 1000 years): darker/bluer tones indicate deeper water, and the flooded footprint generally expands as the return period increases. An OSM basemap is used for geographic context, and the color scale runs from 0 to ~5 m depth. Across all locations, the same trend is clear: moving from RP50 to RP100 to RP1000, flooding becomes both more extensive and more intense, with the deepest flows following the main river corridors, while higher return periods progressively activate adjacent floodplains and low-lying terrain. This expansion is especially pronounced in flatter coastal/delta settings, where inundation spreads laterally and connects into broader continuous flood zones as event rarity increases.

Figure 13: River Flood Inundation Depth Across Return Periods (RP50, RP100, RP1000) in Central Macedonia.

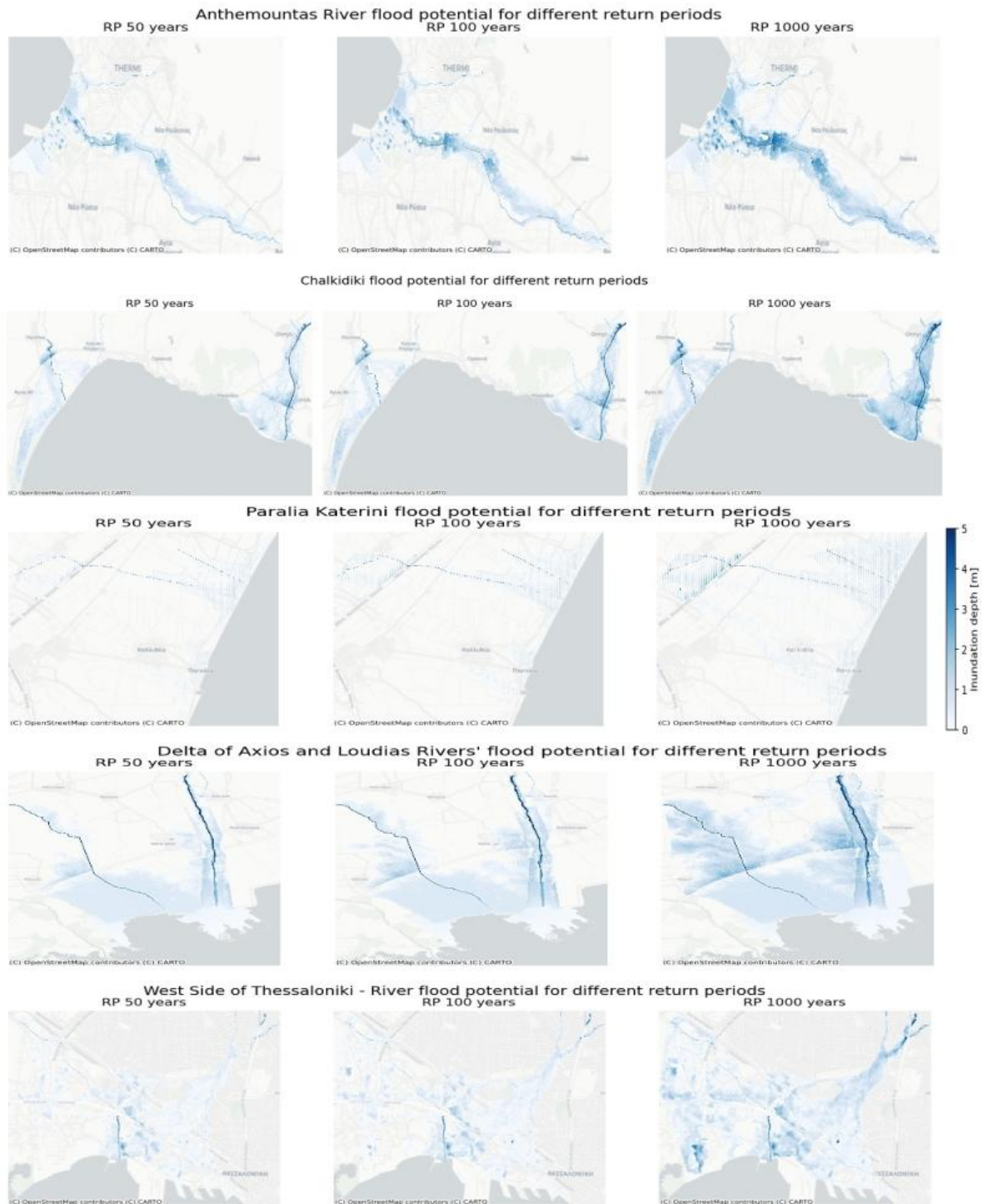


Figure 14 presents Aqueduct Floods River flood-depth maps (in meters) for four locations, each with a distinct flood pattern. Delta Axios exhibits the most extensive and coherent inundation, with depths reaching approximately 4 meters, typical of a broad, low-lying delta or floodplain. Chalkidiki features smaller, fragmented patches with lower depths (about 0 to 1 meter), indicating localized low-lying areas rather than a continuous floodplain. Paralia Katerini appears to be extremely shallow and spatially limited, with depths of up to 0.05 meters, and appears in only a few coarse-

grid cells. The Thessaloniki area shows broader coverage with moderate depths, consistent with a flat coastal or urban plain where flooding spreads widely but does not reach the depths seen in the delta. Please note that each panel uses a different depth scale, so similar colors do not always represent the same absolute depth. Additionally, the Aqueduct products show no flooding in the Anthemountas River, suggesting a data gap in this area compared to regional and European flood datasets.

Figure 14: Aqueduct floods (baseline ca.1980): River Inundation Depth for a 1-in-100 Year Event Across Selected Central Macedonia Case-Study Areas.

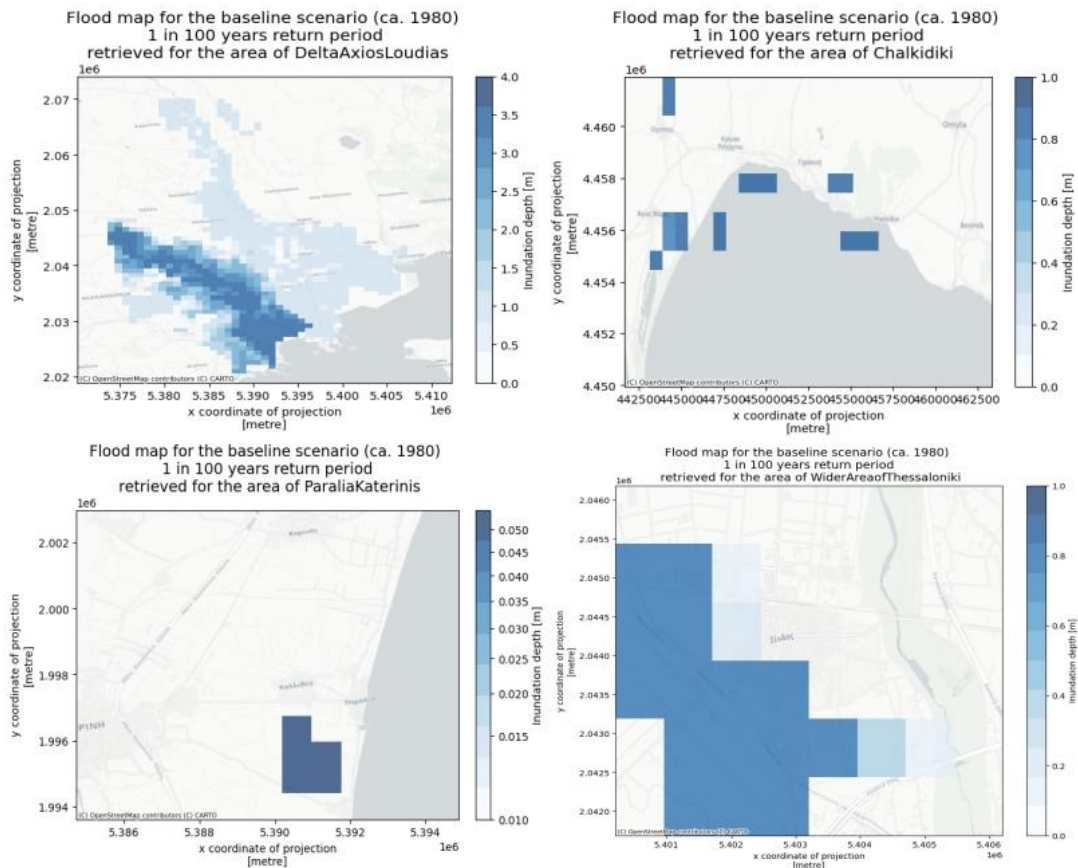
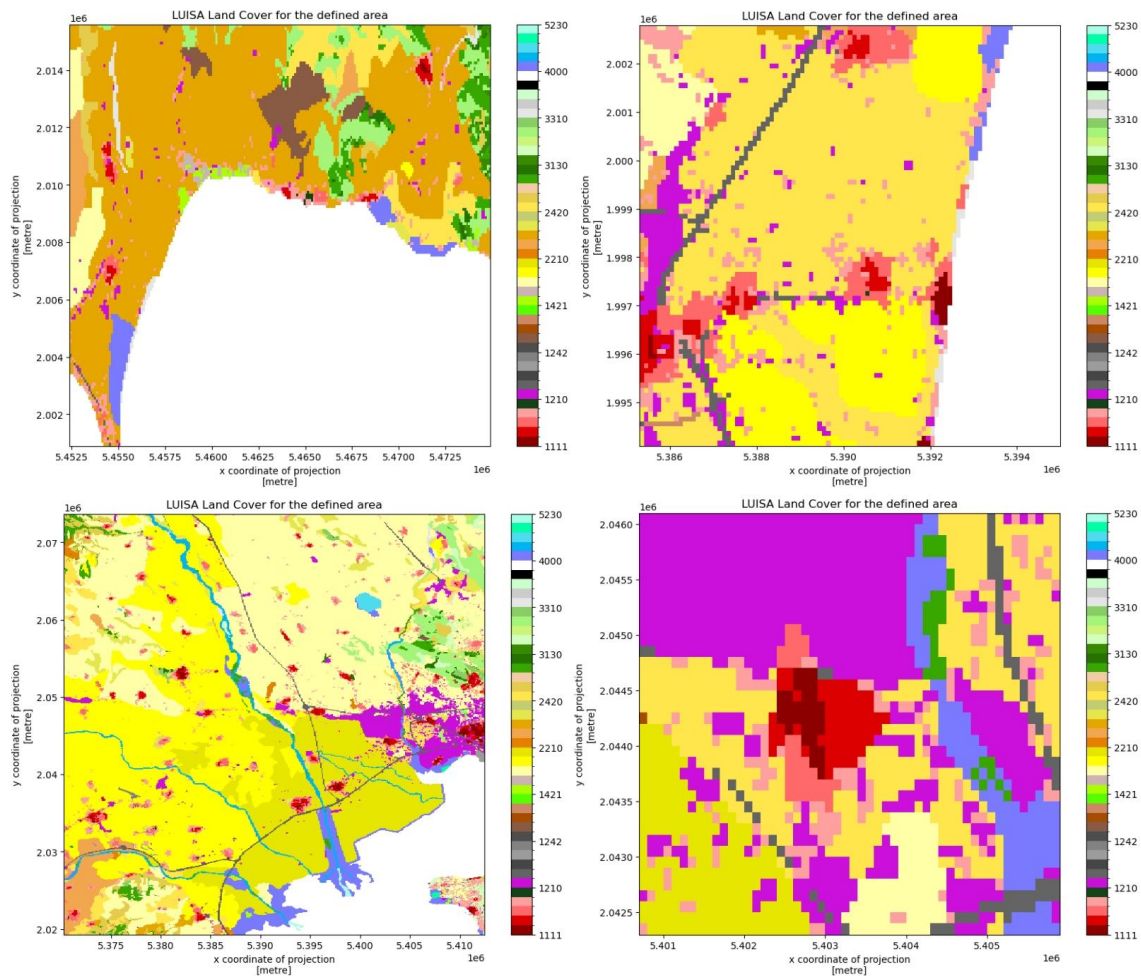


Figure 15 presents LUISA land cover maps (at 100 m resolution), clipped to the case-study areas. Each categorical LUISA class is displayed using a fixed color palette. Broad land-use patterns are distinguishable across the panels: urban and built-up classes cluster around settlements and transport corridors, agricultural classes dominate flatter lowland zones, and natural, forest, or vegetation classes are found in more rugged regions. Water bodies and coastal features are represented as distinct classes along shorelines and river mouths. The color bar provides LUISA class codes (e.g., 1111-5230), ensuring that colors and codes are consistent across all panels. The pixelated or blocky appearance in the bottom-left panel is expected due to two factors. First, LUISA is a categorical raster with a 100 m resolution, resulting in a blocky appearance at the local scale. Second, this specific area spans a larger area or is displayed at a zoom level where each 100 m cell is visually prominent, resulting in class boundaries resembling a mosaic. This visual effect is a normal characteristic of a discrete land-use grid being clipped and plotted for a relatively zoomed ROI, rather than an error in processing.

Figure 15: LUISA Land Cover (2018, 100 m): Categorical Land-Use Maps for Selected Case-Study Areas. Top left represents Chalkidiki, top right Paralia Katerini, bottom left, Delta of Axios, and bottom right a selected area in the Wider area of Thessaloniki (zoomed in).



2.3.1.2.2 Example case studies using regional data: Delta of Axios River and Wider area of Thessaloniki (toy example)

The Axios River delta, together with the nearby Loudias River and its proximity to the western boundaries of the greater Thessaloniki area and the adjacent industrial zone, renders this region highly susceptible to river flooding and makes it an exemplary case study. The broader area will be analyzed using regional flood maps and compared with a smaller, more focused area near the industrial zone of Thessaloniki, specifically a village with approximately 9,000 inhabitants. This comparison aims to illustrate the flood impact of a hazard event in a context that may serve multiple purposes, as outlined in the previous example. The same methodology and notation will be applied to the flood maps to characterize hazards. For risk assessment, the land-use damage curve will be used (see also Deliverable 1, pages 60-61), based on modified data specific to Greece. The land-use code assigned to a total €/m² is expected to remain consistent across both cases, and flood-damage vulnerability curves for the respective cover types will be incorporated. The analysis will clarify the potential economic damage to infrastructure and highlight the most significant economic losses. The bounding box and the coordinates of the areas are shown in the table below.

Bounding box	Area
22.467529,40.486066,22.881107,40.928973	Axios Delta
22.781476,40.655923,22.837205,40.682066	Wider Area of Thessaloniki

Results

Figure 16 presents a comparison of two flood map examples derived from distinct data products and value conventions. The Axios RP50 panel (left) appears to represent a flood extent or footprint layer rather than a processed inundation-depth raster. The colorbar scaling, which displays an extreme scientific-notation factor, suggests that the underlying values may contain nodata or invalid placeholders, or may reflect a scaling or encoding issue. In contrast, the West Thessaloniki panel (right) serves as a standard inundation-depth map, with a practical 0-5 m scale and depth gradients concentrated along channels and in low-lying areas.

Figure 16: Flood hazard mapping based on the regional high-resolution river flood map dataset for the present-day scenario for the wider area of the West Side of Thessaloniki, and for the wider Axios Delta area.

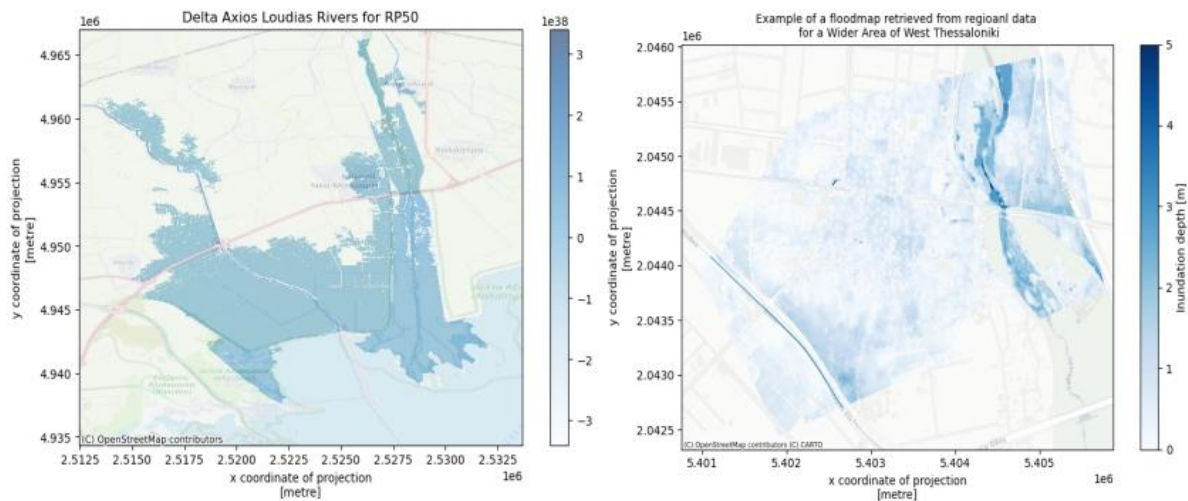


Figure 17 compares modeled river inundation depth across three return periods (RP50, RP100, RP1000) for the same area, shown over an OSM basemap. As the return period increases, the flooded footprint becomes more extensive, and the depth signal (darker blues) becomes stronger, especially along the main river channels. The Axios delta panel (bottom row) highlight how flooding concentrates along the river corridors and then spreads into adjacent low-lying land at higher return periods. Overall, the trend is consistent: rarer events do not just deepen existing flooded zones, cultivating more of the floodplain. The wider area shows a remarkable flooding event for 100 and 100 years indicating the possibility for more intense effect of climate change.

Figure 17: River flood potential for various return periods in both study cases. The upper section illustrates the Wider Area of Thessaloniki, while the lower section shows the Delta area.

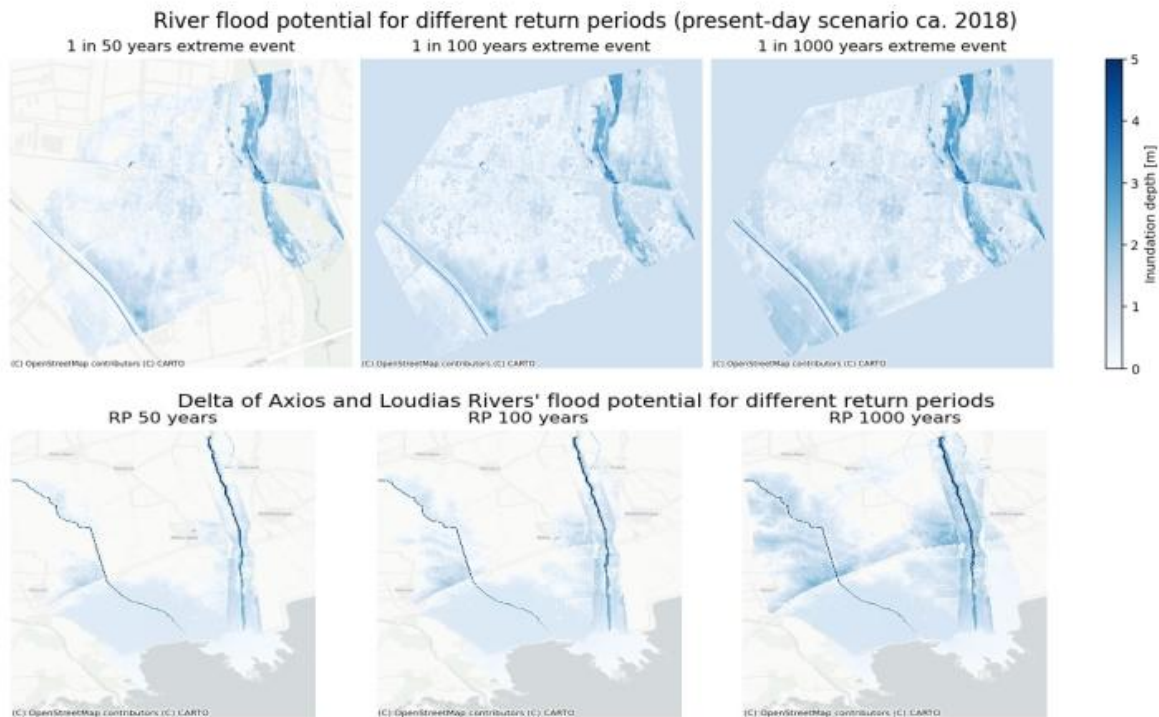
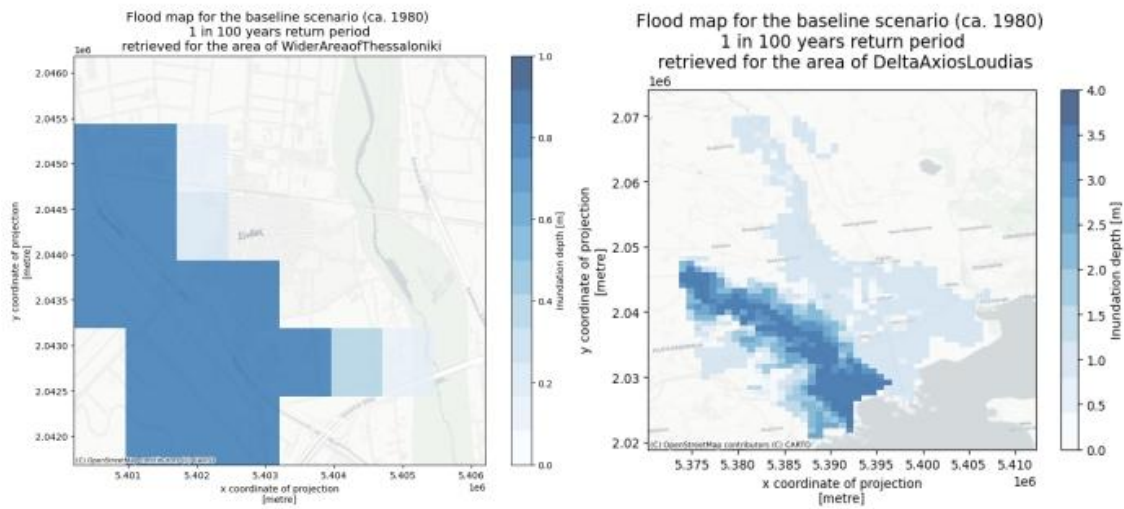


Figure 18 compares baseline (circa 1980) river flood inundation depths for a 1-in-100-year event in two distinct settings: the wider West Side Thessaloniki area (left) and the delta (right). The Thessaloniki panel displays broad, blocky coverage with generally shallow inundation depths, which reflects the coarse grid of the Aqueduct product and the relatively flat urban and coastal plain context. In contrast, the Axios delta panel exhibits a more pronounced floodplain signal, with deeper inundation (up to approximately 4 m) and a more continuous footprint along low-lying terrain. Each subplot employs a unique depth scale; therefore, color intensity is not directly comparable between the two panels.

Figure 18: Flood map for the baseline scenario (ca. 1980) for 1 in 100 years return period for the two (2) selected example areas: on the left, the wider area of the West Side of Thessaloniki, and on the right, the Axios Delta wider area.



In the RCP4.5 Figure 19, the 1-in-100-year inundation depth maps indicate broadly similar spatial patterns across the three (3) time slices, with inundation staying restricted to the same low-lying passages in each case-study area. The corresponding difference panels (future minus 1980 baseline) show a predominantly coherent sign over the mapped domain, suggesting that projected shifts under RCP4.5 manifest primarily as a systematic offset in flood depth rather than a substantial reconfiguration of the flooded footprint. In the wider West Thessaloniki panels (upper set), inundation depths remain within the low range shown, and changes relative to baseline appear spatially smooth, consistent with a modest, spatially consistent shift in modeled water depths through time. By contrast, the RCP8.5 figure exhibits a stronger late-century indication, particularly in the Axios delta figure (lower set). While the overall inundation shapes continue to follow the fluvial network and adjacent floodplain, the depth scale extends to higher values, and the 2080 map displays more pronounced inundation intensities than the corresponding RCP4.5 case. The difference figures under RCP8.5 imply greater divergence from the baseline scenario, consistent with an increase in flood hazard under the higher-emissions scenarios. Overall, the comparison indicates that scenario choice affects the magnitude of projected inundation depths more than the spatial pattern of inundation, with RCP8.5 producing the clearest intensification by the late century, whereas RCP4.5 retains a comparatively quiet release from baseline conditions.

Figure 19: Flood maps for the RCP4.5 emission scenario, for return periods 1 in 100 years for 2030, 2050, and 2080 projections.

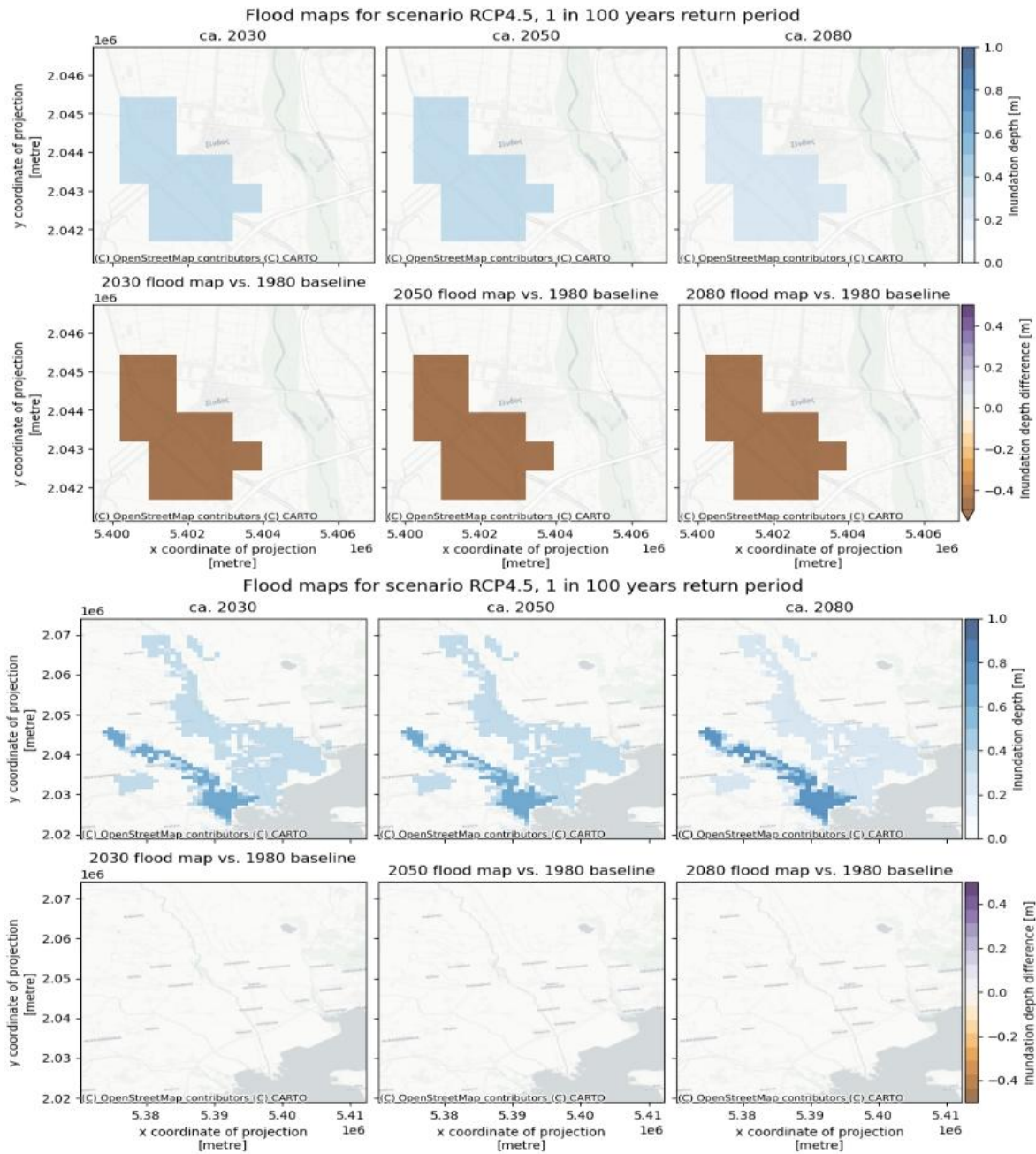
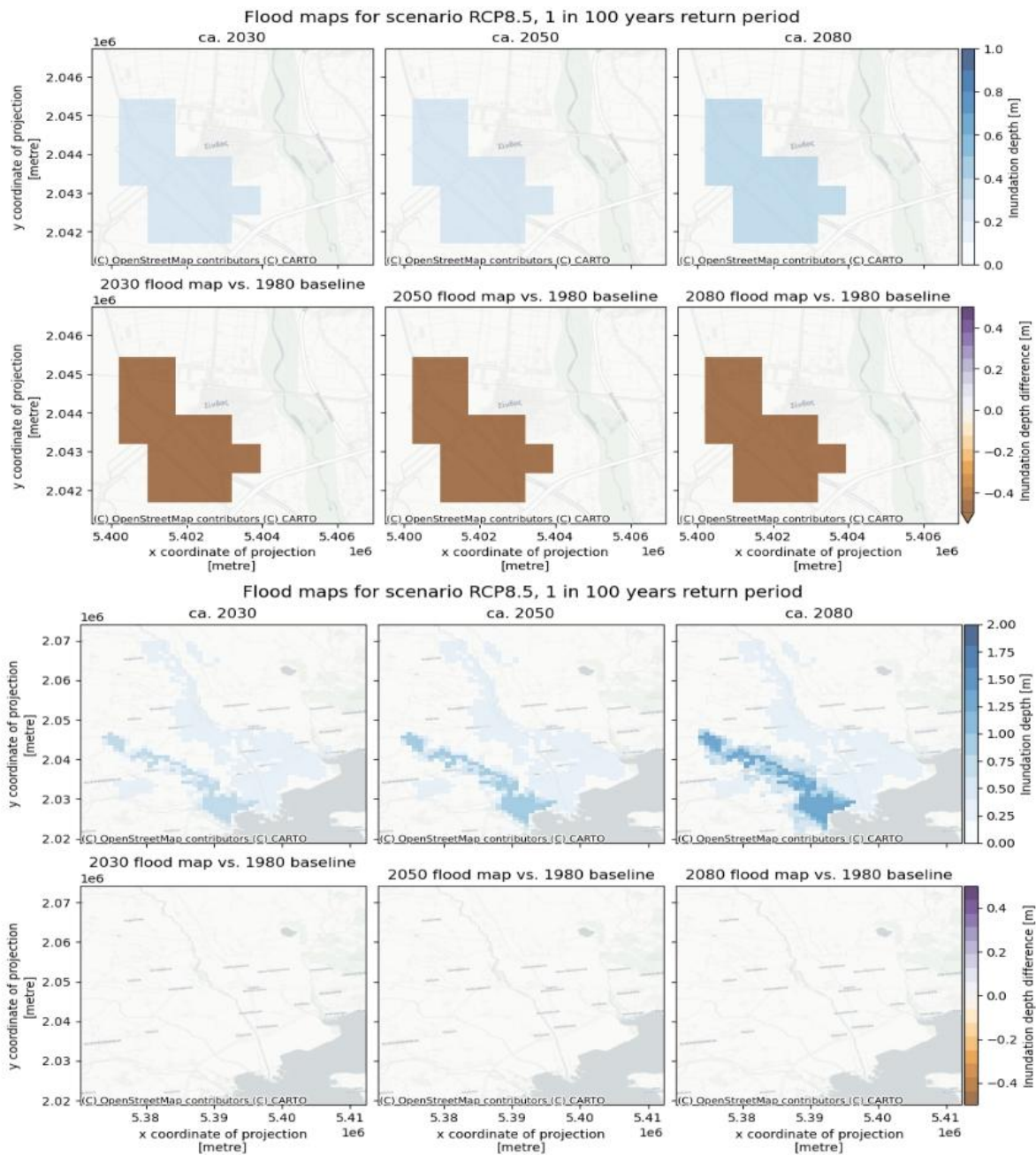


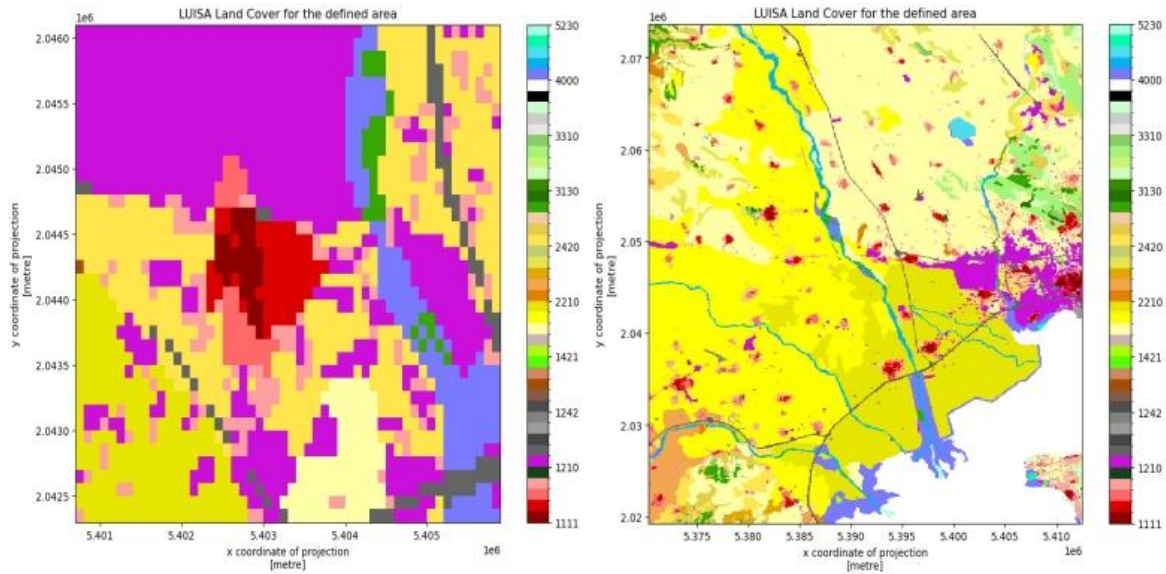
Figure 20: Flood maps for the RCP8.5 emission scenario, for return periods 1 in 100 years for 2030, 2050, and 2080 projections.



2.3.1.2.3 Risk assessment

The risk assessment methodology commences with the acquisition and processing of regional data, using utilizing the LUISA basemap at a 100-meter resolution. Integration of land-use information with regional flood hazard maps enables the identification of critical intersections between climate hazards and human assets.

Figure 21: LUISA Land Cover map for the selected area. On the left the wider area of the West Side of Thessaloniki, and on the right the Axios Delta.



Vulnerability – Flood Damage Curve for Land Use Types

Vulnerability was quantified using the local vulnerability layers we prepared for RCM (e.g., population, economic, and ecological vulnerability rasters), clipped to the AOI and aligned to a common analysis grid (same CRS, extent, and resolution as the hazard layer), so that each pixel has both a hazard value and a vulnerability class/value. Vulnerability is then categorized into three classes (low/medium/high) using either thresholds or quantiles, matching the categorical logic used later in the risk computation. Risk is computed by combining hazard and vulnerability classes pixel-wise using a contingency (risk) matrix, producing separate risk maps for the historical and future scenarios. In Figure 9 the depth and vulnerability curves are given.

Figure 22: Depth-damage curves as given by the JRC (left). Vulnerability curves for the first ten (10) LUISA land cover types are given following the "LUISA_damage_info_curves_greece.xlsx".

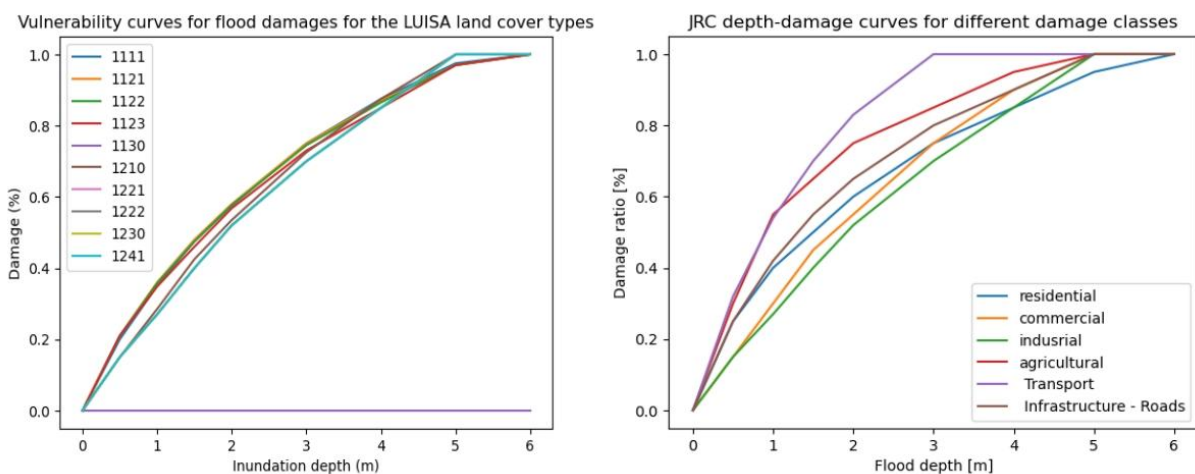


Table 10 presents the calculated maximum potential damage values, expressed in €/m², for the identified LUISA land-use categories. These values represent total replacement or reconstruction costs and are adjusted according to regional GDP per capita to reflect local economic conditions.

Assigning these monetary baselines to the spatial grid enables the model to estimate value-at-risk for each 100-meter cell. This tabular data serves as the multiplier for the damage ratios derived from the vulnerability curves, facilitating the generation of high-resolution economic damage maps.

Table 10: Maximum damage for reconstruction in €/m² for the first land use codes.

Land use code	total €/m ²
1111	435.471384
1121	301.449853
1122	177.769315
1123	50.409522
1130	0.000000
1210	288.913514
1221	28.666369
1222	401.329170
1230	171.998216
1241	401.329170

Calculate potential economic damage to infrastructure

Economic damage was estimated using the DamageScanner Python library, which enables explicit damage calculation by integrating hazard, exposure, and vulnerability data within a unified framework. Damage calculations were conducted for all return periods (for example, 50, 100, and 100 years), resulting in a loss data frame with estimated economic losses for each land use category. Table 11 presents the results for the two study areas, RP50 and RP100, as representative examples of the library's output.

Table 11: Codes with the highest economic damages for Axios Delta and the wider area of the West Side of Thessaloniki.

Wider Area of Thessaloniki	Description	RP50	RP100	Delta Axios	Description	RP50	RP100
2130	Rice fields	1035.916025	1332.560737	2130	Rice fields	208.208108	246.375323
2120	Permanently irrigated land	569.623420	1003.875059	2120	Permanently irrigated land	8.638295	27.781761
2220	Fruit trees and berry plantations	253.475938	423.983863	1121	Medium density urban fabric	45.059782	168.510468
4000	Wetlands	335.201692	406.936094	4000	Wetlands	70.303680	91.990479

1210	Industrial or comercial units	146.616650	234.347462	1122	Low density urban fabric	11.781852	61.161292
2420	Complex cultivation patterns	105.069614	210.770715	1111	High density urban fabric	7.761298	41.240512
2110	Non irrigated arable land	115.014472	157.960832	1123	Isolated or very low density urban fabric	7.187788	21.311018
1123	Isolated or very low density urban fabric	46.821502	89.824805	1210	Industrial or commercial units	2.056537	14.406417
1122	Low density urban fabric	37.886435	79.365053	2310	Pastures	0.000000	1.924507
1330	Construction sites	17.416434	57.504144	2110	Non irrigated arable land	0.033220	0.087725

Figure 23: River flood damages for extreme river flow scenarios in current day climate. The same scheme is followed with the previous figures regarding the areas that are depicted.

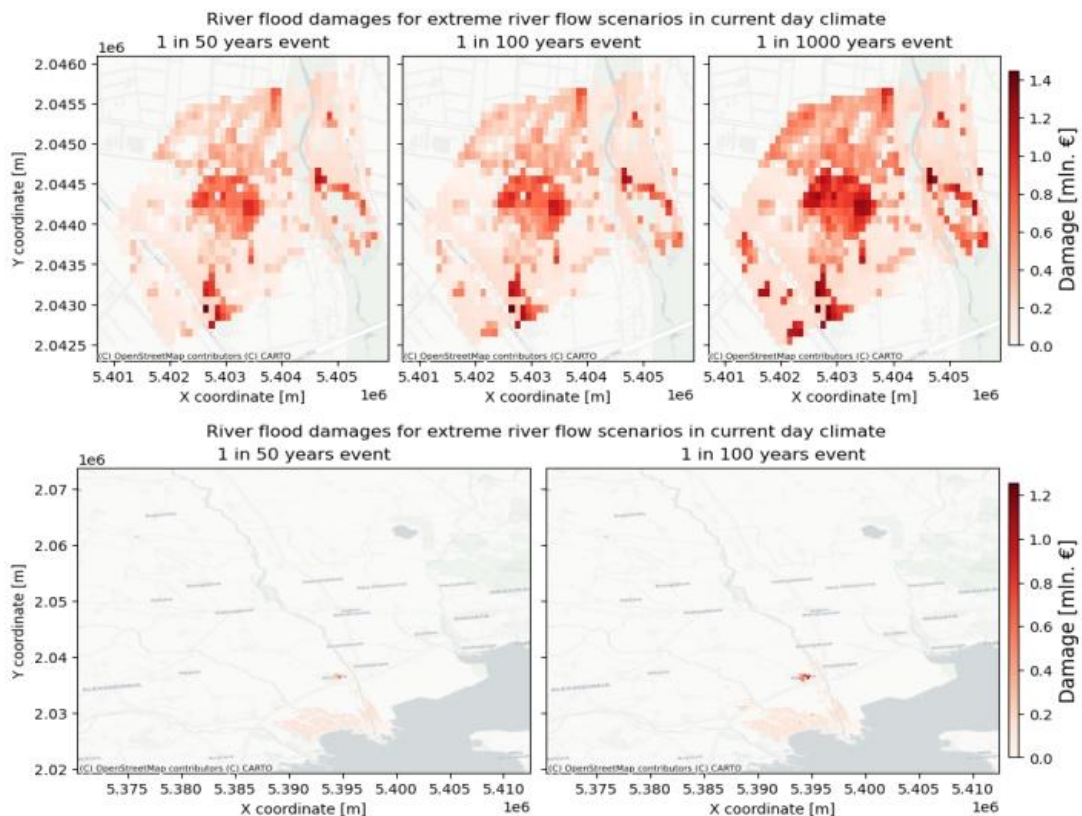
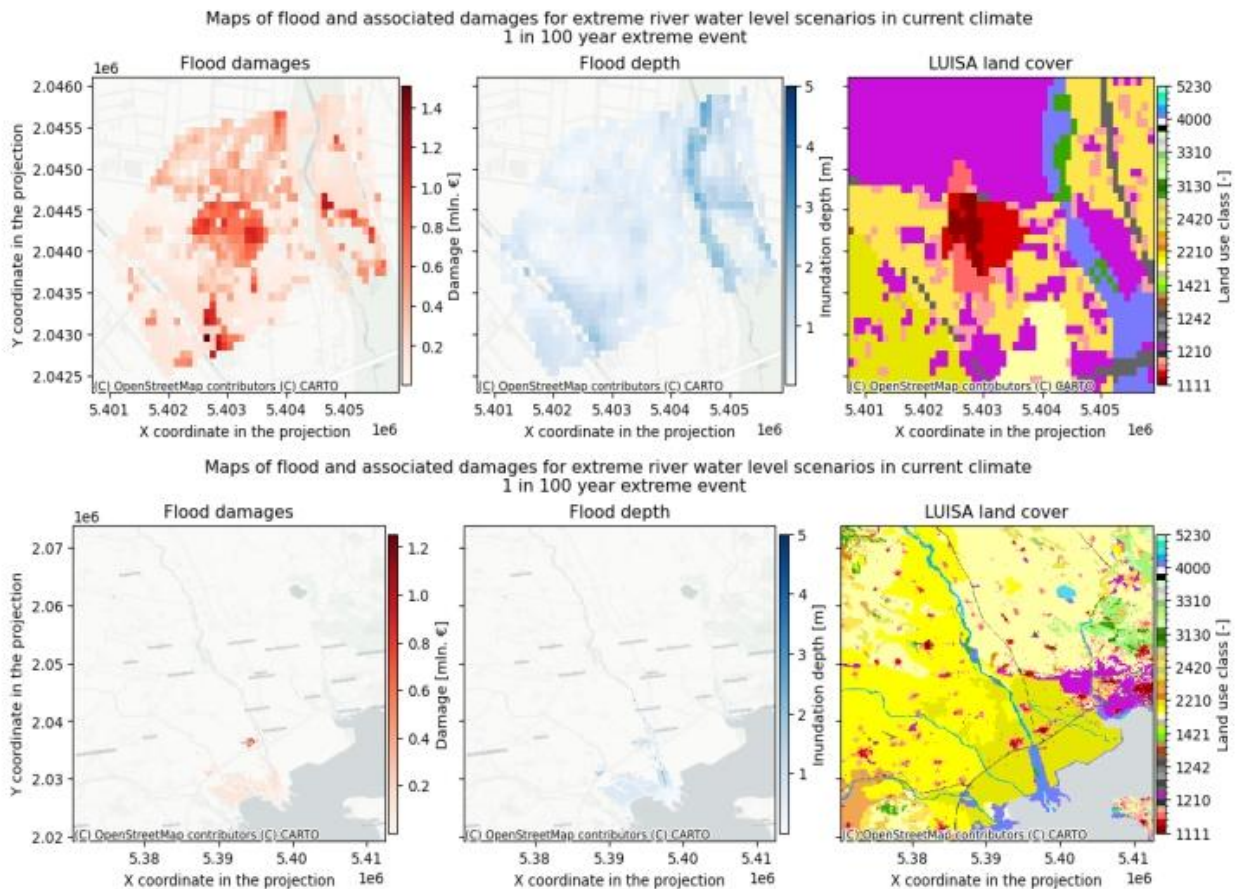


Figure 24: Maps of flood and associated damages for extreme river water level scenarios in current climate 1 in 100-year extreme event.



The final step of the workflow integrates regional river flood hazard (inundation depth), LUISA land cover, and vulnerability or damage estimation to derive potential economic damages for a 1-in-100-year flood event under present-day conditions. The updated results, as shown in Figure 24, present each case-study area as a consistent three-fold set: (i) estimated flood damages, (ii) modeled flood depth (m), and (iii) LUISA land-cover classes. This structure enables a direct visual link between the location of flooding, the exposed assets, and the concentration of losses. The new maps indicate that damage hotspots do not necessarily correspond to the deepest inundation zones. In the top example, damage clusters align with areas of more economically intensive land use, even where flood depths are only moderate. In contrast, the lower example shows a more confined inundation signal, with damage remaining comparatively localized. These findings illustrate the central risk mechanism: losses occur where flood depth coincides with higher-value exposure, while areas with visible inundation may yield limited losses if the affected land cover is associated with lower asset values. The comparison further highlights the importance of grid alignment and consistent reprojection or resampling between the flood-depth product and the LUISA land-use layers. Although these maps provide a coherent screening of potential damage across the RCM, interpretation should be cautious, as results may be sensitive to land-use class valuation, vulnerability, and the spatial precision of the underlying flood-depth product.

2.3.1.3 Flooding buildings and population exposure

Figures 25, and 26 present modeled flood depths for three return periods (50-, 100-, and 1000-year) at two spatial scales: a wide-area perspective (top and middle panels) and a detailed Axios Delta view (bottom row). On the wide-area maps, inundation is most pronounced along the main river corridor on the eastern side, where the deepest water (purple to red on the 0–6 m scale) follows the channel and extends into adjacent low-lying areas. As the return period increases from 50 to 1000 years, the flooded area becomes more continuous. It expands outward from the river, with larger regions transitioning from shallow (blue) to moderate or deeper depths. The bottom-row zoom illustrates a similar pattern at the local scale: flooding clusters in the southern delta and coastal zone as well as along connected drainage paths, with affected patches becoming denser and more extensive as the return period increases. The green outlines indicate the model or domain boundaries used for each set of panels, facilitating comparison of flood extent changes with event severity.

Figure 25: River flood maps for the case study areas for selected return periods for the given bounding box shapefile.

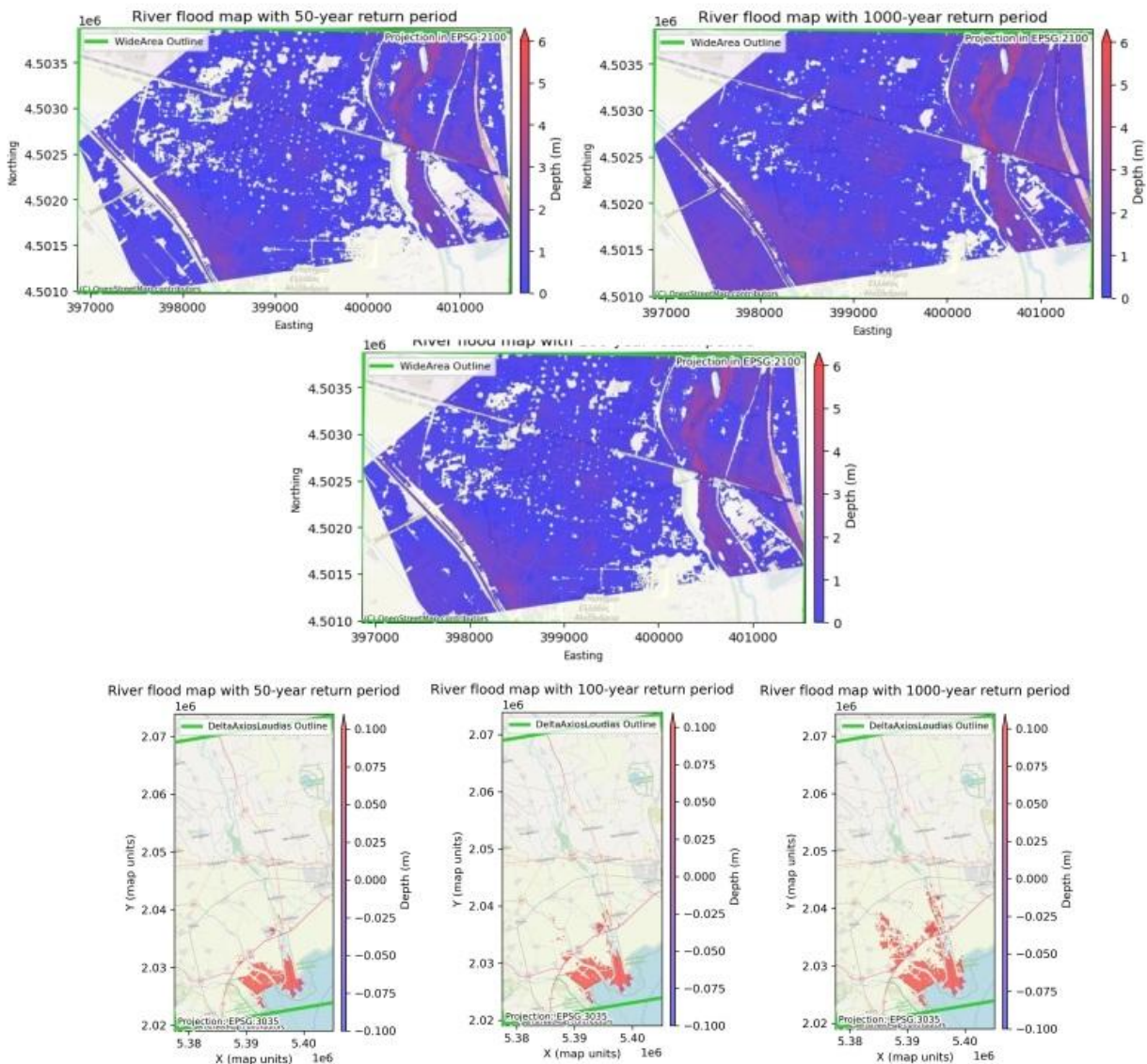


Figure 26: Difference in the river flood maps for the case study areas for selected return periods.

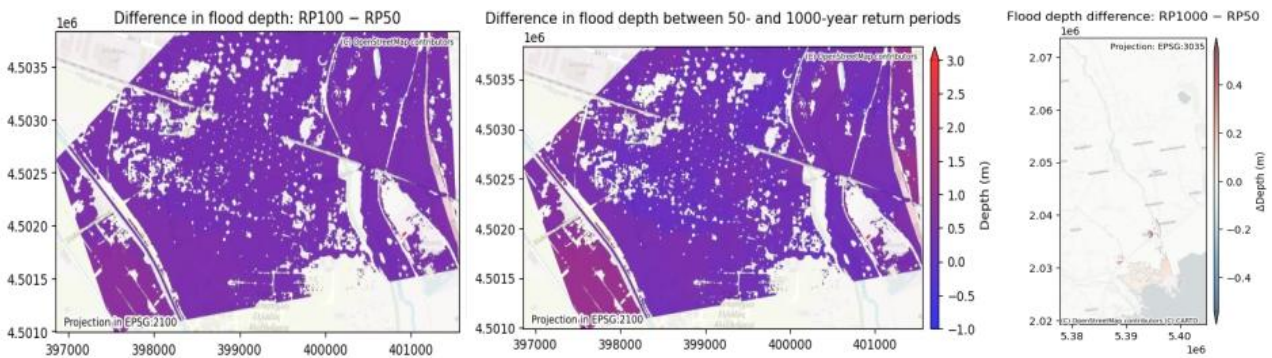


Figure 27 presents a 2025 population raster at two spatial extents: a detailed view within the wider area of the West Side Thessaloniki outline (left) and a broader view within the Axios Delta outline (right). Population values are represented on a 0–100 scale with higher values forming distinct hotspots and corridors rather than being evenly distributed across the landscape, reflecting the tendency for human populations to cluster. In the wide-area panel, population distribution appears relatively continuous but still varies at the cell level, highlighting denser pockets and lower-density gaps. In the regional panel, the contrast is more pronounced: most of the area exhibits low population density, while higher-density cells are concentrated around settlements and along major linear features. This spatial structure is particularly relevant for subsequent overlays of hazards or infrastructure.

Figure 27: Population map for the case study areas for the selected bounding box areas.

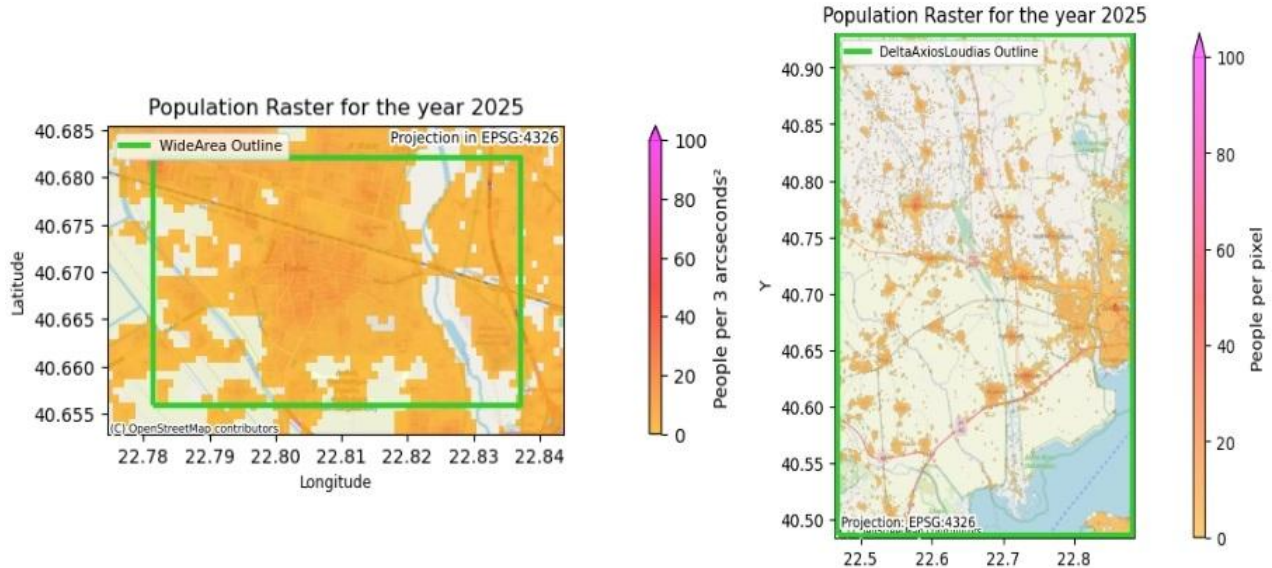


Figure 28 illustrates changes in the OSM building layer when original building tags are consolidated into broader Residential, Commercial, and Industrial classes, and addresses the treatment of unclassified buildings. The left panels depict the pre-classification state, in which buildings have a variety of detailed tags, including numerous “unknown” entries. The middle panels present the dataset after unclassified buildings are removed, resulting in a visually cleaner map but introducing significant gaps in building coverage, particularly outside the urban core. The right panels retain these buildings by assigning them to a “Universal” class, yielding a more spatially

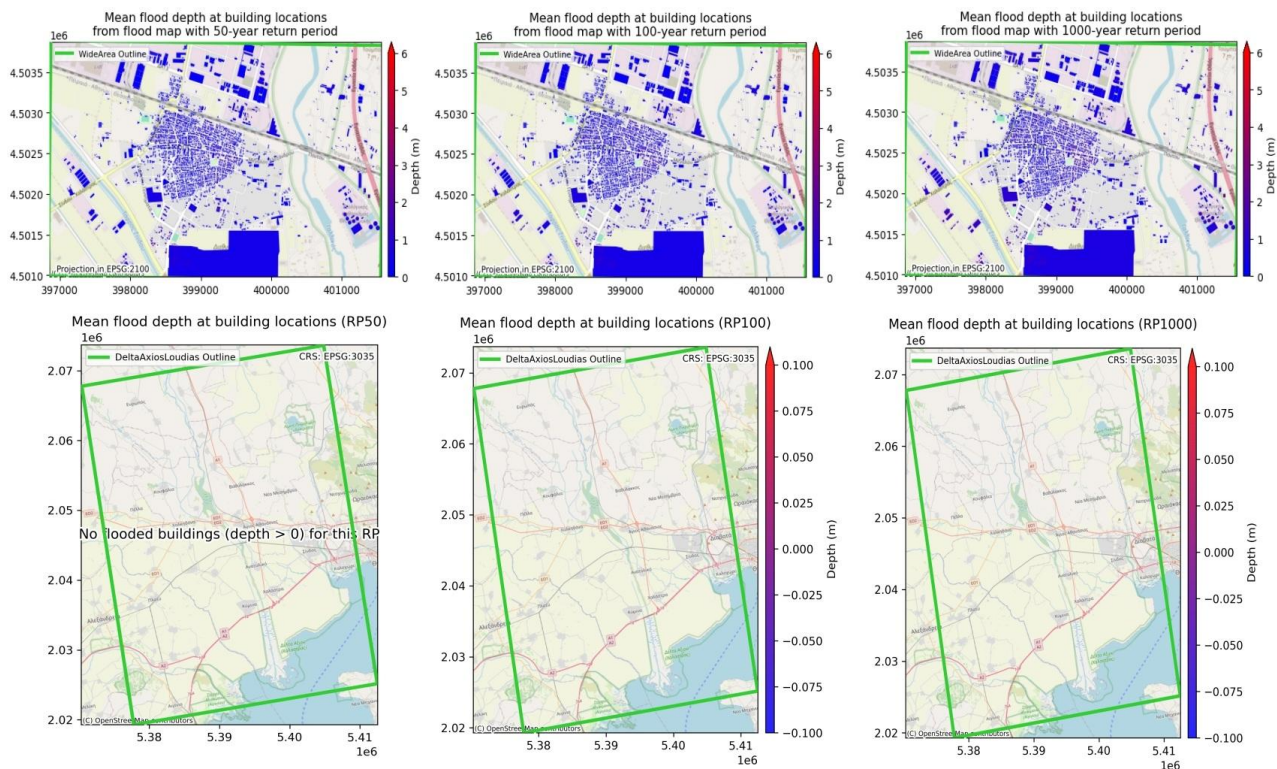
complete layer that preserves large building footprints while maintaining distinctions among industrial, commercial, and residential areas. The paired wide-area and regional views (green outlines) demonstrate, at two spatial scales, that the method used to handle unclassified buildings substantially alters the apparent building stock and, consequently, any subsequent exposure or risk assessments.

Figure 28: Unclassified buildings for the case study areas.



Figure 29 summarizes the mean flood depth sampled at building locations for three return periods, shown at two extents. In the wider area of the West Side of Thessaloniki's maps (top row; EPSG:2100), most buildings are shaded near the lower end of the 0–6 m scale (dark blue), while a smaller subset shows higher depths, with the 1000-year scenario displaying the strongest and most widespread non-zero values compared with the 50-year and 100-year panels. The Axios Delta maps (bottom row; EPSG:3035) show essentially no mapped inundation at building locations: the RP50 panel explicitly states no flooded buildings (depth > 0), and the RP100/RP1000 figures use a very tight color scale with little visible building-level signal, indicating depths are clustered around zero within that outline.

Figure 29: Mean flood depth maps for the 50-, 100-, and 1000-year return periods.



Calculating economic damage to buildings, and total damage to buildings

Figure 30 presents estimated building damage based on mean flood depth for three return periods (50-, 100-, and 1000-year), shown for both the wider area of the West Side of Thessaloniki (top row) and Axios Delta (bottom row) views. In the West Side of Thessaloniki figures, most buildings experience low or near-zero damage (dark blue), while a few locations, particularly a large building block in the south and several scattered sites, show the highest losses (pink/magenta). As the return period increases from 50 to 1000 years, the spatial pattern remains similar, but the severity of damage in these hotspots intensifies, reflecting deeper and more extensive flooding. In the Axios Delta' figures, damage is negligible for RP50, with the color scale tightly centered around zero. The colorbar range increases for RP100 and especially RP1000, suggesting that significant damage is likely only during rarer, more extreme events, although the affected areas remain limited. This is an artifact of the methodology due to the specific topography of the wider delta area.

Figure 30: Mean flood depth damage to buildings based on the flood maps for 50-, 100-, and 100-years return periods.

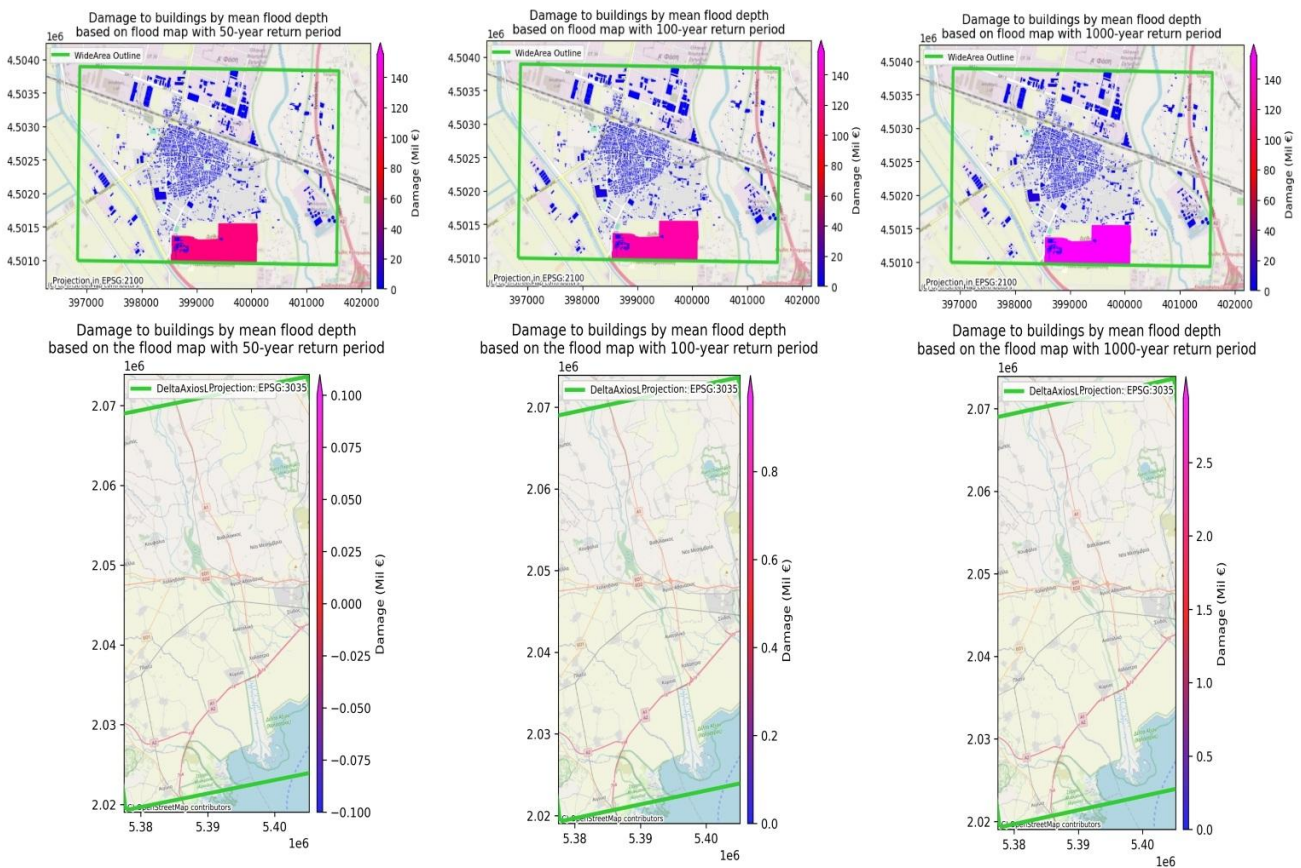
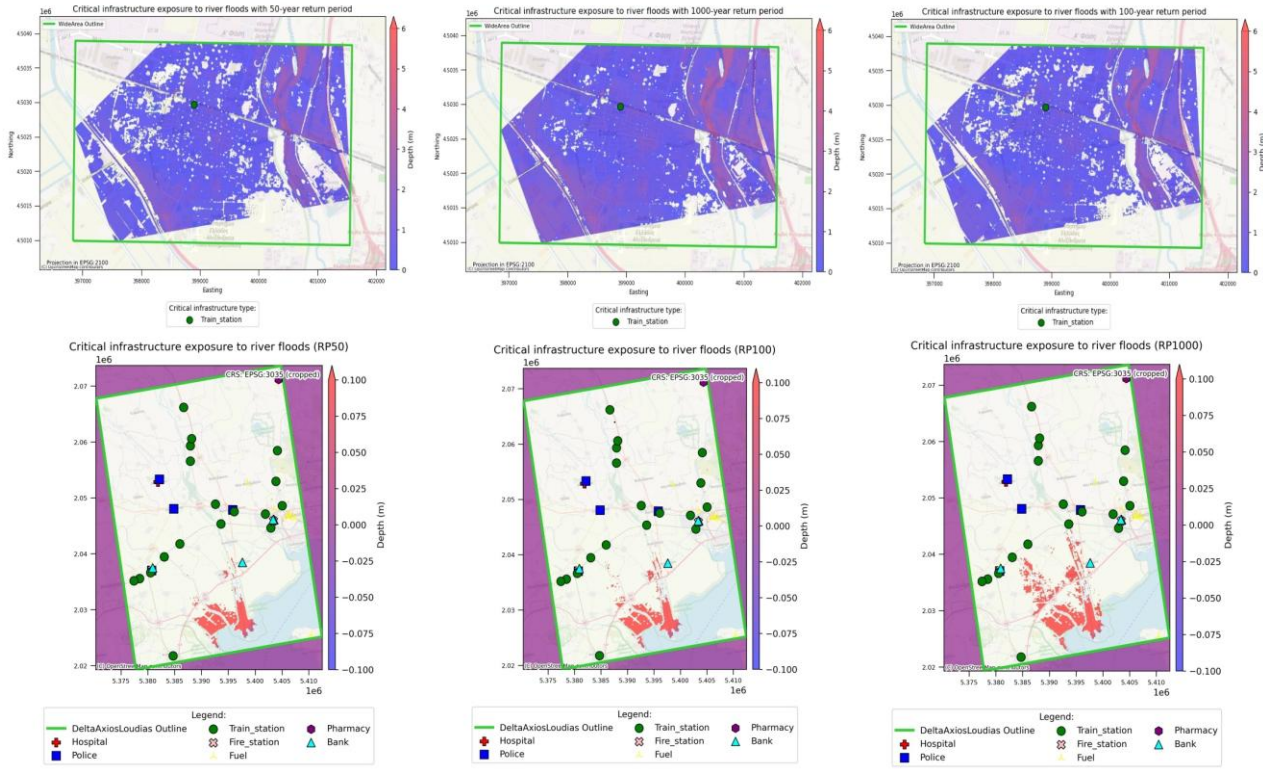


Figure 31 overlays critical infrastructure locations on modeled river flood depths for three return periods (RP50, RP100, RP1000), shown at both a wide-area scale (top row) and a cropped Axios Delta' scale (bottom row; depth scale centered near zero). In the wide-area panels, the single mapped asset (a train station, Green Point) is located in an area of shallow flooding, while deeper water remains along the main river corridor. The inundation pattern becomes more continuous as the return period increases. In the regional panels, multiple infrastructure types (train stations, hospitals, police and fire stations, fuel stations, pharmacies, banks) are displayed against the flood footprint. The largest inundated patches cluster in the southern and coastal areas and along low-lying corridors. Most infrastructure points remain outside these hotspots, indicating limited direct exposure under RP50 and RP100. Under RP1000, the inundated area expands and approaches more assets, indicating increased proximity and potential exposure as events become rarer and more severe. The first-row area is an Industrial area which depicts a crucial data gap in the building classification which plays a key role in the calculation of the critical infrastructure and of the reparation cost of such areas. In the second row, all critical infrastructure locations located far from any flooding events which is the case as it depict a wetland.

Figure 31: Critical infrastructure with 50-, 100-, and 1000-year return periods are depicted.



Exposed and displaced population

Figure 32: Exposed population for 50-, 100-, and 1000-years return periods.

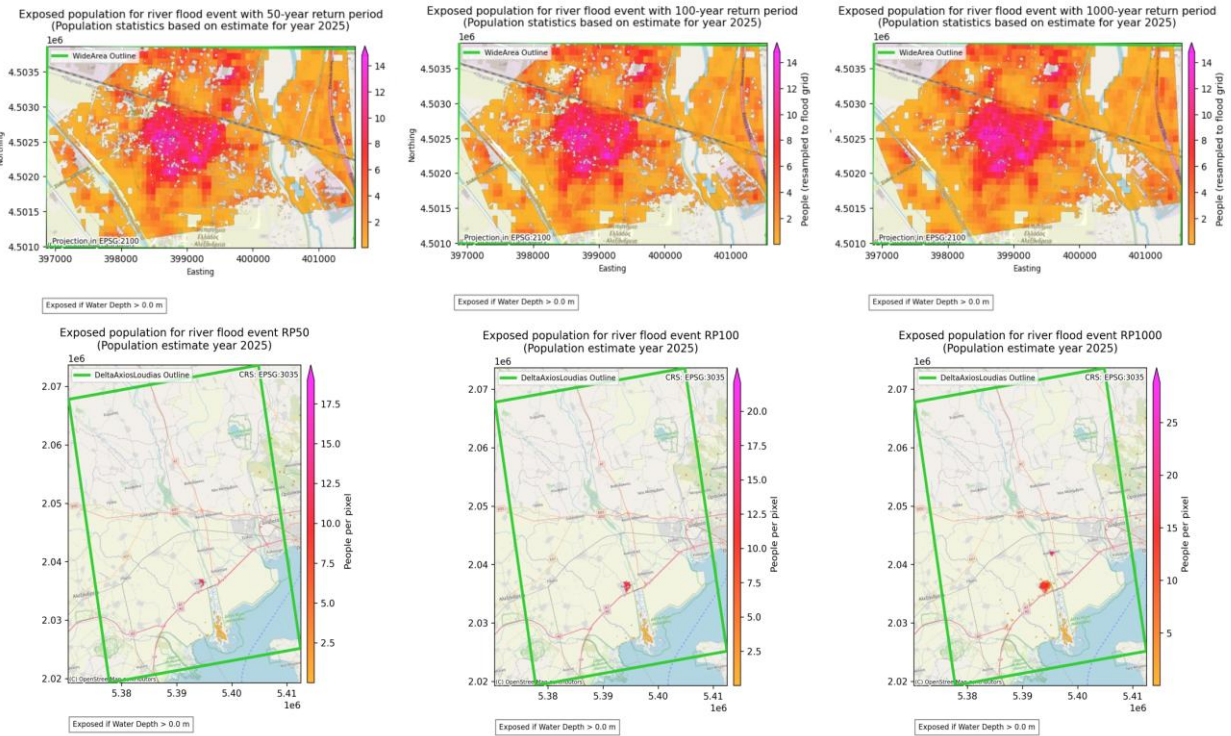
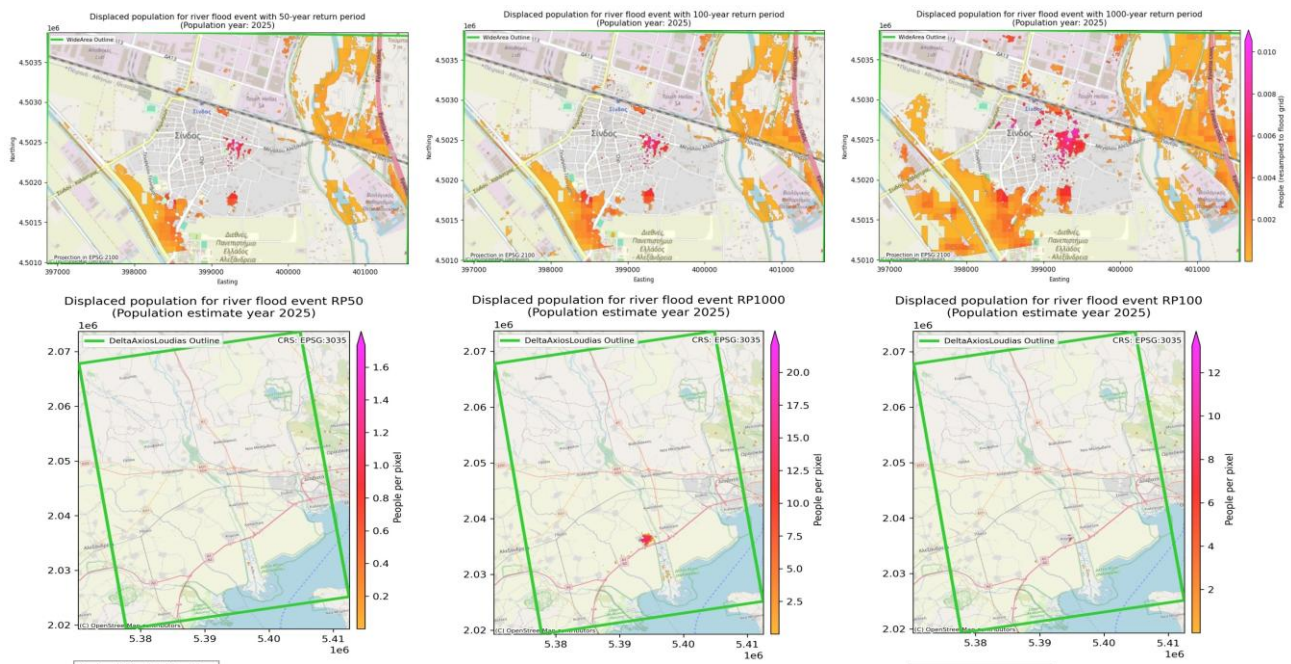


Figure 33: Displaced population for 50-, 100-, and 1000-years return periods.



2.3.2 Hazard #2 – Wildfires

The wildfire hazard and risk assessment workflow quantify hazard and risk under variables such as fire weather indicators, response surface modelling, and population exposure. Wildfire hazard is influenced by multiple climatic factors, and alterations in mean temperature and precipitation must be considered jointly to construct a reliable picture of future fire susceptibility. While increasing temperatures tend to extend the fire season, increased atmospheric moisture in a warmer climate can partially offset fire hazard, underscoring the need for a multivariate assessment. The hazard component is based on a numerical indicator of potential fire intensity that integrates weather observations such as temperature, relative humidity, wind speed, and precipitation to estimate potential wildfire severity. The workflow models the response of FWI statistics to changes in mean temperature and precipitation in relation to a baseline climate. A key metric derived as the yearly probability of exceedance of a predefined FWI threshold, expressed as a value in a continuous spectrum between 0 and 1. Higher values indicate a greater likelihood that fire danger conditions exceed the desired threshold in a given year. To model this response, a response surface is derived empirically linking perturbations in both variables to corresponding FWI exceedance probabilities. The risk component is provided by combining projected wildfire hazard with population exposure. For specified FWI thresholds, the workflow quantifies the population areas where those thresholds are exceeded and estimates the evolution of the affected population.

Datasets

The response surface is constructed from a reference dataset of historical FWI simulations. These simulations are perturbed to span mean temperature changes from 0 to +5°C and mean precipitation changes from -40% to +60% relative to the historical climate. Climate projections of yearly-mean temperature and precipitation are derived from climate indicators from 1940 to 2100 dataset, which is based on reanalysis and EURO-CORDEX climate model projections. Population

exposure is derived from a global gridded population dataset for 2020-2100. The dataset has a spatial resolution of 30 arcseconds (approximately 1 km), is consistent with shared socioeconomic pathway (SSP) national population projections. A summary of the model characteristics can be seen in the table below.

Table 12: Overview of the FWI response model: Assumptions, capabilities, and limitations.

Aspect	Description
Scenario neutrality	The model is agnostic to a range of temperature and precipitation change scenarios
Visualization	Direct visualization and analysis of the FWI exceedance probabilities is allowed
Robustness	The model predicts FWI statistics for changes that otherwise would be considered as unsuitable for direct statistical estimation
Uncertainty	Sensitivity to uncertainty along climate change trajectories can be quantified
Limitations	The index does not include land use or fuel availability; climate change by considering the selected variables is simplified (for example, other variables such as wind are excluded)
Spatial coverage	Reference data are focused on Europe and the Mediterranean region

A list of the wildfire workflows and their progress based on the first and second deliverables can be summarized in the Table below. All results are based on the data availability, especially for the regional data collection where the local sources might experience scarcity of data and data gaps.

Table 13: Workflows' data availability and progress status.

Workflow	EU data	Deliverable /Progress	Regional data	Deliverable/Progress
Wildfire (FWI)	Obtained	1/Achieved	Not available	2/ Not available
Wildfire (ML Approach)	Not available	Not available	Obtained	2/Achieved
Fire Response Model	Obtained	2/Achieved	Not considered	2/ Not available

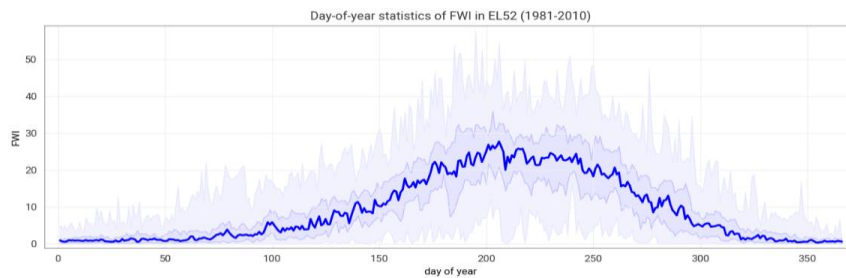
2.3.2.1 Wildfire – FWI Response Model – European data

2.3.2.1.1 Hazard assessment: historical climate

This part of the workflow focuses on data for historical time series for the RCM. The link from the CLIMAAX mirror was not always at functional mode, thus the full dataset with the thirty-six (36) GRIB files was downloaded from the Zenodo repository, using the wildcard expression given in the workflow methodology: "FWI_EU_1981_2010/FWI_T*_P*_EU_1981_2010.grib", where the wildcard character ranges from 0 up to 5 for the "T" and an interval from 0.2 to 1.6 with a 0.2 step for the "P". The primary parameters, precipitation ("dp") and temperature ("dt") perturbations, were maintained at their default values of 0 and 1.0, respectively, corresponding to no change in precipitation and no warming. Future analyses may consider parameter pairs representing extreme

scenarios, such as a 40% increase in precipitation and/or a 10°C rise in temperature, to evaluate the methodology's capacity to simulate extreme cases.

Figure 34: Day of Year Statistics of FWI in EL52 for the period from 1981 to 2010.



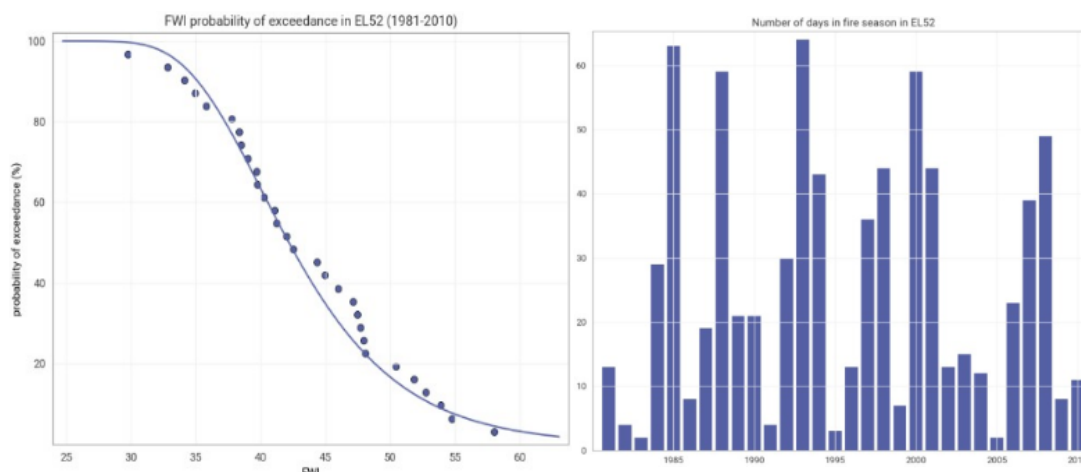
The first result of the analysis is the visualization of the yearly evolution of FWI for the selected NUTS area, as seen in Figure 34. Additionally, a table with the estimation of the return period of the max FWI in the given year can be seen in table below.

Table 14: Table of ranked years for precipitation and temperature perturbations for estimating the maximum return period of FWI (only the first ten (10) values are displayed for demonstration).

Rank	Time	FWI	PE	RP
1.0	2000	58.0	3.2	31.0
2.0	2007	54.7	6.5	15.5
3.0	1998	53.9	9.7	10.3
4.0	2008	52.8	12.9	7.8
5.0	1997	51.8	16.1	6.2
6.0	1993	50.4	19.4	5.2
7.0	2002	48.1	22.6	4.4
8.0	1989	48.0	25.8	3.9
9.0	1992	47.7	29.0	3.4
10.0	1991	47.5	32.3	3.1

This would mean that the highest value of the FWI seen in the year 1991 at the selected location was approximately 47.5, making it the 10th highest-ranking year of the full timeseries. The probability of exceedance (PE) for experiencing an FWI larger or equal to 47.5 in any given year is estimated at around 32.3% based on the data, with a corresponding return period of 3.1 years. Additionally, the probability of exceedance plot can be seen in Figure 35 below (left). The duration of the average fire season is defined as the number of days where the FWI exceeds half the values of the 20-year return period in EL52 and that is 57.5. A complementary diagram can be seen in Figure 35 (on the right side).

Figure 35: FWI probability of exceedance based on a Gumbel fitted distribution model together with the estimated probability of exceedance (left). Number of days in the fire season for EL52 (right).



2.3.2.1.2 Hazard assessment: response surface methodology

Initially, for the second part of the workflow, the selected NUTS area remains the same while the perturbed FWI simulations will be in use as introduced in the previous step, where historical hazard assessment data were considered. The given FWI threshold value was kept as the default, that of 0.6, as the trends of the values for the selected area did not show an extreme deviation from the example table values. For EL52, the input data range covers FWI values from 38.975 to 55.908. A response surface for the PE of the specified threshold was fitted using data from unperturbed and perturbed historical FWI simulations. Annual maxima of FWI from all simulations were modeled using a Gumbel distribution, which was fitted to represent the statistical behavior of extreme values. The fitted distribution was then used to compute the PE, obtained by evaluating the cumulative distribution function at the threshold and expressing the result as a percentage. The resulting two-dimensional array of PEs, defined as a function of temperature and precipitation perturbations relative to the historical climate, constitutes a discrete response surface. For convenient access and subsequent analysis, this response surface was stored as a tabulated response matrix. The response table can be seen below.

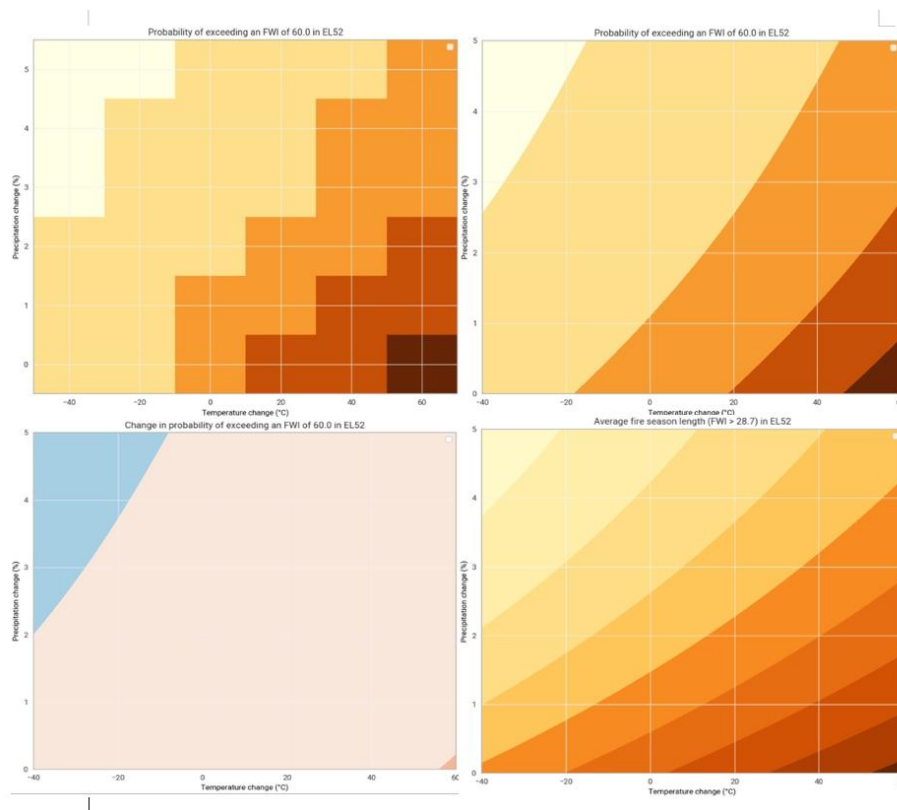
Table 15: Model output values for combined variations in perturbations of dp and dt respectively.

dt	0.0	1.0	2.0	3.0	4.0	5.0
dp						
-40.0	36.0	39.9	44.5	48.3	52.1	56.8
-20.0	30.0	33.6	37.5	41.6	45.5	48.8
0.0	25.4	28.9	32.4	36.1	39.9	43.8
20.0	22.1	25.1	28.7	32.2	35.6	39.3
40.0	19.4	22.5	25.5	28.9	32.5	35.7
60.0	17.4	20.3	23.4	26.0	30.0	33.0

From the response table, the PE of the selected FWI threshold in a given year is estimated to increase in a climate that is 2°C warmer ($dp = 0.0$, $dt = 2.0$) than the unperturbed historical climate ($dp = 0.0$, $dt = 0.0$). A warming of 5°C under otherwise unchanged precipitation conditions ($dp =$

0.0, $dt = 5.0$) is associated with a further increase in the PE to 9.9%. If temperature remains unchanged relative to the historical reference period ($dt = 0.0$) but precipitation increases by 40% ($dp = 40.0$), the PE decreases, indicating a dampening effect of increased precipitation on extreme FWI values. A precipitation increases of 60% leads to a further reduction of the PE under unperturbed temperature conditions. The response surface further reveals non-linear interactions between temperature and precipitation perturbations. For example, in a climate characterized by a 2°C temperature increase and a 40% increase in precipitation relative to the historical reference ($dp = 40.0$, $dt = 2.0$), the probability of exceedance is estimated at 4.0%. This value exceeds the probability obtained under historical precipitation conditions with the same warming, reduced by the precipitation effect alone, indicating that the combined response cannot be represented as a simple linear superposition of individual effects. Similar interaction effects are evident across the response surface, with warming increasingly dominating the PE under larger temperature perturbations, even in the presence of substantial precipitation increases. The plot of the precipitation changes for the probability of exceeding an FWI of 60.0 in EL52 can be seen in Figure 36 below.

Figure 36: Response surfaces of FWI exceedance probability and fire season length under temperature and precipitation changes in EL52.



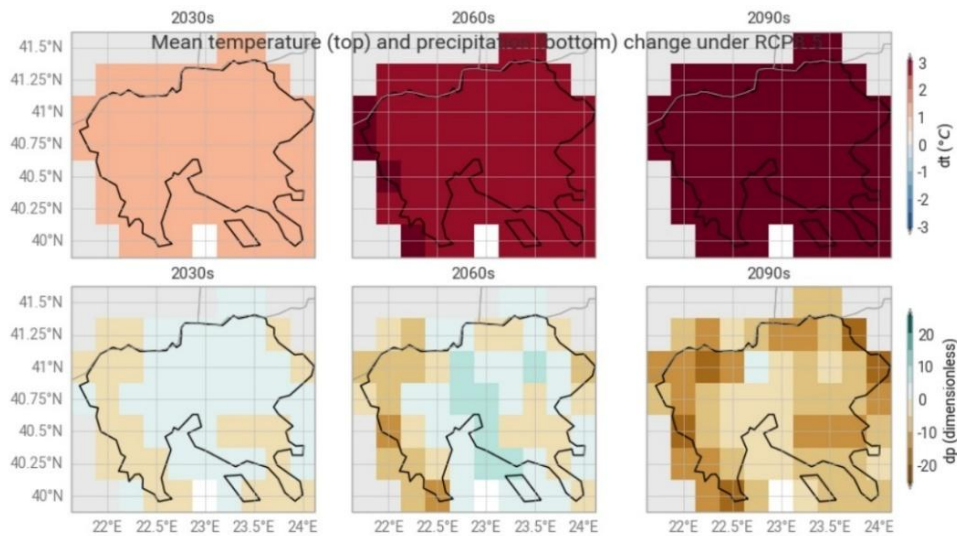
The response-surface plots illustrate how the probability of exceeding a high FWI for the EL52, and the average fire season length, respond to combined changes in temperature and precipitation. Results show that increasing temperature consistently increases the probability of exceeding critical FWI thresholds, whereas precipitation changes have a weaker and partly compensating effect. The strongest increases occur under high temperature change combined with low or neutral precipitation change. Changes relative to the historical climate indicate a systematic shift toward higher wildfire danger across most of the explored space. The average fire season length

also increases with warming, indicating longer periods of elevated fire risk under future climate conditions. The left and right panels of the first row in Figure 36 illustrate the discrete response table and its smoothed representation for the probability of exceeding an FWI threshold of 60.0 in EL52 as a function of temperature and precipitation perturbations. The left panel shows the response surface as derived from the response table. The contours of the fitted response surface provide insight into the dependencies of the estimated probability of exceedance. Predominantly vertical contours indicate that the probability of exceedance is strongly dependent on temperature changes and weakly influenced by precipitation over large parts of the space. The absence of extended horizontal contours suggests that the probability of exceedance is rarely independent of temperature, even with substantial increases in precipitation. The spacing of the contours conveys information about the strength of the response. Regions with closely(wider) spaced contours, particularly at higher(lower) temperature perturbations, indicate a strong(weaker) sensitivity of the PE to small changes in temperature. However, the mitigating effect of increased precipitation diminishes under stronger warming, as evidenced by the persistence of high exceedance probabilities at large temperature perturbations even for substantial precipitation increases. The response surface therefore provides a quantitative depiction of how wildfire hazard, as represented by the FWI, responds to concurrent changes in temperature and precipitation, highlighting the dominant role of temperature. On the left side of the second row, the change in probability of exceeding an FWI of 60.0 in EL52 (Figure 36) shows the change in exceedance probability relative to the historical climate and is consistent with the preceding response surfaces. Warming increases probabilities across most of the parameter space, while increased precipitation reduces exceedance only under limited, low-temperature conditions, confirming the dominant influence of temperature. In the right panel of the second row (Figure 36), the response surface shows that the average fire season length increases with warming and decreases with increased precipitation. As for exceedance probabilities, temperature changes dominate the response, while precipitation acts as a secondary modulating factor.

2.3.2.1.3 Hazard assessment: climate projections

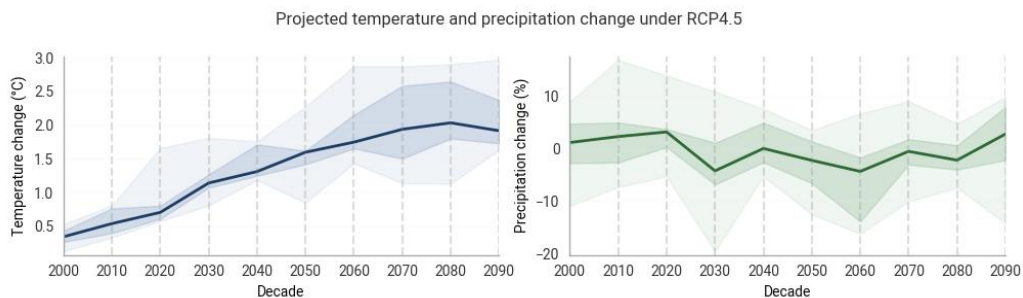
At this stage of the workflow, projections of temperature and precipitation from climate model simulations are combined with the response model developed in the earlier response-surface analysis. This approach derives projections of future wildfire hazard. Temperature and precipitation serve as driving variables because they are standard outputs of climate models and are more widely available than direct projections of fire weather indices. These are processed to compute decadal changes relative to a historical reference period. The resulting changes are then used to evaluate the response model and assess how key wildfire hazard metrics evolve under different climate scenarios and future time horizons. Figure 37 shows projected changes in mean temperature (top row) and precipitation (bottom row) for the 2030s, 2060s, and 2090s under the RCP8.5 scenario. Temperature increases are spatially consistent and intensify over time, while precipitation changes exhibit greater spatial variability, with a shift toward drier conditions by the end of the century.

Figure 37: Projected changes in mean dt and dp for RCM under RCP8.5.

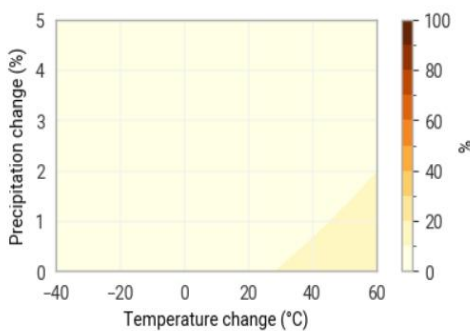


To complement the spatial maps, the figure presents regionally aggregated temperature and precipitation change over time, derived as area-weighted averages across the study region. The visualization summarizes the multi-model ensemble response and its spread across future decades under the selected climate scenario.

Figure 38: Spatially aggregated projections of temperature and precipitation change under RCP4.5.



In the next step, the fitted response surface model is loaded and sampled to verify its behavior prior to its application to climate projections. This figure shows the response surface derived from the fitted wildfire hazard model, evaluated across a range of temperature and precipitation changes.



It presents the probability of exceeding an FWI threshold of 60 as a continuous function of temperature and precipitation perturbations, obtained by sampling the trained response model. The visualization is used to verify that the loaded model seems to behave consistently with the response table and associated metadata defined in earlier workflow stages, before it is applied to projections for scenario-based analysis.

based analysis.

In the next step, where wildfire hazard projections are evaluated by overlaying climate change signals on the response surface, projections of dt and dp vary from the climate-model ensemble are overlaid on the fitted response surface to translate these signals into projected wildfire hazard.

Figure 39: EL52 | RCP8.5: Climate-projection distributions overlaid on the FWI \geq 60 exceedance response Surface (2030s–2090s).

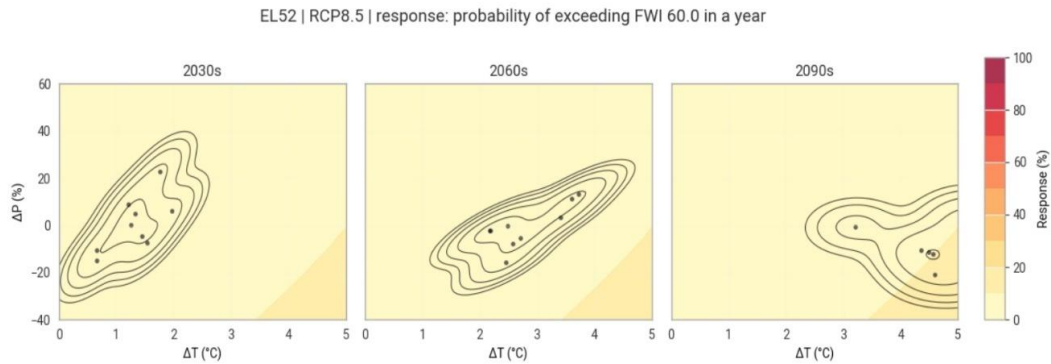
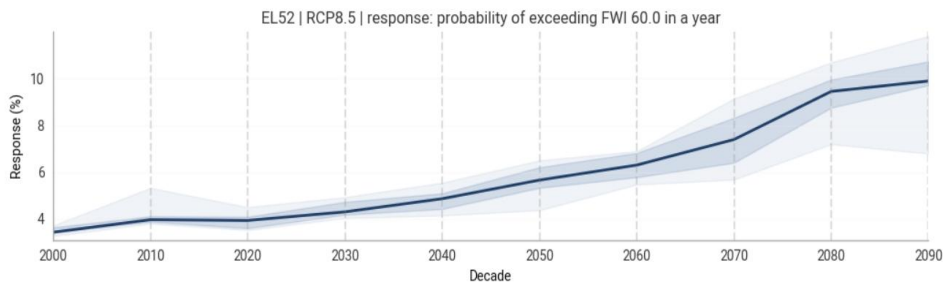


Figure 39 shows the response surface for the annual probability of exceeding an FWI threshold of 60, with decade-specific climate projection distributions overlaid as contour lines and individual climate model realizations shown as markers for the 2030s, 2060s, and 2090s. The overlays illustrate how projected temperature and precipitation changes intersect with the response surface across successive future periods. The temporal evolution of wildfire hazard under climate change is assessed by evaluating the response model with projected temperature and precipitation time series from each climate model run. The resulting plot summarizes the ensemble response over time and offers a concise representation of variability across models and decades.

Figure 40: response probability plot for exceeding FWI threshold in a year for EL52 under RCP 8.5.



The figure shows the evaluated response model output for the annual probability of exceeding FWI 60, computed by applying the response surface model to the area-weighted regional mean ΔT and ΔP time series for each climate-model run. The central line represents the median across runs for each decade, while the shaded bands indicate the interquartile range (25-75%) and the full ensemble range.

Figure 41: Ensemble statistics of spatially resolved FWI \geq 60 exceedance probability in a year, for 2000-2020s and 2030-2050s decades.

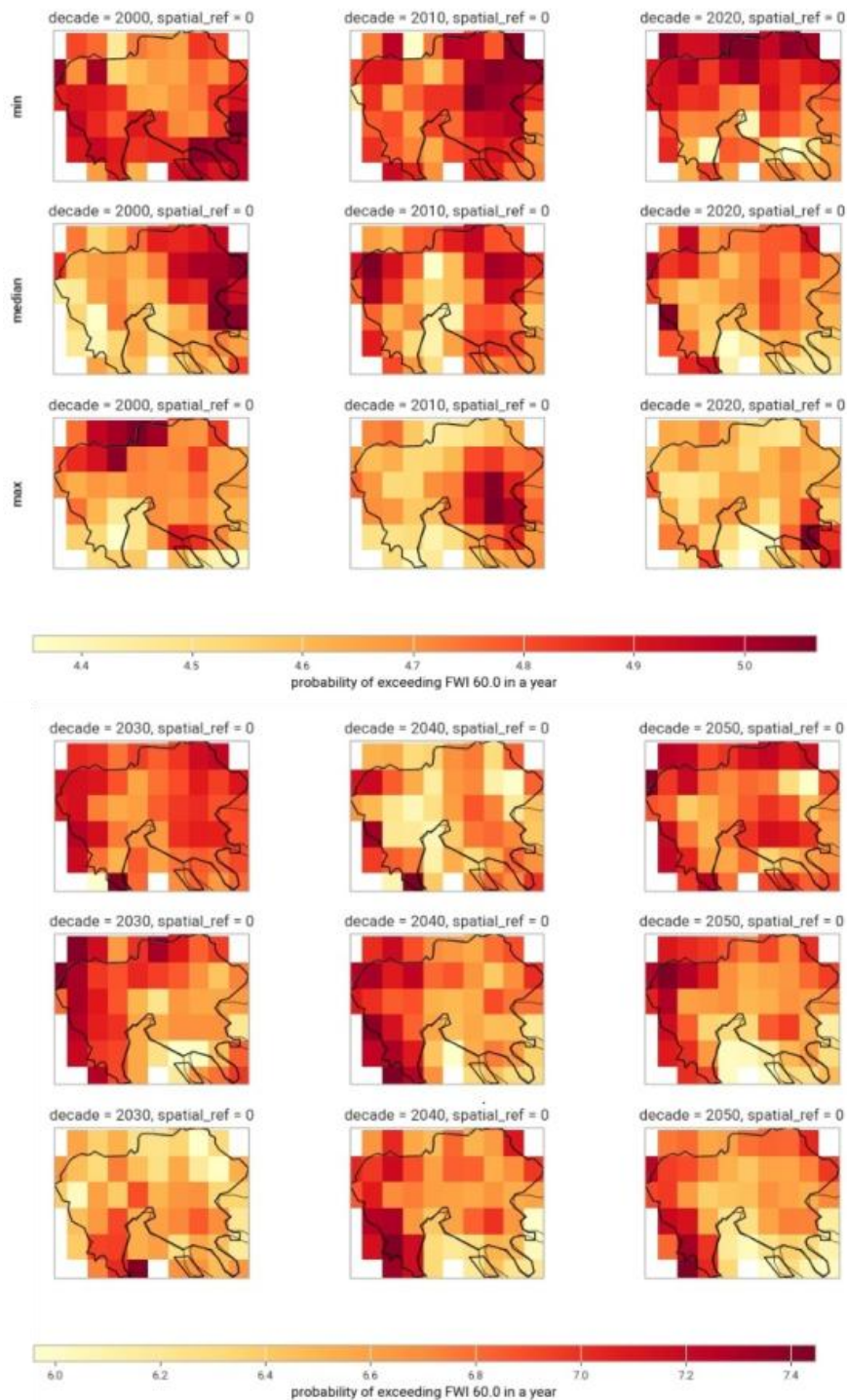
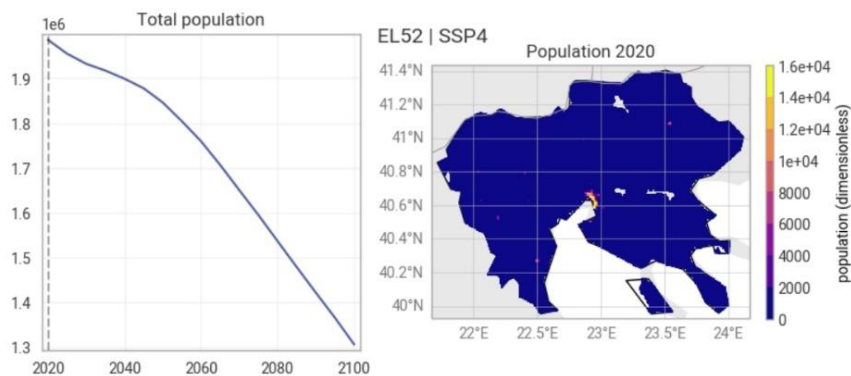


Figure 41 presents spatially resolved ensemble statistics of the evaluated response model, computed by applying the response surface independently at each grid point of the climate model data. Maps show the minimum, median, and maximum probability of exceeding an FWI threshold of 60 across the climate-model ensemble for selected decades, providing an overview of spatial variability in the projected wildfire hazard.

2.3.2.1.4 Risk assessment: affected population

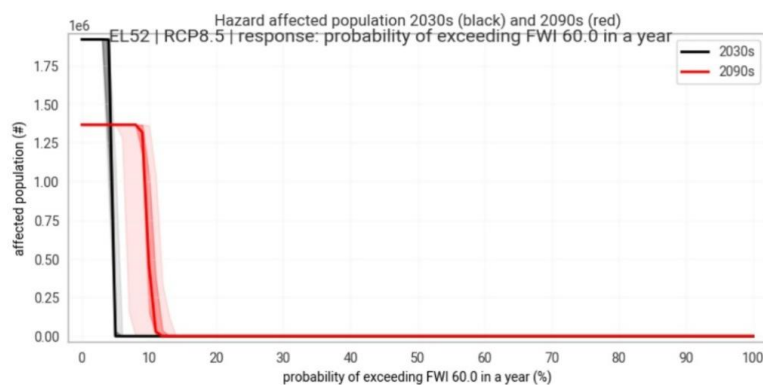
The final step of this workflow involves calculating the affected population and modeling global population distribution from 2020 to 2100 in 5-year increments under five Shared Socioeconomic Pathway scenarios (SSPs): (i) SSP1: "Taking the Green Road", (ii) SSP2: "Middle of the Road", (iii) SSP3: "A Rocky Road", (iv) SSP4: "A Road Divided", and (v) SSP5: "Taking the Highway". For this workflow, SSP4 is selected for EL52. Population data is extracted from the Zenodo¹⁵ repository, and a year coordinate is assigned based on the dataset's values. This process creates population maps for the chosen years and delineates the selected region, including data up to 2020.

Figure 42: Population distribution and projected total population change under SSP4 for EL52.



The left subfigure shows the projected evolution of total population in the region from 2020 to 2100 under the SSP4 scenario, indicating a steady decline over time up to 2100. The right subfigure shows the spatial distribution of population in 2020, with population density concentrated in urban areas (red or yellow color) and very low values across most of the region's territory (blue color and shades of blue color). In comparison with the example provided in the CLIMAAX framework, this population diagram shows a decline without any recovery and without any potential max points.

Figure 43: Affected Population as a Function of Wildfire Hazard Level (FWI ≥ 60) under RCP4.5.

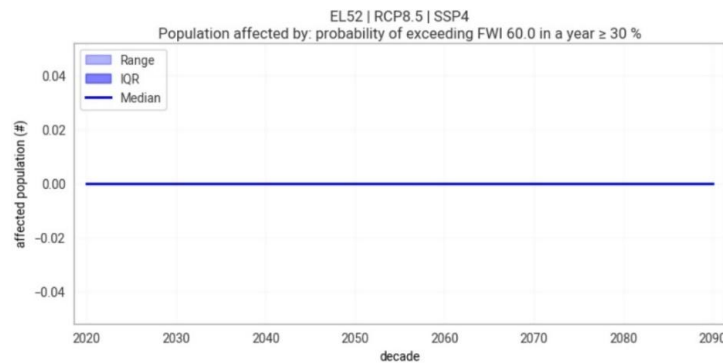


This figure shows a population-based wildfire risk assessment by combining projections of the probability of exceeding an FWI threshold of 60 with spatial population data. For selected future decades, it presents the number of inhabitants living in areas where different hazard levels are exceeded, based on climate and hazard projections. The visualization enables comparison

¹⁵ [CLIMAAX's Zenodo Repository](#).

between decades and demonstrates how changes in wildfire hazard affect population exposure across the region. Finally, in Figure 44, the total population affected for the RCP8.5 in EL52 under the SSP4 is depicted.

Figure 44: Affected Population under a High Wildfire Hazard Threshold (FWI ≥ 60 , $P \geq 30\%$).



The figure presents a time series of population affected by a wildfire hazard threshold, defined as a probability of exceeding FWI 60 of at least 30%, in EL52 for RCP8.5 under SSP4. For all decades from 2020 to 2090, the median, interquartile range, and full ensemble range of the affected population remain at zero. There is no temporal variation, indicating that none of the climate model realizations project population exposure above this threshold. Therefore, under the selected threshold (FWI ≥ 60 with probability $\geq 30\%$), no grid cells with population exceed the hazard level in any projection. This suggests the threshold is too high for this region and scenario, resulting in no population being classified as affected.

2.3.2.2 Wildfire – FWI (ML)

The wildfire risk assessment workflow uses a machine-learning (ML) framework to quantify and project fire susceptibility by integrating historical fire events with multidimensional environmental drivers. Central to this process is the Random Forest Classifier, which is trained to recognize the complex spatial relationships between past fire occurrences (from datasets such as the Forest Fire 1986–2022 inventory and for the RCM region from 2020-2024) and geophysical predictors. To ensure technical consistency, all datasets including the Digital Elevation Model (DEM) used to derive slope, aspect, and roughness are reprojected to a metric coordinate system (EPSG:2100 for Greece) and harmonized to a standard 100-meter resolution via resampling. The ECLIPS-2.0 dataset, a high-resolution gridded climate resource for Europe, significantly enriches the hazard assessment. This dataset provides 80 distinct annual, seasonal, and monthly climate variables, such as Mean Warmest Month Temperature (MWMT) and Summer Precipitation (PPT_sm), across historical (1961–2010) and five future periods (up to 2100). By utilizing two greenhouse gas concentration scenarios (RCP 4.5 and 8.5), the workflow projects how shifts in climate indices will alter future fire susceptibility. Furthermore, the workflow incorporates CORINE Land Cover data as a critical proxy for fuel availability. During the preprocessing stage, land cover rasters are reclassified into "burnable" and "non-burnable" categories to mask out waterbodies and urban centers, ensuring the machine learning model focuses only on viable fuel sources. The final transition from susceptibility (the likelihood of a fire starting) to hazard (the potential intensity) is achieved by considering different plant functional types. This processed hazard map is ultimately intersected with exposure layers, such as residential infrastructure or critical road networks,

through a contingency table approach to produce a definitive Risk Index (1–4), facilitating evidence-based climate adaptation and regional disaster management.

Data availability and dataset creation

The RCM dataset was developed based on the structure of the Catalonia example dataset. All files and datasets were organized according to the workflow's folder structure. The components are described below:

- **Boundaries:** Shapefiles for Thessaloniki were created using GIS software and data from the NUTS website ("NUTS_RG_01M_2024_3035.shp.zip"). The bounding box was verified to represent the RCM accurately.
- **Climate:** The following files, as listed in the Catalonia example, were downloaded and used for the RCM dataset: "ECLPS2.0_199110" or "HIST_199110", "CLMcom_CLM_4.5", and "CLMcom_CCLM_4.5". Files were modified as needed during workflow execution.
- **DEM:** The original YPEN regional DEM data were used. Due to hardware limitations, processing the entire RCM region was not feasible. Therefore, a modified, clipped version of the original DEM was used.
- **Exposure:** All exposure data were obtained in QGIS using the QUICKOSM plugin, applying the relevant OSM tags to each feature (e.g., highway=primary, amenity=school, etc.). Shapefiles were clipped and reprojected to EPSG:2100 as required.
- **Fires:** A dedicated dataset was created using local historical fire data for the RCM from 2020 to 2024. The shapefile was projected to EPSG:2100. For the creation of the historical fire dataset, records were downloaded from the official [Fire Brigade website](#), where data are provided in .xls and .xlsx formats. Although data are available from 200-2012 onward, only records from 2020 onward are georeferenced with x and y coordinates, making them suitable for spatial analysis. The files were cleaned to retain only relevant rows, then merged into a new .xls file. A shapefile was generated to match the keywords specified in the CLIMAAX workflow. The shapefile was subsequently projected to EPSG:2100 and used as the layer for Step 6 of the workflow. For all purposes QGIS software was used when needed.
- **Land cover:** The LUISA Land Cover dataset, as "U2018_CLC2018_V2020_20u1," was used, sourced from the Copernicus Store via the Corine Land Cover 2018 website.
- **Vulnerability:** All vulnerability layers and the burned area map (Sentinel-2/MODIS images) were downloaded from the [EFFIS website](#), using the data provided through the EFFIS data request form.

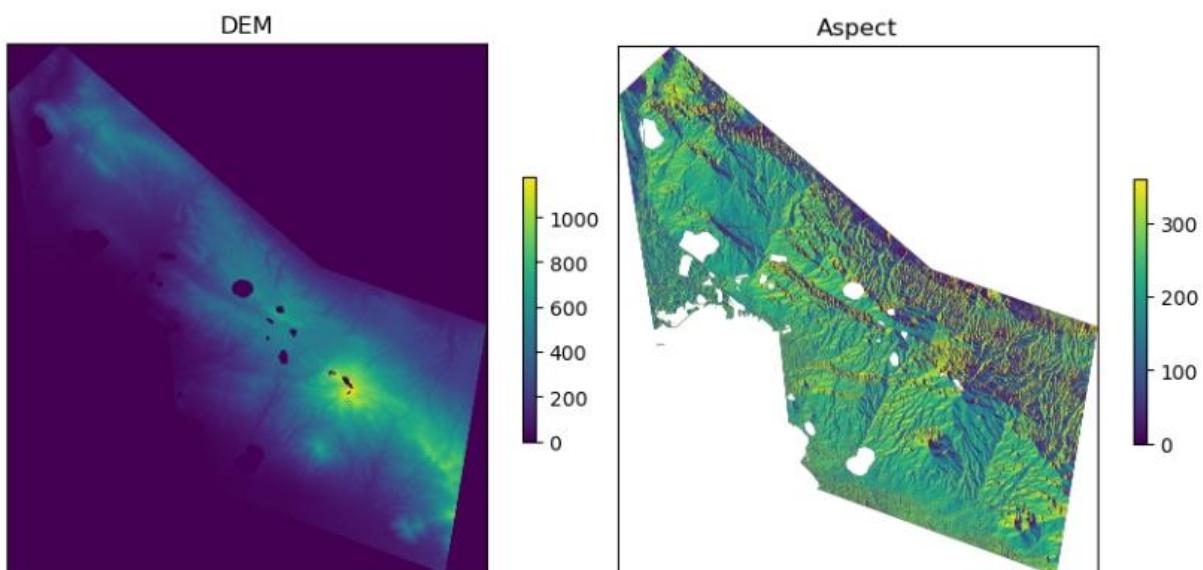
2.3.2.2.1 Hazard assessment (ECLIPS)

The wildfire risk assessment workflow uses a machine-learning (ML) framework to quantify and project fire susceptibility by integrating historical fire events with multidimensional environmental drivers. Central to this process is the Random Forest Classifier, which is trained to recognize the complex spatial relationships between past fire occurrences (from datasets such as the Forest Fire 1986–2022 inventory and for the RCM region from 2020-2024) and geophysical predictors. To ensure technical consistency, all datasets, including the Digital Elevation Model (DEM) used to

derive slope, aspect, and roughness, are reprojected to a metric coordinate system (EPSG:2100 for Greece) and harmonized to a standard 100-meter resolution via resampling. The ECLIPS-2.0 dataset, a high-resolution gridded climate resource for Europe, significantly enriches the hazard assessment. This dataset provides 80 distinct annual, seasonal, and monthly climate variables, such as Mean Warmest Month Temperature (MWMT) and Summer Precipitation (PPT_{sm}), across historical (1961–2010) and five future periods (up to 2100). By utilizing two greenhouse gas concentration scenarios (RCP 4.5 and 8.5), the workflow projects how shifts in climate indices will alter future fire susceptibility. The workflow also integrates CORINE Land Cover data as a key proxy for fuel availability. During preprocessing, land cover rasters are reclassified into "burnable" and "non-burnable" categories to exclude water bodies and urban areas, ensuring the machine learning model focuses exclusively on viable fuel sources. The transition from susceptibility (the likelihood of fire ignition) to hazard (potential fire intensity) is accomplished by incorporating different plant functional types. The resulting hazard map is intersected with exposure layers, such as residential infrastructure and critical road networks, using a contingency table approach to generate a definitive Risk Index (1–4). This process supports evidence-based climate adaptation and regional disaster management.

The regional dataset compiled for the RCM was utilized to implement the CLIMAAX FWI-based wildfire hazard workflow in a reproducible manner. Data acquisition and preprocessing were conducted in GIS software, and modelling was executed according to the CLIMAAX stepwise structure. Historical wildfire events were obtained from the Fire Brigade website; these records are officially georeferenced and include x–y coordinates, which enabled direct spatial integration and rasterization on the analysis grid. A DEM provided by YPEN was prepared as a core topographic input by clipping it to the RCM extent and reprojecting it to reduce file size and computational burden. Terrain derivatives, including aspect, were generated to support subsequent modelling and are reported in Figure 45.

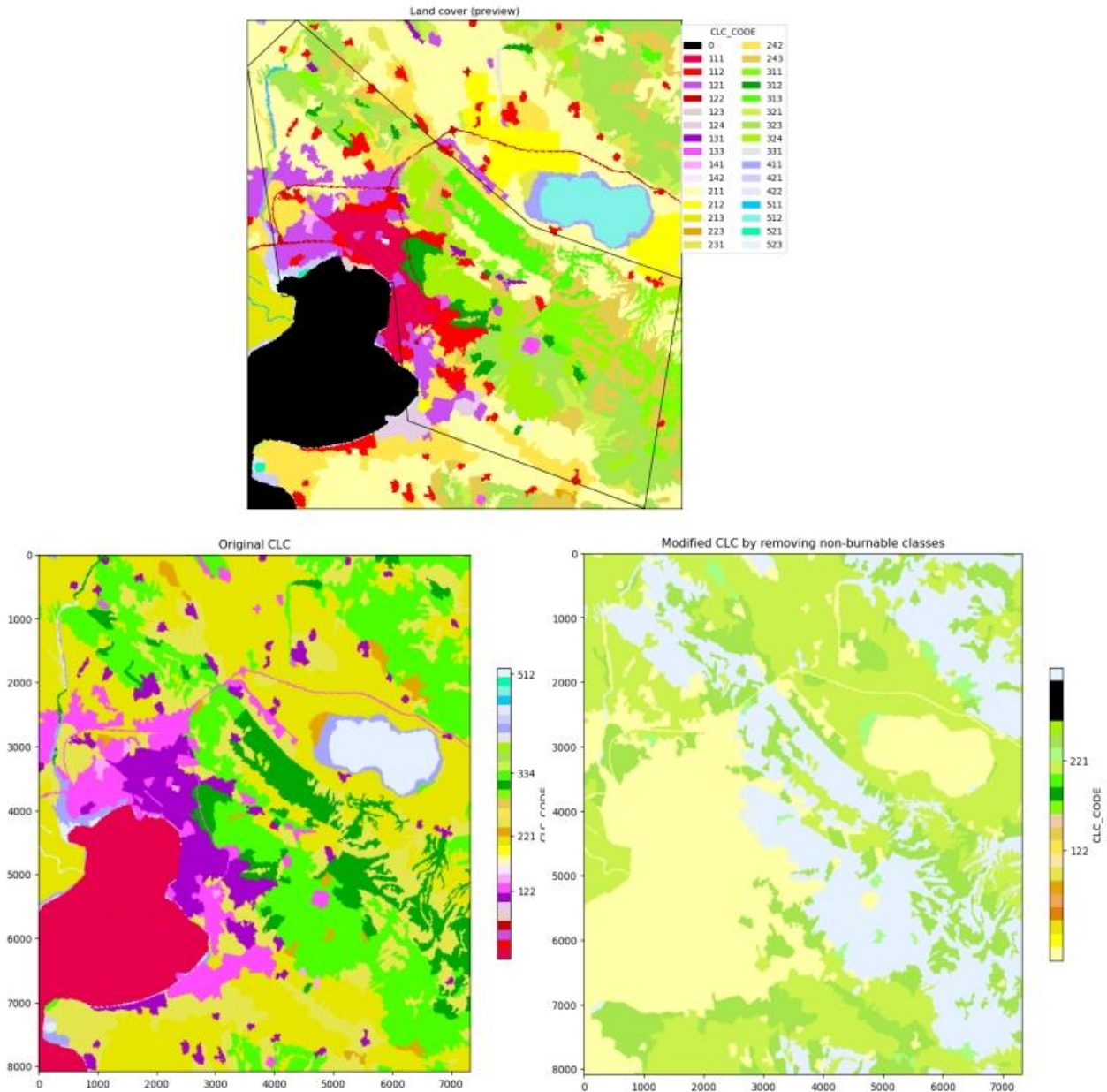
Figure 45: DEM and Aspect figures for the selected area of Thessaloniki.



Climatic predictors were sourced from ECLIPS-2.0 and assembled into the CLIMAAX input set. These included summer-oriented temperature descriptors (MWMT, TD, DD_{below0}, DD_{above18}, MAT, Tave_{sm}, Tmax_{sm}), summer heat–moisture interaction indices (AHM, SHM), and

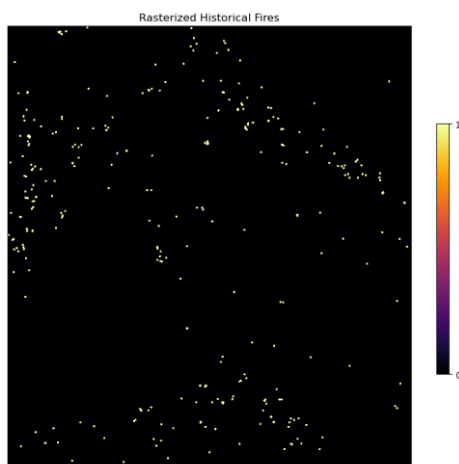
precipitation descriptors capturing totals and seasonality (MAP, PPT_at, PPT_sm, PPT_sp, PPT_wt). The historical training baseline was set to hist_period = "199110" (1991–2010), one of the two ECLIPS-2.0 historical periods available, with the other being 1961–1990. Land cover was prepared from CORINE Land Cover (CLC) through the creation of the original land-cover layer, a raster in which non-burnable classes were set to zero, and a modified CLC where non-burnable classes were removed, as illustrated in Figure 46.

Figure 46: Figure of the Land Cover map (top), and the original and modified CLC (down).



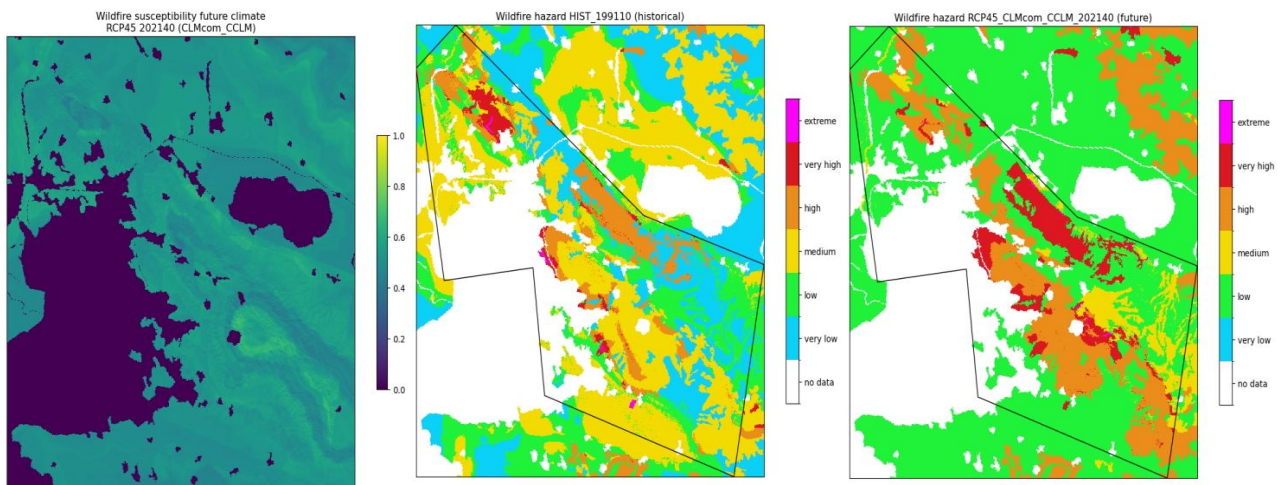
The rasterized historical fire layer used for model development is shown in Figure 47.

Figure 47: Rasterized historical fires map. The sparsity of the map is related to the number of fire events occurred in the selected area of Thessaloniki in the given period between 2020 and 2024.



The modelling implementation adhered strictly to the CLIMAAX workflow, including the definition of a raster-handling structure to standardize paths and metadata and the assembly of the raster input collections required by the model. In Step 8 (Historical climate), the machine-learning model was trained on historical conditions and applied to generate a susceptibility surface using a Random Forest classifier with probabilistic output. Because susceptibility values are bounded between 0 and 1, interpretation and subsequent classification relied on extracting the specific quantiles from the non-negative susceptibility distribution to define meaningful thresholds consistent with the model's probability scale. The resulting susceptibility map for the historical (present) climate is presented in Figure 48 (Wildfire susceptibility, Historical Climate; ECLIPS2.0). Future projections were generated using ECLIPS-2.0 climate model inputs derived from bias-corrected EURO-CORDEX simulations selected to represent available RCM-GCM combinations and driven under RCP4.5 and RCP8.5. For this analysis, the future configuration was specified as `future_scenario = "RCP45"`, `future_period = "202140"` (2021–2040), and `climate_model = "CLMcom_CCLM"`. The corresponding climate fields were downloaded, spatially subset to the study region, and reprojected to align with the prepared DEM grid. The trained model was then projected onto the future climate inputs to produce a future susceptibility surface (Figure 48; Wildfire susceptibility, future climate for RCP4.5). In Step 10 (Hazard), hazard was derived by combining susceptibility with an intensity representation based on fuel type, produced by converting the modified CLC to aggregated fuel categories using a dedicated correspondence table. Hazard classes were then generated and visualized for both the historical baseline (`hist_199110`) and the selected future scenario (RCP4.5; CLMcom_CCLM; 202140), enabling a consistent comparison of wildfire hazard between present and future climate conditions (Figure 48).

Figure 48: Wildfire susceptibility and hazard mapping for the RCM under historical climate (1991–2010) and future scenario RCP4.5 (2021–2040; CLMcom_CCLM). (left) Wildfire susceptibility (probability) under future climate: RCP4.5, 2021–2040 (CLMcom_CCLM). (middle) Wildfire hazard classes under historical climate: 1991–2010 (HIST_199110). (right) Wildfire hazard classes under future climate: RCP4.5, 2021–2040 (CLMcom_CCLM).



2.3.2.2.2 Risk assessment

The wildfire risk assessment notebook presents a systematic methodology for quantifying absolute wildfire risk by integrating machine learning-based hazard data with vulnerability and exposure layers. Figure 49 employs a standardized color scale ranging from green (low) to yellow (moderate), orange (high), and red (very high) to illustrate the spatial overlap of fire threats with human and environmental assets. Initial figures display Vulnerability and Sensitivity Maps, which classify the fragility of population, economic, and ecological sectors using JRC data. These maps often convert continuous percentile data into discrete grid classes to facilitate computational analysis. Subsequent figures depict exposure and asset layers, identifying specific at-risk elements such as hospitals, schools, hotels, and rasterized road networks derived from OSM data. The primary visual outputs are integrated risk grids that represent the $Risk = Hazard \times Vulnerability \times Exposure$ calculation and provide side-by-side comparisons of historical and projected climate scenarios to highlight areas where increasing hazards coincide with high vulnerability. The workflow concludes with Administrative and Infrastructure risk figures that aggregate pixel-level results into NUTS3 boundaries and municipal zones. Additionally, specialized maps evaluate risk to primary, secondary, and tertiary transportation routes to inform regional evacuation and emergency planning. In Figure 49 the vulnerability indicators can be seen. The figure illustrates the transition from raw environmental data to actionable wildfire risk indicators by processing JRC vulnerability products for population, economy, and ecology. The first figure displays the continuous vulnerability maps, showing raw sensitivity scores clipped and resampled to the specific resolution and extent of the study area (e.g., Thessaloniki) using a bilinear method for visual clarity. The second figure demonstrates the categorized vulnerability, where these continuous values are reclassified into discrete "Low," "Medium," and "High" classes based on defined thresholds. This transformation is a critical preprocessing step, converting complex percentile data into a standardized format that can be mathematically intersected with wildfire hazard levels to produce the final risk assessment.

Figure 49: Vulnerability indicators for Thessaloniki (100 m resolution): continuous normalized surfaces and three-class categorical maps (population, economic, ecological).

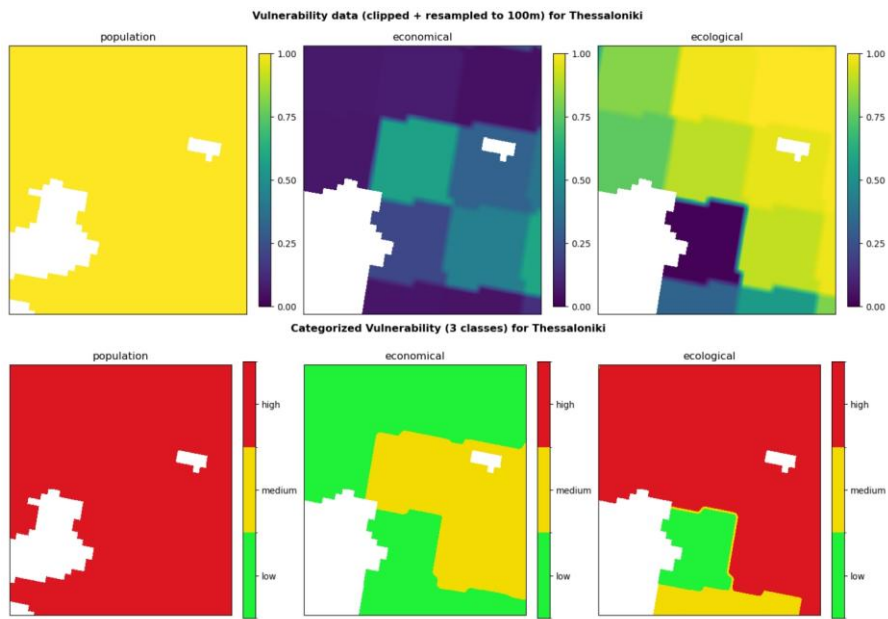


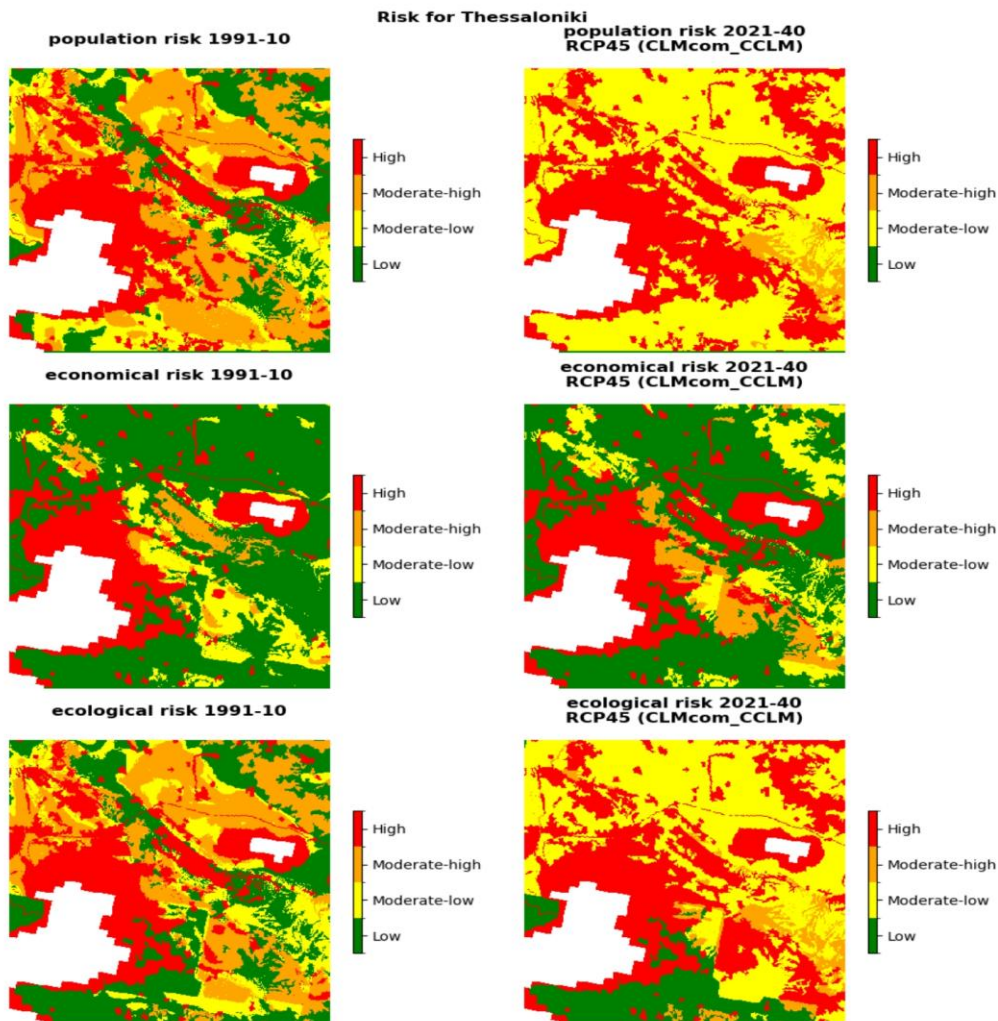
Figure 50 shows the exposure assessment phase. Vector data from OSM, including hospitals, schools, and roads, is mapped as point and line layers to display asset distribution. These layers are then converted into rasterized exposure data, creating a 100m-resolution binary grid that aligns with the hazard and vulnerability maps.

Figure 50: Exposure datasets for Thessaloniki used in the risk analysis, shown as (top) vector layers and (bottom) rasterized previews within the study-area boundary, including point-based assets (hospitals, hotels, schools, shelters) and road network classes (primary, secondary, and tertiary roads).



Figure 51 presents the main results of the wildfire risk assessment. These results were produced by intersecting categorized vulnerability layers with machine learning hazard maps using a 3x4 contingency matrix. The side-by-side maps compare historical and future risk levels for population and economy, using a standard four-class color scale from Green (Low) to Red (High). This visualization highlights geographic hotspots where changing climate conditions are expected to increase the socio-economic impact of wildfires.

Figure 51: Wildfire risk maps for Thessaloniki under historical (1991–2010) and future (2021–2040, RCP4.5; CLMcom_CCLM) climate conditions, showing categorized risk levels (low, moderate-low, moderate-high, high) for three vulnerability dimensions: population (top row), economic (middle row), and ecological (bottom row).



2.4 Key Risk Assessment Findings

The Key Risk Assessment step reviews the results from Phase 2 by considering three main factors: the severity of the impacts, the urgency of action based on future risks and hazards, and the local strategy's ability to anticipate, respond to, and recover from challenges. This evaluation followed the CLIMAAX approach. The results are intended to be examined with decision-makers, experts, and focus groups, helping to determine the importance of risk management and adaptation.

2.4.1 Mode of engagement for participation

Risk evaluation engagement in Phase 2 involved targeted coordination with institutional stakeholders in climate risk management and Civil Protection. Discussions included the RCM, the Decentralized Administration of Macedonia and Thrace, the Ministry of Environment, Civil Protection services, and senior regional Fire Service leadership. Engagement consisted of one in-person meeting and follow-up emails. Feedback highlighted the relevance of wildfire risk metrics, the need for clear and interpretable outputs, and improved access to regional datasets (See also Section 2.6). Stakeholders showed interest in applying the results to operational planning and confirmed their intention to participate more actively in Phase 3, especially to integrate CLIMAAX outputs into preparedness and response strategies.

2.4.2 Gather output from Risk Analysis step

Risk evaluation in Phase 2 uses outputs from the Risk Analysis step for both fluvial flooding and wildfires. For river flooding, outputs include projections of river discharge indicators derived from European-scale climate inputs, supporting qualitative assessment of flood hazard evolution under current and future conditions. For wildfires, outputs include response-surface-based projections of the probability of exceeding an FWI threshold, plots showing temporal evolution across climate model ensembles, maps of minimum, median, and maximum hazard levels, and population-based exposure estimates combining hazard projections with SSP-based population data. Together, these outputs support comparisons of hazard severity over time, assessments of uncertainty across climate projections, and evaluations of potential impacts on exposed populations, providing a common evidence base for risk prioritization across hazards.

2.4.3 Assess Severity

Hazard	Severity
River flooding	Significant
Coastal flooding	Moderate
Wildfires	Critical

River Flooding: currently, constitutes a substantial climate risk, with projections indicating a shift to critical under future scenarios. Historical records and hazard maps document recurrent inundation in major river basins, severely affecting agricultural floodplains, transportation networks, and human settlements. Quantitative flood hazard maps across return periods reveal pronounced

vulnerabilities in low-elevation, high-exposure zones. Future projections underscore a marked escalation. In the Strymonas (EL11) and Axios (EL10) basins, modelled economic damages are estimated at a few billion under RCP4.5/8.5 scenarios, driven primarily by inundation of permanently irrigated lands and rice paddies. These losses threaten agricultural productivity, industrial operations, and urban functionality. Beyond direct impacts, flooding induces irreversible effects (including but not limited to soil salinization, permanent loss of arable land, and wetland degradation) along with cascading failures in critical infrastructure. Insights from regional technical services and civil protection authorities affirm that intensifying extreme events are overwhelming recovery capacities, justifying the critical future classification. **Wildfires:** Wildfire susceptibility in the RCM presently merits a substantial rating, evidenced by recurrent ignitions, persistent high-risk zones, and documented effects on forests, agroforestry systems, and peri-urban areas. FWI analyses and historical burn data delineate stable, alongside elevated risks in mixed-use landscapes exacerbated by agricultural abandonment and fuel accumulation. Projections anticipate intensified severity from rising temperatures, and prolonged fire seasons.

While current impacts remain relatively localized compared to flooding, the rising frequency of extreme FWI conditions elevates specific hotspots to critical status. Fire management authorities highlight strained suppression resources under future regimes and underscore decision-makers' grasp of evolving fire dynamics.

2.4.4 Assess Urgency

Hazard	Urgency
River flooding	Action needed
Coastal flooding	Monitoring needed
Wildfires	Action needed

River flooding: as a rapid-onset hazard, river flooding delivers acute impacts over short timescales. High-damage events are feasible under extant climate variability, with severity set to rise imminently. Urgent priorities encompass reinforcing flood defense infrastructure, rigorous enforcement of land-use planning, and elevating preparedness in vulnerable locations. This classification

accounts for both ongoing disruptions and projected near-term risk amplification. All urgency considerations refer to single hazard events following CLIMAAX workflows. Compound or cascade events cannot be excluded as additional hazards whose urgency must be considered in climate resilience discussions. **Wildfires:** Wildfire risk integrates gradual precursors such as land-use shifts, and fuel loading with high-consequence events post-ignition. Empirical trends predict deterioration within a few years, marked by earlier fire season onset and extended duration. Thus, the sparsity of the available datasets with geolocations of the historical fires, points towards a limitation for training datasets for data-driven models.

2.4.5 Understand Resilience Capacity

The RCM exhibits medium resilience to flooding and wildfires, underpinned by established civil protection frameworks, flood risk strategies, and fire response protocols from prior regional and national initiatives. Natural buffers, including wetlands and forested floodplain zones, complemented by extant infrastructure. Persistent constraints temper this capacity. Vulnerabilities persist in exposed infrastructure, while nature-based solutions remain underexploited in management paradigms. Interdepartmental coordination and structured stakeholder involvement warrant strengthening. Integration of CLIMAAX methodologies marks a pivotal enhancement, supplying refined spatial risk profiles, informed investment pathways, and the embedding of CLIMAAX outputs into policy could elevate resilience to substantial levels in the ensuing phases (see also Section 2.6).

2.4.6 Decide on Risk Priority

A risk priority table was assigned by combining severity and resilience capacity results, and by integrating stakeholder feedback on critical assets. The prioritization was performed at the regional scale, with the intention that the ranking be validated and refined through subsequent engagement activities, including public-facing dialogue mechanisms when regional data will be included. This table merely offers a qualitative approach; it is not a dedicated synthetic table that accounts for more detailed information on each hazard, its combinations, or even compound or cascade events.

Table 16: Risk priority table for the selected hazards for the RCM.

Hazard	Severity Current/Projected	Planning	Resilience	Priority
Fluvial floods	Low-Moderate/Moderate	Increase preparedness	Low	High
Pluvial floods	Moderate/Moderate-High	Increase preparedness	Low	Medium
Coastal floods	Low-Moderate/Moderate	Monitoring	Medium	Medium
Wildfires	High/High	Informed action plans	Low	Very High

2.5 Monitoring and Evaluation

Phase 2 improves the applicability of decisions by structuring the assessment for regionalization within the CLIMAAX framework. It enables integration of regional data and indicators and ensures a consistent baseline assessment using EU datasets. A significant challenge was limited access to regional datasets, as government agencies did not respond to data requests within the project timeframe. As a result, implementation relied on a specific set of workflows based on regional and EU data, including but not limited to river flood discharge estimation and an FWI response model. Both were applied at the regional scale to compare flood and wildfire hazard patterns under current and future climate conditions. Standardized EU datasets ensured methodological consistency and reproducibility. Phase 2 clarified the value of regional data for increasing spatial detail and decision relevance, and defined the technical and institutional requirements for future integration. Overall, Phase 2 established a structured baseline and a clear pathway for further regional refinement, while maintaining transparency and coherence. Next steps include expanding workflows to incorporate regional data as it becomes available, further enhancing the accuracy and utility of the assessment for the most vulnerable areas of the RCM.

2.6 Work plan Phase 3

The third phase will use the European and regional data collected so far, together with the calculated indicators and maps produced for wildfires and floods. A series of joint working sessions will be organized with local and regional units, including Civil Protection and other relevant authorities, to review the maps and agree on priority risk areas and key findings. These sessions will focus on discussing feasible adaptation measures and how the identified priorities can be integrated into existing climate resilience and adaptation strategies. The phase will not address new hazard modelling or detailed impact assessments, as the emphasis is on consolidating results and supporting practical follow-up by authorities. Additionally, when needed, CLIMAAX workflows for floods and wildfires will be considered, to study case study area, on specific regions that specialists consider as prone to climate disasters. Finally, a discussion on data gaps and on the applicability and transferability of regional data in combination with currently available European databases will be considered for further evaluation.

3 Conclusions Phase 2- Climate risk assessment

Phase 2 demonstrates that the CLIMAAX workflows for river floods (flooding maps), river flood discharges, Fire Weather Index (FWI) machine learning hazard and risk assessment, and FWI-based wildfire hazard are consistently applicable at the regional scale and provide a coherent analytical framework for climate risk assessment in the RCM. The results indicate that European Union datasets are adequate for establishing a common baseline, assessing climate sensitivity, and comparing hazard variation, while maintaining methodological transparency and consistency. Although integrated regional datasets are included, the results remain primarily hazard-focused and indicative, requiring further calibration to local exposure, vulnerability, and damage data. Consequently, conclusions regarding absolute risk levels, location prioritization, and cost-effective adaptation measures remain provisional and are expected to evolve. Data gaps are particularly evident for regional datasets, which are often limited or dispersed across various government agencies, complicating data collection. Nevertheless, the combined use of regional and European datasets offers a robust foundation for enhancing regional climate resilience strategies. While the workflows currently address single-hazard events, consideration of compound and cascading events is essential in future strategy development among regional and municipal climate resilience authorities. The CLIMAAX workflows provide a transferable set of tools for all hazards studied. The open-source nature of the language and datasets facilitated modifications that improved the usability of the available code. Ultimately, Phase 2 establishes a baseline and initiates further engagement with authorities and stakeholders in the subsequent phase, while allowing for additional workflows tailored to specific case studies within the RCM.

Phase 3 will be better positioned to support targeted, climate resilience-oriented decision-making for the RCM. Phase 2 provides clarity by identifying areas where regional data can enhance accuracy, specifying which workflow components benefit most from local refinement, and outlining how future analyses can transition efficiently from hazard screening to risk evaluation. This establishes a robust technical and organizational foundation for Phase 3, during which the integration of pending regional datasets will be critical to operationalizing the analytical system for regional planning, civil protection, and adaptation decision-making.

4 Progress evaluation

This phase focused on selecting available data from regional and local sources and fully implementing the CLIMAAX methodology in the RCM. This approach produced valuable outputs for both flood and wildfire risk workflows. All hazard, exposure, and vulnerability datasets were processed, and key outputs, such as spatial risk maps and quantitative damage assessments, were delivered as planned. The tables below summarize the achieved Key Performance Indicators (KPIs) and milestones for this reporting period. These results will inform adaptation planning, measure prioritization, and regional engagement in the next project stage. The work completed to date ensures technical readiness for integrating climate risk outputs into operational and strategic frameworks at the regional level.

Table 17: Overview key performance indicators.

KPIs	Progress
T2.1. Collection of regional data and addressing any data gaps. Integration of regional data categories and resolution of any data gaps – Use all the collected regional datasets for at least two (2) different types of climate risks – Three (3) stakehold	A vast majority of possibly available data was collected. KPI is fulfilled.
T2.2 Application of the framework for the improved risk assessments – Measurement of the CLIMAAX’s effectiveness in improving the quality of risk assessments. The task will produce maps, for at least two (2) different types of climate risks showing exp	Newly added workflows were validated. KPI is fulfilled.

Table 18: Overview milestones.

Milestones	Progress
CLIMAAX Workshop BCN	Milestone has been reached.
Regional Data Verification and Collection Completion	A vast majority of possibly available data was collected. Milestone has been reached.
Enhanced risk management	Newly added workflows were validated. Milestone has been reached.

5 Supporting documentation

Regional data and links of the sources, technical data, analytical results, or visual materials produced at this deliverable have been included and described in this deliverable, following the detailed step-by-step process as given in the CLIMAAX framework. Accordingly, no additional, shareable, and transferable datasets or outputs have been generated to date that would qualify for publication on Zenodo or other open-access repositories. All data were sourced from regional or governmental repositories after request. A number of the regional data can be considered as open-source by the governmental entities, but there is no rationale for all available data. Some of the data were obtained through an official request from RCM. If the technological implementation generates any extra relevant outputs, these will be recorded, appropriately curated, and shared in the Zenodo repository in compliance with the project's open science and data management guidelines. Upon request by the CLIMAAX consortium, all materials, including visual outputs, communication pieces, and structured datasets will be prepared and shared accordingly as the project advances into its next stage(s). Outputs produced during this stage:

- Main report for Phase 2,
- Visual outputs for both floods and fire hazards, including figures and *.geotiff* files.
- Regional datasets: no specific reproducible and transferable datasets were produced. The dataset for the FWI-ML workflow was based on national data for fire events including the RCM, however, it is only a *.geotiff* file and it cannot be used for/transferred to any other region other than the RCM.

All produced materials are available, and when needed can be uploaded and classified in the Zenodo repository, following the required format and standards for open-access dissemination. RCM, and the external collaborator (CDXi), remain dedicated to the FAIR data initiative supporting the open sharing of “Findable, Accessible, Interoperable, and Reusable” data.

6 References

Berg, P., Photiadou, C., Bartosova, A., Biermann, J., Capell, R., Chinyoka, S., Fahlesson, T., Franssen, W., Hundecha, Y., Isberg, K., Ludwig, F., Mook, R., Muzuusa, J., Nauta, L., Rosberg, J., Simonsson, L., Sjökvist, E., Thuresson, J., and van der Linden, E., (2021): Hydrology related climate impact indicators from 1970 to 2100 derived from bias adjusted European climate projections. Copernicus Climate Change Service (C3S) Climate Data Store (CDS). DOI: 10.24381/cds.73237ad6.

Isberg, K. (2017). EHYPE3_subbasins.zip [Dataset]. Zenodo. <https://doi.org/10.5281/zenodo.581451>.

CLIMAAX: Deliverable 1.4 – Climate risk assessment framework. WP1 – Framework for local and regional climate risk assessment. [CLIMAAX – Horizon Europe, Grant Agreement No. 101093864]. Available at: https://files.cmcc.it/climaax/Deliverables/CLIMAAX_D1.4_Climate%20Risk%20Assessment%20Framework_revised.pdf, 2023.

CLIMAAX: Deliverable 2.1 – Report on the specifications for toolbox methods. WP2 – Co-design of the supporting toolbox. [CLIMAAX – Horizon Europe, Grant Agreement No. 101093864]. Available at: https://www.climaax.eu/wp-content/uploads/2023/07/CLIMAAX_D2.1_v3_corrected.pdf, 2023.

CLIMAAX: Deliverable D2.2 – Report on hazard tools of relevance to the CRA Toolbox. WP2 – Co-design of the supporting toolbox [CLIMAAX – Horizon Europe, Grant Agreement No. 101093864]. Available at: https://www.climaax.eu/wp-content/uploads/2024/07/CLIMAAX_D2.2.pdf, 2024.

CLIMAAX: Deliverable D2.3 - Report on pan European vulnerability and exposure projections. WP2 – Co-design of the supporting toolbox. [CLIMAAX – Horizon Europe, Grant Agreement No. 101093864]. Available at: https://www.climaax.eu/wp-content/uploads/2024/07/CLIMAAX_D2.3.pdf, 2024.

CLIMAAX: Deliverable D2.4 – Report on integrated risk assessment tools of relevance to the CRA Toolbox. WP2 – Co-design of the supporting toolbox. [CLIMAAX – Horizon Europe, Grant Agreement No. 101093864]. Available at: https://files.cmcc.it/climaax/CLIMAAX_D2.4.pdf, 2024.

Muis S, Irazoqui Apecechea M, Dullaart J, de Lima Rego J, Madsen KS, Su J, Yan K and Verlaan M, A High-Resolution Global Dataset of Extreme Sea Levels, Tides, and Storm Surges, Including Future Projections. *Front. Mar. Sci.* 7:263, <https://doi.org/10.3389/fmars.2020.00263>, 2020.

Dottori, F., Alfieri, L., Bianchi, A., Skoien, J., and Salamon, P.: A new dataset of river flood hazard maps for Europe and the Mediterranean Basin, *Earth Syst. Sci. Data*, 14, 1549–1569, <https://doi.org/10.5194/essd-14-1549-2022>, 2022.

Trucchia Andrea, Meschi Giorgio, Fiorucci Paolo, Provenzale Antonello, Tonini Marj, Pernice Umberto, Wildfire hazard mapping in the eastern Mediterranean landscape. *International Journal of Wildland Fire* 32, 417-434, <https://doi.org/10.1071/WF22138>, 2023.

El Garroussi, S., Di Giuseppe, F., Barnard, C., & Wetterhall, F., Europe faces up to tenfold increase in extreme fires in a warming climate. *Npj Climate and Atmospheric Science*, 7(1). <https://doi.org/10.1038/s41612-024-00575-8>, 2024.

Jacome Felix Oom, D., De Rigo, D., Pfeiffer, H., Branco, A., Ferrari, D., Grecchi, R., Artes Vivancos, T., Durrant, T., Boca, R., Maianti, P., Liberta`, G. and San-Miguel-Ayanz, J., Pan-European wildfire risk assessment, EUR 31160 EN, Publications Office of the European Union, Luxembourg, 2022, ISBN 978-92-76-55137-9, doi:10.2760/9429, JRC130136.

Aerts, J.C.J.H., Bates, P.D., Botzen, W.J.W. et al. Exploring the limits and gaps of flood adaptation. *Nat Water* 2, 719–728, <https://doi.org/10.1038/s44221-024-00274-x>, 2024.

Bachmann, M., Mechler, R., Higuera Roa, O., Pirani, A., Pal, J., Reimann, L., Mazzoleni, M., Buskop, T., and Mysiak, J.: An adaptive and flexible Climate Risk Assessment Framework for regions, EGU General Assembly 2024, Vienna, Austria, 14–19 Apr 2024, EGU24-16910, <https://doi.org/10.5194/egusphere-egu24-16910>, 2024.

Kendon, E. J., Jones, R. G., Kjellström, E., and Murphy, J. M. (2010). Using and Designing GCM–RCM Ensemble Regional Climate Projections. *Journal of Climate*, 23(24), 6485-6503. <https://doi.org/10.1175/2010JCLI3502.1>.

Di Baldassarre, G., Mazzoleni, M., and Mondino, E. (2021). Flood fatalities in Africa: From diagnosis to mitigation. *Earth System Dynamics*, 12(4), 1543–1553. <https://doi.org/10.5194/esd-12-1543-2021>.

Kim, E., Kim, T., Mun, T. et al. Multimodel GCM-RCM ensemble-based projections of tropical cyclone activities over CORDEX East Asia domain. *Clim Dyn* 63, 143 (2025). <https://doi.org/10.1007/s00382-025-07627-6>.

Appendix

In connection to 2.1.3 and 2.1.5, the following data can be found for a discussion organized by RCM, including CDXi, representatives from the local authorities, the head of the fire department, and the head of the regional civil protection unit:



Συνάντηση Τοπικής Ομάδας Υποσ
Παρασκευή 14 - 11 - 2025
Θεσσαλονίκη

A/A	Όνοματεπώνυμο	Φορέας	Θέση
1	Μαρία Καραβίτση	ΑΔΑΠ/ΔΚΥ	Αν. Προϊκ. Δ/νση 22
2	Κωνσταντίνος Τσοπάνης	ΠΕΠΥΣΑΜ	Προϊκ. Γρ. Επιτελ. 2
3	Καλλιόπη Αρβυλάκη	ΠΕΠΥΑΚΜ	Διοικητική 2
4	Στέφανος Τριανταφύλλης	ΔΙΠΥΝ ΘΕΣ/Π/ΚΥ	Προϊκ. Διαχ. 2
5	Στέφανος Αρβυλάκης	ΔΤΕ/ΠΚΥ	Υπόδημος 22
6	Νικόλαος Ανδριανός	ΑΔΥΚΕ ΠΚΥ	ΣΜΕ 22
7	Ηλίας Γιαλαμουνάκης	CDXi solutions	ΕΕΟ 65
8	Αναστασία Μουκρτζή	CDXi solutions	ΣΤΟ 69
9	Παναγιώτης Νηλίας	π.κ.μ.	Διαχειριστική 65
10	Παναγιώτης Νηλίας	π.κ.μ.	Υποδημος 69
11	Αθανάσιος Αρβυλάκης	ΕΤ	Υποδημος 69
12	Γεωργία Σω	ΠΚΥ	Υποδημος 6

ΘΕΜΑ : Πρόσβαση σε δεδομένα στο πλαίσιο υλοποίησης του ευρωπαϊκού έργου CLIMAAX-Datable με τίτλο "Κλιματική προσαρμογή ευάλωτων περιφερειών χρησιμοποιώντας την εργαλειοθήκη του CLIMAAX" από την Περιφέρεια Κεντρικής Μακεδονίας

Η Περιφέρεια Κεντρικής Μακεδονίας συμμετέχει στο ευρωπαϊκό έργο «climate aDAPtation for vulnerABle regions using the "CLIMAAX" framEwork - Κλιματική προσαρμογή ευάλωτων περιφερειών χρησιμοποιώντας την εργαλειοθήκη του CLIMAAX". ΑΚΡΩΝΥΜΙΟ: "DATABLE"» το οποίο χρηματοδοτείται από το Ευρωπαϊκό Πρόγραμμα Horizon Europe 2021-2027. Το έργο υλοποιείται με την συνεργασία της Αυτοτελούς Διεύθυνσης Πολιτικής Προστασίας της Π.Κ.Μ.

Το CLIMAtE risk and vulnerability Assessment framework and toolboX (CLIMAAX) είναι ένα τετραετές πρόγραμμα «Ορίζοντας Ευρώπη», το οποίο θα παρέχει οικονομική και τεχνική υποστήριξη για τη βελτίωση των περιφερειακών σχεδίων διαχείρισης κινδύνων λόγω κλιματικής αλλαγής και ευρύτερων εκτάκτων αναγκών. Το πρόβλημα που προσπαθεί να επιλύσει το έργο είναι ότι το πεδίο, σε ευρωπαϊκό επίπεδο διαχείρισης των κινδύνων καταστροφών και της προσαρμογής στην κλιματική αλλαγή, δεν παρουσιάζει ομοιομορφία.

Στο πλαίσιο υλοποίησης του Ευρωπαϊκού έργου CLIMAAX, δημοσιεύτηκε ανοιχτή πρόσκληση που καλούσε Περιφέρειες της Ευρώπης να υποβάλλουν πρόταση για εφαρμογή της μεθοδολογίας και εργαλειοθήκης του CLIMAAX στις αντίστοιχες περιοχές. Η Περιφέρεια Κεντρικής Μακεδονίας επιλέχθηκε, ανάμεσα σε πολλές άλλες, για να χρηματοδοτηθεί και να υλοποιήσει το έργο DATABLE και τις παρακάτω δράσεις σε 3 φάσεις:

ΦΑΣΗ 1: Εφαρμογή της μεθοδολογίας CLIMAAX σε περιφερειακό/τοπικό επίπεδο χρησιμοποιώντας τη διαθέσιμη εργαλειοθήκη του έργου.

Η πρώτη φάση των εργασιών που πρέπει να γίνουν είναι η εφαρμογή της μεθοδολογικής προσέγγισης CLIMAAX με τη χρήση της υποστηρικτικής εργαλειοθήκης CLIMAAX, η οποία περιέχει δεδομένα και κατευθυντήριες γραμμές για εφαρμογή της μεθοδολογίας σε επίπεδο Περιφέρειας ή/και σε πιο τοπικό επίπεδο. Στη πρώτη φάση, θα γίνει χρήση κοινών ευρωπαϊκών βάσεων δεδομένων για το κλίμα (παρελθούσες παρατηρήσεις, μελλοντικές προβλέψεις) και θα αξιοποιηθούν κοινές μεθοδολογίες για τον υπολογισμό των αλλαγών στις συχνότητες των σχετικών κλιματικών δεικτών που χαρακτηρίζουν τους πολλαπλούς κινδύνους.

ΦΑΣΗ 2: Βελτιωμένη εφαρμογή της μεθοδολογίας εκτίμησης κινδύνων με τη χρήση περιφερειακών/τοπικών δεδομένων υψηλής κλίμακας.

Η δεύτερη φάση των εργασιών είναι η βελτίωση/εξειδίκευση της εκτίμησης κινδύνου που διενεργήθηκε στη φάση 1. Η πρόταση πρέπει να προσαρμόζεται στη διεξαγωγή της καλύτερης δυνατής μελέτης πολλαπλών κινδύνων από την κλιματική αλλαγή αξιολόγηση σε περιφερειακή/τοπική κλίμακα για την τοποθεσία/κοινότητα του αιτούντος, με στόχο να εκτιμηθεί η μεταβολή των κινδύνων λόγω της κλιματικής αλλαγής και να παρασχεθεί υποστήριξη για το σχεδιασμό σε στρατηγικές προσαρμογής και τη βελτίωση των τοπικών σχεδίων διαχείρισης κινδύνων με σκοπό την αύξηση της περιφερειακής ανθεκτικότητας.

ΦΑΣΗ 3: Αξιολόγηση των αποτελεσμάτων των φάσεων 1 και 2 και διερεύνηση προτάσεων στρατηγικής προσαρμογής σε τοπική κλίμακα για την αντιμετώπιση των κινδύνων και των τρωτών σημείων που εντοπίστηκαν από την ανάλυση.

Κατόπιν των ανωτέρω, θα επιθυμούσαμε εφόσον είναι εφικτό για την συγκατάθεση και άδεια στην ανάκτηση στοιχείων από τις αντίστοιχες βάσεις δεδομένων σας, όπως αυτά καταγράφονται στο συνημμένο πίνακα pdf (μετεωρολογικά δεδομένα, πλημμυρικά φαινόμενα, πυρκαγιές, κ.λ.π.), προκειμένου να χρησιμοποιηθούν τα δεδομένα αυτά στην υλοποίηση του έργου Climax-Datafile.

Σας ευχαριστούμε εκ των προτέρων και είμαστε στην διάθεσή σας για οποιαδήποτε άλλη διευκρίνιση.



ΑΚΡΙΒΕΣ ΑΝΤΙΓΡΑΦΟ

Μ.Ε.Π.

Η ΑΝ. ΠΡΟΣΤΑΜΕΝΗ ΤΗΣ ΑΥΤΟΤΕΛΟΥΣ ΔΙΕΥΘΥΝΣΗΣ



ΥΛΑΠΤΙΣΗ ΜΑΡΙΑ
Π.Ε. Μηχανικός
με βαθμό Α

ΜΑΡΙΑ ΓΟΥΛΑΠΤΣΗ

ΕΣΩΤΕΡΙΚΗ ΔΙΑΝΟΜΗ:
Αρχείο ΦCLIMAAX-DATABLE

ΠΙΝΑΚΑΣ ΑΠΟΔΕΚΤΩΝ:

1. Υ.Π.Ε.Ν:
2. Υπ. Κλιματικής Κρίσης & Πολιτικής Προστασίας:
3. ΟΦΥΠΕΚΑ:
4. ΑΔΜΘ:
5. ΕΠάδαΠ:
6. Α.Π.Θ.:
7. ΚΤΗΜΑΤΟΛΟΓΙΟ:
8. ΕΜΥ:



Πρόγραμμα: Horizon Europe 2021–2027

Τίτλος έργου: „Κλιματική προσαρμογή ευάλωτων περιφερειών χρησιμοποιώντας την εργαλειοθήκη CLIMAAX _ climate adApTation for vulnerABLE regions using the “CLIMAAX” framEwork

Ακρωνύμιο: DATABLE

Θεματικό πεδίο ενδιαφέροντος: Προσαρμογή στην Κλιματική Αλλαγή

Site: <https://www.climaax.eu>

Περίληψη έργου:

Το έργο DATABLE θα επικεντρωθεί στην αντιμετώπιση των σημαντικότερων κλιματικών κινδύνων που αντιμετωπίζει η Περιφέρεια Κεντρικής Μακεδονίας εφαρμόζοντας τη μεθοδολογία εκτίμησης κλιματικών κινδύνων που αναπτύσσεται στο πλαίσιο του Ευρωπαϊκού έργου CLIMAAX. Το CLIMAtE risk and vulnerability Assessment framework and toolboX (CLIMAAX) είναι ένα τετραετές έργο του προγράμματος «Ορίζοντας Ευρώπη», το οποίο θα παρέχει οικονομική και τεχνική υποστήριξη για τη βελτίωση των περιφερειακών σχεδίων διαχείρισης κινδύνων λόγω κλιματικής αλλαγής. Το πρόβλημα που προσπαθεί να επιλύσει το έργο είναι ότι το Ευρωπαϊκό πλαίσιο της διαχείρισης του κινδύνου καταστροφών και της προσαρμογής στην κλιματική αλλαγή δεν είναι καθόλα ομοιόμορφο. Το CLIMAAX βασίζεται σε υφιστάμενα πλαίσια, μεθόδους και εργαλεία εκτίμησης κινδύνου και προωθεί τη χρήση συνόλων δεδομένων και πλατφορμών υπηρεσιών για την ανάπτυξη σε τοπική και περιφερειακή κλίμακα. Στόχος του είναι να αναπτύξει ένα ισχυρό και συντονισμένο πλαίσιο συνεπών, εναρμονισμένων και συγκρίσιμων εκτιμήσεων κινδύνου. Το έργο ξεπερνά τα υπάρχοντα εργαλεία και υπηρεσίες και με την βοήθεια της τεχνολογίας αιχμής, δίνει προτεραιότητα στην περαιτέρω ανάπτυξη της προσαρμοστικότητας, της καθοδήγησης, της προσαρμογής στα τοπικά δεδομένα, της ερμηνείας και της υιοθέτησης από αντιπροσωπευτικές αρχές διαχείρισης κινδύνου καταστροφών και πολιτικής προστασίας.

Στο πλαίσιο υλοποίησης του Ευρωπαϊκού έργου CLIMAAX, δημοσιεύτηκε ανοιχτή πρόσκληση που καλούσε Περιφέρειες της Ευρώπης να υποβάλλουν πρόταση για εφαρμογή της μεθοδολογίας και εργαλειοθήκης του CLIMAAX στις αντίστοιχες περιοχές. Η Περιφέρεια Κεντρικής Μακεδονίας επιλέχθηκε, ανάμεσα σε πολλές άλλες, για να χρηματοδοτηθεί.

Δράσεις Περιφέρειας Κεντρικής Μακεδονίας:

Το έργο DATABLE είναι δομημένο σε 3 φάσεις με τα αντίστοιχα παραδοτέα.

ΦΑΣΗ 1: Εφαρμογή της μεθοδολογίας CLIMAAX σε περιφερειακό/τοπικό επίπεδο χρησιμοποιώντας τη διαθέσιμη εργαλειοθήκη του έργου.

Η πρώτη φάση των εργασιών που πρέπει να γίνουν είναι η εφαρμογή της μεθοδολογικής προσέγγισης CLIMAAX με τη χρήση της υποστηρικτικής εργαλειοθήκης CLIMAAX, η οποία περιέχει δεδομένα και κατευθυντήριες γραμμές για εφαρμογή της μεθοδολογίας σε επίπεδο Περιφέρειας ή/και σε πιο τοπικό επίπεδο. Στη πρώτη φάση, θα γίνει χρήση κοινών ευρωπαϊκών βάσεων δεδομένων για το κλίμα (παρελθούσες παρατηρήσεις, μελλοντικές προβλέψεις) και θα αξιοποιηθούν κοινές μεθοδολογίες για τον υπολογισμό των αλλαγών στις συχνότητες των σχετικών κλιματικών δεικτών που χαρακτηρίζουν τους πολλαπλούς κινδύνους.

ΦΑΣΗ 2: Βελτιωμένη εφαρμογή της μεθοδολογίας εκτίμησης κινδύνων με τη χρήση περιφερειακών/τοπικών δεδομένων υψηλής κλίμακας.

Η δεύτερη φάση των εργασιών είναι η βελτίωση/εξειδίκευση της εκτίμησης κινδύνου που διενεργήθηκε στη Φάση 1. Η πρόταση πρέπει να προσανατολίζεται στη διεξαγωγή της καλύτερης δυνατής μελέτης πολλαπλών κινδύνων από την κλιματική αλλαγή αξιολόγηση σε περιφερειακή/τοπική κλίμακα για την τοποθεσία/κοινότητα του αιτούντος, με στόχο να εκτιμηθεί η μεταβολή των κινδύνων λόγω της κλιματικής αλλαγής και να παρασχεθεί υποστήριξη για το σχεδιασμό σε στρατηγικές προσαρμογής και τη βελτίωση των τοπικών σχεδίων διαχείρισης κινδύνων με σκοπό την αύξηση της περιφερειακής ανθεκτικότητας.

ΦΑΣΗ 3: Αξιολόγηση των αποτελεσμάτων των φάσεων 1 και 2 και διερεύνηση προτάσεων στρατηγικής προσαρμογής σε τοπική κλίμακα για την αντιμετώπιση των κινδύνων και των τρωτών σημείων που εντοπίστηκαν από την ανάλυση.

Προϋπολογισμός Περιφέρειας Κεντρικής Μακεδονίας: 185.000,00 €

Το έργο χρηματοδοτείται 100% από Ευρωπαϊκούς πόρους.

Χρονοδιάγραμμα υλοποίησης έργου: 22 μήνες

Έναρξη έργου: 1/10/2024.



ΠΕΡΙΦΕΡΕΙΑ
ΚΕΝΤΡΙΚΗΣ ΜΑΚΕΔΟΝΙΑΣ

ΠΕΡΙΦΕΡΕΙΑΚΕΣ ΕΝΟΤΗΤΕΣ

Περιφέρεια Κεντρικής Μακεδονίας

SITE MAP

[Επικοινωνία](#)
[Σύνδεσμοι](#)
[Για τον πολίτη](#)
[Ενημέρωση](#)
[Ψηφιακές](#)
[Υπηρεσίες](#)
[Δήλωση](#)
[προσαρμοστικότητας](#)

[Πολιτική Προστασίας](#)
[Προσωπικών Δεδομένων](#)
[Υπεύθυνος Προστασίας](#)
[Δεδομένων](#)
[Υπηρεσίες προς Υπαλλήλους](#)
[Διαύγεια](#)
[Προηγούμενη ιστοσελίδα](#)

ΔΙΑΥΓΕΙΑ
Διαύγεια
Διαφάνεια στο κράτος

GOV.gr
gov.gr
Κατά το έδαφος υπηρεσία που
έχει κεντράει να γράφει



Όροι Χρήσης & Πολιτική Απορρήτου

Σχεδιασμός και υλοποίηση από την Crowdpolity